UNIVERSITY OF CALGARY

Loop-Mediated Isothermal Amplification for Diagnosis of Major Infectious Diseases in Resource-Limited Settings

by

Paul Mintchev

A THESIS

SUBMITTED TO THE FACULTY OF GRADUATE STUDIES

IN PARTIAL FULFILMENT OF THE REQUIREMENTS FOR THE

DEGREE OF MASTER OF SCIENCE

GRADUATE PROGRAM IN BIOMEDICAL ENGINEERING

CALGARY, ALBERTA

JULY, 2015

Abstract

Major Infectious Diseases (MIDs) continue to pose major global health-care challenges in 2015, particularly in resource-limited settings. Alongside the recent global Human Immunodeficieny Virus (HIV)/Acquired Immunodeficieny Syndrome (AIDS) pandemic, there has been a marked resurgence in fatalities related to Malaria and Leishmaniasis in Lower-to-Middle-Income Countries (LMICs). With the recent development of Loop-Mediated Isothermal Amplification (LAMP), researchers are hoping to bring rapid and inexpensive point-of-care diagnostics, based on nucleic acid amplification, to LMIC settings. We explored the possibility of a portable, low-cost LAMP-based diagnostic device targeting HIV, Malaria, and Leishmaniasis, for use in resource-limited settings, in an idealized proof-of-concept study. Design and build an inexpensive functional prototype with the potential to quantify disease severity that demonstrates the feasibility of this diagnostic tool for the desired application was the primary outcome; however, much work remains to be done in order to optimize the method to a reliable and repeatable clinical tool.

Preface

As I wrote this thesis, I couldn't help but chuckle as I reflected on how the execution of this project mirrored its goal so perfectly.

I shocked myself by pursuing a Master of Science degree almost constantly – even well into my experimental work – because, although I've always had an intense passion for science, not long ago I was on the verge of withdrawing from even my undergraduate studies.

In my last year of High School, for the first time in my life, I suffered an intense grand-mal seizure. My breathing and my heartbeat both stopped for almost two minutes, and I am only alive today because of a course of emergency Cardio-Pulmonary Resuscitation quickly administered (albeit, ironically enough, very incorrectly) by two loved ones. The attack left me in a coma for three days; however, I made a full recovery soon afterward, completed the twelfth grade and enrolled at McGill University to study Biochemistry, while neurological follow-ups showed no abnormalities, and the incident was dismissed as a sort of freak-accident.

Almost three years after my first seizure, two days after my last final exam of my second year, I suffered a second seizure. This one broke my jaw in three places and left me hospitalized for almost a month while it was surgically reconstructed with titanium implants. I also suffered nerve trauma that has left my face permanently paralyzed and numb in several areas. My third seizure occurred eleven months later. The fourth attack followed

just over four months after the third, two months prior to the start of my fourth year of undergrad – after I had already begun a course of treatment for epilepsy.

Although the third and fourth incidents didn't injure me as the first two did, any scientist familiar with analyzing and extrapolating data trends will, I'm sure, appreciate the terror I found myself in after this upward trend in frequency, particularly as my seizures would always come without any sort of presentiment, or “aura”.

To this day I can't fully explain why I did go back to complete my fourth year of university, other than out of habit, but I questioned the decision daily as I waited for the attacks to recur, according to a morbidly quantified schedule I had prepared graphically on Excel, until they eventually killed me. I had the date of my death scheduled and a bottle of champagne set aside for the occasion.

In the meantime, lectures became a kind of entertainment to pass the time on death-row, so long as the material genuinely interested me – which was often the case with biochemistry. I must have unintentionally done something right somewhere, because they were nice enough to give me a degree for it. I don't remember too much of that, other than thinking it would be one hell of a dark joke to get that fancy piece of paper just in time to be buried with it.

But, my fourth seizure indeed proved to be my final one (knock-on-wood), and my itch for science was a clause that was happily renewed in my second lease on life. This time, I decided to shift gears and explore the more practical side of theory, with this Master of

Science degree in Biomedical Engineering. I eventually ended up making the decision to leave my first project, in the middle of a particularly difficult funding environment.

I entered Dr. Van Marle's lab much like a stray animal to the SPCA. I was funded the minimum stipend through the Biomedical Engineering graduate program itself. However, because of the time I had already spent on my first project, I had less than a year remaining in which to complete a second project before that would expire and I would be forced to withdraw from the program. Dr. Van Marle had an endowment for HIV-related research that paid for reagents and equipment – for the first 7 months – after which we were left entirely without a budget for the remainder of my project, while the renewal process was set in motion for 2015.

Dr. van Marle has invested much of his own money into this project (for which I cannot thank him enough), and I myself have come out-of-pocket to purchase components that I deemed crucial. Most of the time, though, the game was to figure out free solutions to our problems. The prototype I designed had to be built from recycled materials filched from old equipment discarded by other laboratories. The line between “3D-printing” and “cutting out of cardboard” blurred by the day. Meter-long coils of wire became resistors, and even year-old plywood found under the deck wasn't safe. The project took on a very ironic character as it mirrored the real challenges facing health-care practitioners in Lower-to-Middle Income Countries: a tight time-line, and an extremely restricted supply pool.

We set out to explore the feasibility of bringing rapid, portable, low-cost point-of-care diagnostics to people in dire need of these tools in the very near future, who had very limited means with which to pay for them.

We did so, in dire need of a completed project in the very near future, and with very limited resources with which to do it.
What could be more fitting?

I am extremely honored to have been a part of this amazing project and its beautiful humanitarian goal. I regret not being able to pursue many research goals I had in order to bring my prototype to the level of a professional clinical diagnostic, but I hope that, in less than half the time normally given to a project of this kind, and with an extremely budget, I have laid a solid and proven groundwork out of which continued research will produce great things in the future – things that will one day bring people more deserving than myself back from the edge of oblivion, to re-learn what it's like to live life on a blank schedule again, the way I've been doing in between the experiments I have the privilege of sharing with you herein.

Acknowledgments

First and foremost, none of this would not have been possible without the vision, guidance, and input (both scientific and monetary) of my supervisor Dr. Guido van Marle.

Purchases of equipment and reagents in the earlier stages of this project were made possible through the Thomas Norquay Endowment for AIDS research.

My personal stipend was generously supported by Dr. Michael Kallos and the University of Calgary's Biomedical Engineering graduate program for the first few months of my research.

I would also like to express my wholehearted gratitude to:

My co-supervisors Drs. Lashitew Gedamu and Anthony Schryvers, who have contributed both insight and valuable reagents to this project;

Dr. Wendy Anne Hutchins, who has provided me with much guidance and literature, as well as ideas;

Dr. Carla Coffin and her PhD student Dr. Shan Gao, with whom we have shared lab space, equipment, and reagents;

Drs. John Dort and Devon Livingstone, as well as Steve Nakoneshny, who have contributed both reagents and insight into the LAMP technique with their parallel exploration of its merits as a diagnostic tool for other applications;

Joao Prado and Mitchell Rohatensky, who helped me gain my bearings early in the project, while acquiring more data than I could with my own manpower, as I trained them in the LAMP technique;

Sandra Nishikawa, as she has been an indispensable source of wisdom and guidance from a seasoned molecular biology technician;

Dr. Raymond Turner for finding me a Teaching Assistant position, without which this project would have had a time-line of less than 8 months;

Lisa Mayer for her efficient handling of administrative and logistical aspects of my degree;

Alex Jurkov, Joseph & Faustina Wang, and Michael Poscente for their mentorship in electrical design;

My family and friends, of course, for their constant support in its various incarnations.

Table of Contents

List of Tables

List of Figures

List of Symbols, Abbreviations, Nomenclatures

Abbreviations:

DNA, DeoxyriboNucleic Acid

RNA, Ribonucleic Acid

mRNA, messenger RiboNucleic Acid

WHO, World Health Organization

MID, Major Infectious Disease

BSE, Bovine Spongiform Encephalopathy

PrP, Prion Protein

PrP^{c}, Prion Protein: cellular form

PrP^{sc}, Prion Protein: amyloid form

GPI, GlycoPhosphatidylInositol

NAAT, Nucleic Acid Amplification Test

ALS, Amyotrophic Lateral Sclerosis

GDP, Gross Domestic Product

LMIC, Lower-to-Middle Income Country

UNU-WIDER, United Nations University World Institute for Development Economics Research

HIV/AIDS, Acquired Immune Deficiency Syndrome caused by Human Immunodeficiency Virus

HIV, Human Immunodeficiency Virus

UNAIDS, Joint United Nations Programme on HIV/AIDS

SIV, Simian Immunodeficiency Virus

HTLV-1, Human T-Lymphotropic Virus Type 1

HTLV-2, Human T-Lymphotropic Virus Type 2

ssRNA, single-stranded messenger RiboNucleic Acid

tRNA, transfer RiboNucleic Acid

dNTP, deoxyNucleoside TriPhosphate

ELISA, Enzyme-Linked Immunosorbent Assay

RDT, Rapid Diagnostic Test

PCR, Polymerase Chain Reaction

PTC, Peltier Thermoelectric Cooler

AC, Alternating Current

DC, Direct Current

LAMP, Loop-Mediated Isothermal Amplification

Bst, *B. stearothermophilus* DNA polymerase

FIP, Forward-Inner-Primer

BIP, Back-Inner-Primer

LPF, Loop-Primer: Forward

LPB, Loop-Primer: Back

BLAST, Basic Local Alignment Search Tool

NCBI, National Center for Biotechnology Information

LB, Lysogeny Broth

HEPA, High Efficiency Particle Arrestance

LED, Light Emitting Diode

CMOS, Complementary Metal-Oxide Semiconductor

MOSFET, Metal-Oxide-Semiconductor Field-Effect Transistor

CCD, Charge-Coupled Device

IDS, Imaging Development Systems

qPCR, quantitative Polymerase Chain Reaction

BSC, Bio-Safety-Cabinet

HPLC, High Performance Liquid Chromatography

dTTP, deoxyThyine TriPhosphate

dUTP, deoxyUracil TriPhosphate

UNG, Uracil-DNA-Glycosylase

IPTG, Isopropyl β-D-1-thiogalactopyranoside

SDS-PAGE, Sodium Dodecyl Sulfate-Polyacrylamide Gel Electrophoresis

CHAPS, 3-((3-chloramidopropyl) dimethylammonio)-1-propanesulfonate

Ni-NTA, Nickel-Nitrilotriacetic Acid

Symbols:

USD, United States Dollars

CAD, Canadian Dollars

bp, base-pairs

kb, kilo-base-pairs

°C, degrees Celsius

$\bar{Q}$, heat generated on the heat-rejecting side per unit time [of a Peltier Thermoelectric Cooler]

J, Joules (unit of energy)

s, second

min, minute

Π_A, Peltier coefficient of conductor A

Π_B, Peltier coefficient of conductor B

I, current

A, Amperes (unit of current)

mA, milli-Amperes

V, Volts

R, [electrical] resistance

Ω, Ohms (unit of resistance)

mΩ, milli-Ohms

W, Watts (unit of power)

Ah, Ampere-hours

kPa, kilo-Pascals (unit of pressure)

K, potassium

Cl, chlorine

Na, sodium

N, nitrogen

H, hydrogen

O, oxygen

S, sulfur

Mg, magnesium

P, phosphorus

PPi^{4-}, pyrophosphate

Ca, calcium

L, litre

µL, microliter

M, moles per litre (unit of concentration)

µM, micro-moles per litre,

p, p-value obtained in a two-tailed Student's T-test

n, population number used for a two-tailed Student's T-test

rfu, Relative Flurescence Units

X, unknown value

awg, American Wire Gauge

", inches

', feet

cm, centimetres

1. BACKGROUND

1.a Overview of Major Infectious Diseases

Despite decades of research and large sums of money spent by agencies such as the World Health Organization (WHO), the eradication of infectious diseases continues to be only a future goal, even in 2015.

Infectious diseases are usually caused by a micro-organism that has invaded the patient and is proliferating on or within them in a parasitic fashion, causing bodily harm. Most infectious diseases have either a bacterium, virus, or a microscopic eukaryotic parasite as causative agent; a minor sub-group, called the “prion diseases”, are caused by misfolded proteins that have the capacity to induce misfolding in properly folded proteins as well, and are very difficult to test for. Diagnostic tests for the majority of infectious diseases may focus on detecting the causative micro-organism, whose presence directly correlates with the condition. Medical diagnostics of infectious disease is not as clear-cut as it may seem, however, as there are many factors to take into consideration when developing diagnostic assays. It is important to note, for example, that not all bacteria, viruses, and micro-eukaryotes cause disease in humans. Indeed, the human body is estimated to contain ten times more bacterial cells in and on it than it does human cells(1). Viruses can also play non-pathogenic roles in normal physiology, with some experts estimating that

up to 8% of the human genome may have been acquired through the integration of viral genomes that have since become “domesticated” and no longer capable of packaging into infectious virion particles(2). With regard to microscopic eukaryotes, there is a well described balance of several yeast species that live in and on the human body in both sickness and health(3). These relationships with microbes may be commensal, with the human host being largely unaffected by their presence, or even mutualistic, as in the case of many intestinal bacteria, where the micro-organism benefits the human host(1). In other cases, however, the presence of some micro-organisms is almost certainly harmful to the host, and an infectious disease develops. Major Infectious Diseases (MIDs) are largely caused by harmful microbes that are foreign to some extent and, if present in or on the human body in detectable levels, directly correlate with a diseased state. Theoretically this can be done even in the earliest stages of infection, before symptoms arise, with the right diagnostic methods.

For the vast majority of MIDs, there exist not only foreign proteins to test for via protein-based diagnostics, but also a foreign nucleic-acid genome as well, though the latter often needs to be amplified to detectable levels first. Amplification and detection of microbial (i.e. viral, bacterial, or parasitic) genomes is a relatively new advance, and may have several key advantages over protein-based methods. The focus of this work was to explore the merits, drawbacks, and applicability of Nucleic-Acid-Amplification-Tests (NAATs) for the diagnosis of several MIDs, for which other diagnostic methods may not be ideal.

1.b Clinical Diagnostics and the Challenges of Lower-to-Middle-Income-Countries

Of course, most infectious diseases cause symptoms that can be examined by a specialist, and a clinical diagnosis can be made. However, many diseases have symptoms that overlap with others, and this can confound a clinical diagnosis, even to the most experienced clinician. In some cases, improper diagnosis can lead the patient to begin a course of treatment that will not only be ineffective against the condition, but may waste valuable resources, and time, during which proper treatment could have affected the outcome more positively. For example, the neuromuscular symptoms of Lyme Disease can sometimes be misdiagnosed as Amyotrophic Lateral Sclerosis (ALS). Lyme Disease can be treated very effectively using several antibiotics, including ceftriaxone and cefotaxime, administered intravenously; however, once neuromuscular symptoms develop, the disease has already progressed significantly and this treatment must be administered quickly to avoid permanent complications such as partial paralysis(10). ALS has no known cure, and treatments focused on blocking disease-associated sodium receptors using riluzole have no positive effect for sufferers of Lyme Disease(11). Moreover, because ALS is progressive and riluzole treatment only marginally improves some symptoms, the lack of improvement may not be seen as a reason to re-evaluate the clinical diagnosis.

The case described above further serves to underscore the importance of timeliness in the medical field. As in the case of Lyme Disease, there exists a multitude of diseases that

can be treated very effectively in their earlier stages, but which can cause permanent complications or even be fatal if allowed to progress far enough. This danger is particularly apparent in regions where access to clinicians is scarce or absent.

For a number of historical and geographical reasons, many of the tropical regions of our planet have been left sadly underdeveloped in terms of Gross Domestic Product (GDP) and infrastructure. Indeed, a hefty proportion of the world's Lower-to-Middle-Income-Countries (LMICs) are located between the Tropic of Cancer and the Tropic of Capricorn. Figure 1 shows a global distribution of wealth from the year 2000, for graphical illustration of this phenomenon.

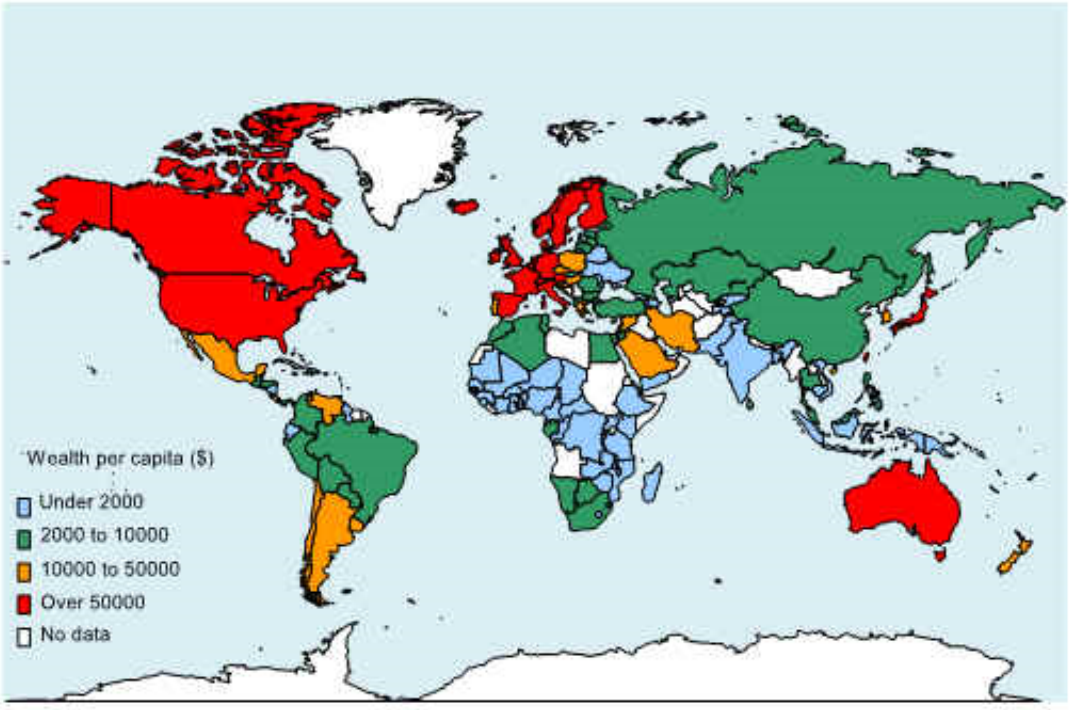

FIGURE 1: Global distribution of per-capita Wealth (USD) in 2000, as estimated by the United Nations University World Institute for Development Economics Research (UNU-WIDER)[1]

LMICs often have a scarcity of clinics, hospitals, and trained clinicians – all of which are costly elements of infrastructure to implement. Many of these LMICs have very significant rural populations as well, perhaps also stemming from underdeveloped urban infrastructure. Not only does this hinder clinical diagnoses, which mostly occurs in urban hospitals and clinics, but the lack of stable electricity and clean water sources also limits other diagnostic options. Many alternative diagnostic methods that could be implemented in underdeveloped rural settings without stable power or clean water sources are unfortunately too costly to be feasible for most LMICs. In addition, the climates of many tropical LMICs pose many additional challenges to potential diagnostic instruments, which need to be extremely robust so as to withstand the high temperatures and humidity levels found in these regions.

Unfortunately, many tropical LMICs are also hot-spots for some very harmful microbes. The malaria-causing *Plasmodium* genus of protozoa, for example, does not generally pose a significant threat to anyone living outside of the tropics, because the climate fluctuates to colder temperatures too dramatically with the changing of the seasons to maintain the populations of their particular mosquito hosts(12). The *Leishmania* genus of eukaryotic parasites, responsible for the “leishmaniasis” group of diseases, also scarcely present problems to people living in temperate climates, for similar reasons, as they also spend a portion of their life-cycles in an insect host that does not thrive outside of the tropics(13). Both of these MIDs, though relatively straightforward to diagnose and treat with the proper resources, have had a dramatic resurgence in lethality in recent years,

owing to frequent co-infection with another, more complex MID: the Acquired Immune Deficiency Syndrome caused by the Human Immunodeficieny Virus (HIV/AIDS)(14). HIV is a global problem that, unlike malaria and leishmaniasis, can cause disease in temperate and tropical climates alike. However, it is thought to have originated in the tropical region of Sub-Saharan Africa, where it remains a significant epidemic that kills an estimated 1.1 million of its 1.5 million total fatalities worldwide (2013 data), likely due in no small part to the regional challenges we have just been discussing(15). In 2013, over 30 million people were living with HIV worldwide.

As three of the most important MIDs challenging medicine in a large number of LMICs, we chose to focus our research into alternative low-cost diagnostic methods for resource-limited settings on HIV, malaria, and leishmaniasis as model diseases. Each of these three possess unique pathophysiologies that may pose challenges to conventional diagnostic methods, as will be discussed in the following sections.

1.c HIV/AIDS

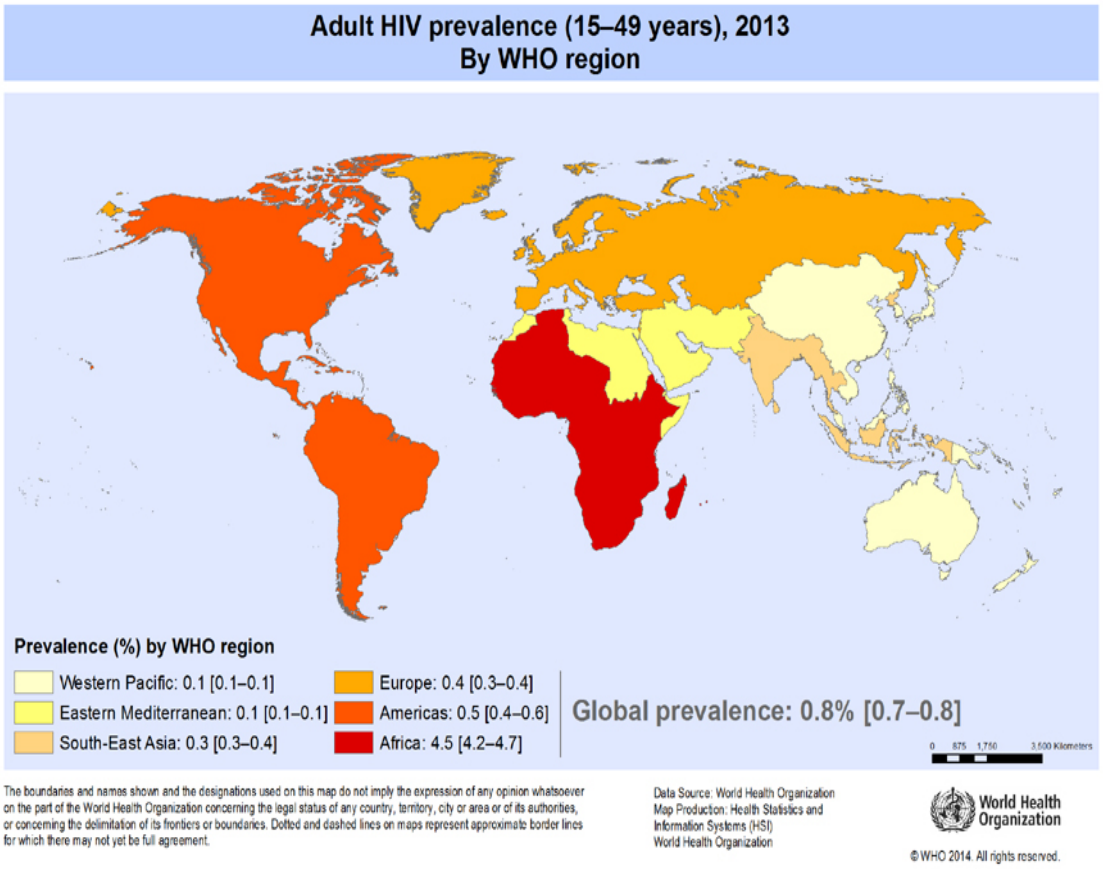

FIGURE 2: Worldwide prevalence of HIV/AIDS as a percentage of infected individuals in the adult population, as estimated by the World Health Organization (WHO) in 2013[2].

Figure 2 shows a recent estimation of the worldwide prevalence of HIV/AIDS, in order to highlight the heavy overlap of its distribution with the lower-to-middle-income tropical regions we have been discussing.

HIV is extremely reliant on its host for survival, as its viral particle is rapidly denatured on contact with air(16). Thus, it is transmitted directly from one person to another through bodily fluids – usually through unprotected sexual intercourse, birth (mother-to-offspring vertical transmission), blood transfusions, or shared injection needles(17). Figure 2 shows that the virus is not actually endemic to the tropics in the way Malaria and Leishmaniasis are, but simply has a much higher prevalence in certain LMICs – most notably in Sub-Saharan Africa. It is thought that HIV jumped species from the similar Simian Immunodeficiency Virus (SIV), which infects certain monkeys and apes, but only causes immune deficiency disease in a small subset of species, and was originally present only in Old World Monkeys and Great Apes in Sub-Saharan Africa before it mutated into the human-infecting virus(18). Perhaps exacerbating the AIDS epidemic are the many economic challenges facing tropical Africa. Without abundant access to diagnostic tests, prophylactic barriers for protected sexual intercourse, and education on the virus, HIV continues to spread in these regions of the world.

HIV is considered one of the biggest challenges to health-care researchers and practitioners of the 21st century(19). It is an extremely atypical and variable virus that can switch between dormant and disease-causing life-cycles unpredictably, confounding many treatment attempts. For starters, HIV is a retrovirus(20). Other than the two types of HIV, HIV-1 and HIV-2, only two retroviruses – Human T-Lymphotropic Virus Type 1 (HTLV-1) and Human T-Lymphotropic Virus Type 2 (HTLV-2) have been shown to cause any disease in humans(21). HIV further distinguishes itself from both of these human-infecting retroviruses by causing a unique diseased state of immunodeficiency, rather

than a form of cancer. HIV infection in and of itself does not appear to have any inherent oncogenic or mutagenic properties(22).

Retroviruses have a life-cycle that can be considered, in many ways, opposite to that of many virus types. A DNA virus, for example, is composed of a DNA genome and a protein coat (capsid), with many animal-infecting viruses also possessing an outer-most phospholipid bilayer called the viral envelope, which can aid their entry into host cells via fusion to the plasma membrane(23). Once inside, these viruses employ the typical biological “central dogma” of “DNA->RNA->Protein” (i.e. RNA is synthesized from a DNA template, and RNA is then translated into proteins), and the host cell's endogenous machinery, to replicate both their viral proteins and their genomes so heavily that they eventually exhaust the cell's resources and kill it, while many more virus particles are released(23).

HIV and other retroviruses do away with a double-stranded DNA genome, and instead do their genetic encoding using a single mRNA strand (ssRNA)(23). Although many other viruses also make use of an RNA genome, retroviruses differ from these as well, in that they reverse the typical DNA->RNA->Protein process. HIV and other animal-infecting retroviruses possess a lipid envelope with receptor-binding glycoproteins, and enter their host cells in a similar membrane-fusion mechanism to the one described for DNA viruses, releasing their capsids intracellularly. In the case of HIV specifically, these envelope proteins include gp120 and gp41, which bind to membrane receptors such as CD4, CCR5, and CXCR4 on immune cells to initiate envelope fusion with the plasma

membrane(24). The ssRNA genome is packaged together with a viral reverse-transcriptase enzyme within the capsid, which activates once it reaches the cytoplasm(25). Reverse-transcriptase is a unique enzyme, in that it alters the classical "DNA->RNA->Protein" model of gene expression by using a transfer-RNA (tRNA) as a primer, to synthesize double-stranded DNA, referred to as "cDNA", from the viral ssRNA genome. Packaged in the capsid along with reverse-transcriptase is a second enzyme called integrase, which then transports the newly synthesized cDNA to the host cell's nucleus and integrates it randomly into the host genome(25). Once integrated, the viral cDNA is referred to as a "provirus", and can remain dormant in the nucleus as part of the genomic DNA for long stretches of time(25). Indeed, this is one of the difficulties faced by health-care practitioners in HIV diagnosis, as symptoms can take years to develop following infection(26). In addition, if any mutations have been introduced in the provirus that interfere with the final re-packaging into a new virion particle, the provirus may in effect become a new component of the host genome that will be passed down to offspring. In fact, through sequence alignment of the human genome with known retroviral sequences, it has been, estimated that 5-8% of the human genome has been derived from various retroviral infections that haven't caused diseases(2). Such mutation events are not uncommon, as reverse-transcriptase is a particularly error-prone enzyme; its propensity to introduce mutations is also, unfortunately, one of the major reasons HIV treatment is such a challenge(27). If retroviral provirus integration takes place within a critical gene, disrupting the coding region, it may cause problems. Because most of the human genome is non-coding, however, the integration is harmless in the vast majority of cases. HIV proviral integration in itself hasn't been shown to be oncogenic or to cause

deleterious mutagenesis, nor have its viral proteins shown any evidence of being oncogenic(22).

The provirus of a retroviral infection is subject to the host cell's gene-regulatory mechanisms surrounding the region of integration, unlike the separate and unregulated DNA fragments of DNA viruses, and will be transcribed into viral ssRNA and viral proteins when the rest of the DNA region is transcribed. While this does take some additional cellular energy and amino-acids, it is usually insignificant, and the retrovirus is able to make a smaller copy number of new virions to bud from the host cell without killing it(23). Antiretroviral drugs can work at any of these stages, as can be seen in Figure 3 which shows the retroviral replication cycle for HIV and lists some common therapies that inhibit the various steps.

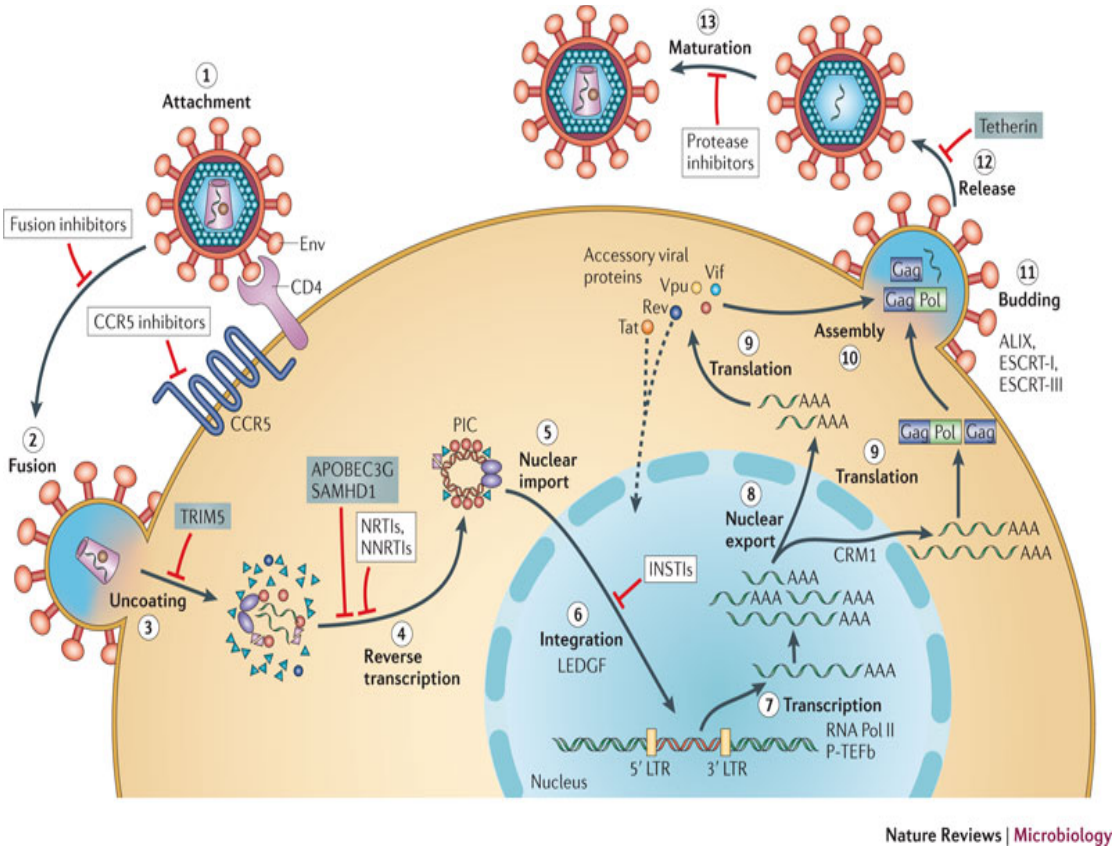

FIGURE 3: Schematic representation of the HIV cycle of infection/replication, with some common drug therapies listed at the steps they inhibit[3].

For the past 30 years since its discovery as the cause of HIV/AIDS, the mechanism(s) whereby HIV actually kills its host cells has remained shrouded in some mystery, and HIV-induced AIDS was largely a phenomenon of correlation that was not fully explained. Only recently have several key mechanisms of HIV-induced cell death been described in detail.

HIV infects cells of the immune system, specifically a class known as CD4+ T-cells. CD4 is one of the membrane receptors HIV binds to in order to initiate infection, the other

being either CCR5 or CXCR4(24). One of the particularly puzzling features of AIDS has been that only a very small minority of CD4+ T-cells are actually infected with the virus, although AIDS is characterized by a massive catastrophic decline in CD4+ T-cells(28). Some studies have shown evidence that HIV-infected CD4+ T-cells express proteins on their plasma membranes that bind to receptors on neighboring CD4+ T-cells and induce the process of apoptosis, or programmed cell suicide without release of intracellular contents. This mechanism would suggest that CD4+ T-cell depletion takes place predominantly in lymph nodes, such as the spleen for example, where T-cells are clustered together tightly(29).

Several recent studies, most notably Doitsh et al. and Monroe et al. (30,31), have implicated *abortive* HIV infection as a crucial player, by the mechanisms summarized herein. Similarly to their DNA virus counterparts, many retroviruses are dependent on the cell-cycle of their target cells in order to initiate a successful infection. In the case of HIV, many immune cells spend a majority of their time in a quiescent state when there are no infections for them to battle, and HIV infection is non-productive. In this state, the cells employ a protein called SAMHD1 to deplete their cytosolic stores of deoxynucleoside triphosphates (dNTPs). As dNTPs are the essential building blocks of DNA, this depletion ensures that energy will not be wasted in replicating the immune cell when no infection is present. When such a cell is infected by HIV, reverse-transcriptase begins the process of making cDNA from the ssRNA viral genome, but soon runs out of dNTPs and is forced to abort the task. Several cellular proteins, notably IFI16, bind this incomplete HIV cDNA and initiate an inflammatory response called pyropoptosis. In contrast to

apoptosis, which is mediated by a cell-death protein called caspase-3, pyropoptosis is mediated by a different protein of the same class, caspase-1, and causes the cell to produce many pro-inflammatory proteins before its programmed death, then finally lyses the cell and releasing these factors, inducing local inflammation in the area. This inflammation is very beneficial to the HIV virus, as it recruits more immune cells, including CD4+ T-cells, to the site *en masse*, where the virus can essentially "try again" to make a productive infection. In the case of a productive HIV infection in the minority of T-cells, studies have shown that fully reverse-transcribed HIV cDNA provides resistance to pyropoptosis and delays cell death, but eventually also kills the cells, via induction of caspase-3 production and classical apoptosis(30,31).

Regardless of the mechanism, depletion of CD4+ T-cells makes HIV/AIDS patients particularly susceptible and vulnerable to other infections. In the tropical regions we have been discussing, this often manifests as malaria or leishmaniasis co-infections, and these otherwise treatable diseases have become some of the main killers of immuno-compromised individuals in Sub-Saharan Africa, as well as regions of India and Brazil(14).

1.d Malaria and the Plasmodium Life-Cycle

The malaria disease is caused by parasitic infection from a species of *Plasmodium* protozoans, which have a fairly intricate polymorphic life-cycle, as reviewed extensively in Cowman et al.(32). In cases of malaria, patients have been bitten by a mosquito of the *Anopheles* genus, of which over 100 species can serve as vectors for *Plasmodium* parasites. *Anopheles* mosquitoes do not, however, host the actual infective form *Plasmodium*. When a female *Anopheles* mosquito bites a mammal infected with a *Plasmodium* species (male mosquitoes do not ingest blood, but rather feed exclusively on plant nectar), it actually takes up the protozoan's gametocytes. Gametocytes are large precursor cells that eventually divide into several smaller mature gametes. Gamete cells are haploid, either male or female, and can fuse with gametes of the opposite gender in order to complete the sexual reproductive life-cycle of *Plasmodium*, and form the so-called ookinete. This occurs in the mosquito's midgut lumen, and the resulting ookinete is a diploid, mobile zygote of sorts. It uses an actin/myosin-dependant form of locomotion called “gliding” to infect the cells of the mosquito's midgut lining, and develop into an oocyst. A large oocyst divides into many sporozoites, which are also motile, and journey up to the mosquito's salivary glands. Sporozoites are still diploid, and, though very small, are still mobile by gliding. When the mosquito bites another mammal, the sporozoites are injected through the salivary glands, along with chemicals such as anticoagulants that are introduced by the mosquito to aid blood-feeding. Sporozoites migrate through the mammalian blood stream to the liver, where they infect hepatocytes and become highly

active intracellularly. Sporozoites feed and mature in their mammalian host's liver cells, growing and making multiple nuclei and organelles as they become schizonts. Schizonts eventually rupture and release thousands of mobile diploid cells called merozoites. Merozoites prefer to infect erythrocytes or reticulocytes (red blood cells and immature red blood cells, respectively) over hepatocytes, and they thus break out of the liver and into the peripheral circulatory system. Within their blood cell host, merozoites mature into large, uninuclear cells called ring-trophozoites. The end-stage of trophozoite maturation is another type of schizont cell, which copies its nucleus and membrane-bound organelles before rupturing, lysing the host red blood cell and releasing many more merozoites into the bloodstream, where they can infect other erythrocytes. This portion of the *Plasmodium* life cycle, dubbed the erythrocytic cycle, is what is responsible for malaria symptoms. Finally, through an unknown mechanism, some merozoites develop into haploid gametocytes after the ring-trophozoite stage in their infected red blood cells, rather than schizonts. Gametocytes, though large, do not rupture their host erythrocytes, and do not develop any further within the mammalian host. For maturation to actual gametes, another *Anopheles* mosquito must ingest the erythrocytes containing *Plasmodium* gametocytes. After the insect digests the mammalian erythrocyte in the lumen of its midgut, the parasitic gametocytes are free to mature into many haploid gametes, which can then fuse sexually to begin the diploid life cycle once again(32).

As mentioned, the erythrocytic stage of the *Plasmodium* life cycle is the portion responsible for the symptoms of malaria. In addition to the anemia caused simply by depletion of erythrocytes, the bursting of a merozoite-containing schizont also releases toxins such as hemozoin(33). Hemozoin is a crystallized form of heme pigment produced

by the parasite after it feeds from the protein component of hemoglobin, leaving only the heme pigment(33). Since the heme pigment catalyzes the formation of reactive oxygen species, and is thus toxic to the protozoan, it is converted to hemozoin through biocrystallization(34). When released into the mammalian bloodstream, however, hemozoin causes several toxic effects to the mammalian host organism such as inhibition of erythropoeisis, which slows down production of new red blood cells and further contributes to the anemia commonly found in malaria. It is also partially responsible for the alternating cycle of fever and chills characteristic to malaria(33). Several effective anti-malarial medications, including cholorquine and mefloquine, work by binding free heme and inhibiting its biocrystallization to hemozoin, eventually poisoning the parasite(35).

Anopheles mosquitoes, like the vast majority of insects, are poikilothermic, meaning they cannot generate body heat and have internal temperatures comparable to the ambient environment. For this reason, they cannot survive metabolically during the winter in any region outside the tropics; since *Plasmodia* are dependent on their mosquito vectors for sexual reproduction and as host vectors to infect mammals for the mammalian portion of their life-cycle, the parasite is rarely found outside the tropics(36). Nevertheless, malaria caused over 500 000 deaths worldwide in 2013, and continues to be a major worldwide health care concern(37). Of these, the majority are caused by the species *Plasmodium falciparum*, which is associated with a much more severe form of the disease that also requires a more aggressive treatment to purge, though *Plasmodium vivax, Plasmodium*

malariae, *Plasmodium ovale, and Plasmodium knowlesi* can all cause milder forms of malaria(12). Figure 4 showcases the global distribution of the malaria disease.

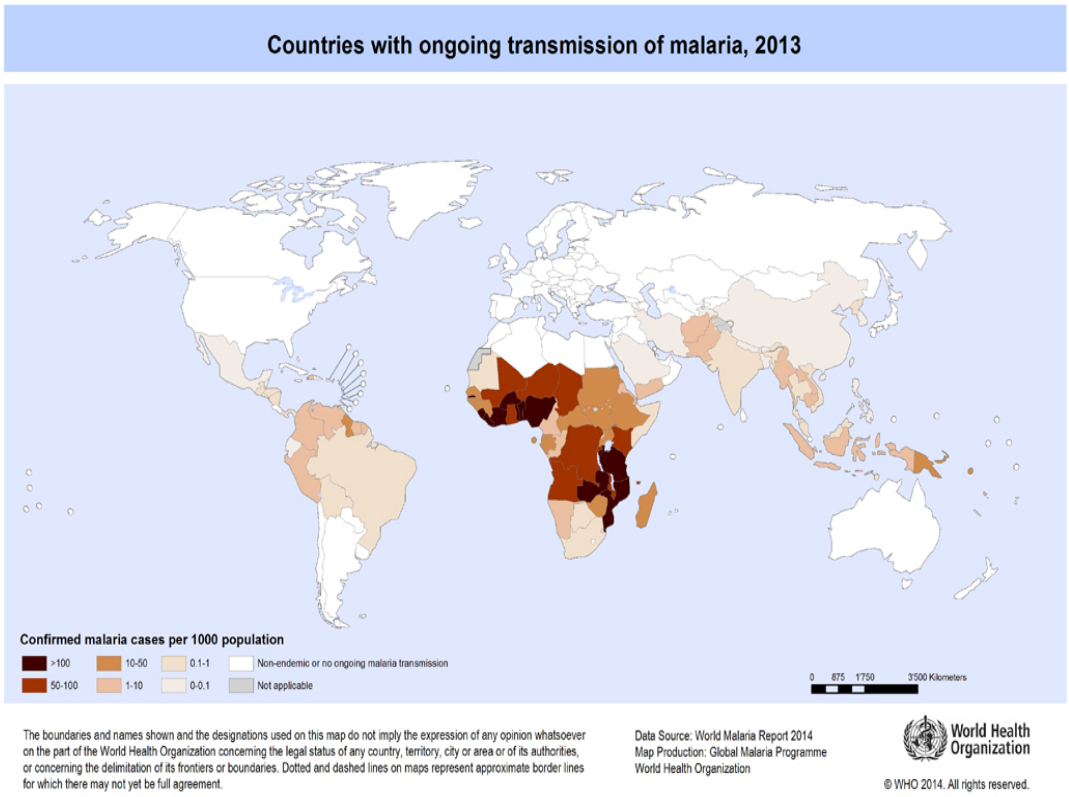

FIGURE 4: Global distribution of human malaria cases per 1000 population confirmed by the WHO, in 2013[4].

1.e Leishmaniasis and the Leishmania Life-Cycle

Another MID endemic to the tropics that can be fatal to humans is leishmaniasis(13). As can be seen through an extensive review of its pathophysiology in McMahon-Pratt, et al., it shares many infectious characteristics with malaria, though it is generally much milder(38). For example, leishmaniasis is also caused by an eukaryotic protozoan parasite – this time of the genus *Leishmania*, of which over 20 species can infect humans. Like malaria, the disease-causing agent of leishmaniasis is transmitted through an insect bite. In the case of leishmaniasis, the insect vector is the female sandfly, genus *Phlebotomus*, of which many species, similarly to the female mosquito, need to feed on blood in order to produce eggs. The sandfly uses its mouth-parts to pierce mammalian skin and start bleeding, after which it sucks up blood using its proboscis, while also injecting saliva doped with anticoagulants into the wound to promote bleeding. This latter process introduces *Leishmania* parasites into the bloodstream through the pharyngeal valve, particularly as the protozoans may be so numerous as to block the valve initially, compelling the sandfly to regurgitate this plug (or "clear its throat") before it can suck. These parasites are of the metacyclic promastigote form, meaning they possess a flagellum which makes them highly mobile and infective, and they do not divide. Metacyclic promastigotes are capable of actively infecting macrophages that are recruited to the bite wound, or may be taken up into these cells by phagocytosis as part of a normal immune response. Once inside macrophages, metacyclic promastigotes change morphologically into amastigotes, which lack a flagellum and are thus immobile, and

which divide actively. The amastigote cells reside within macrophages, feeding and dividing into more amastigotes until the macrophage lyses and releases them. At this point, the amastigotes can infect other macrophages, or can infect other tissue types. For many *Leishmania* species these other tissues are skin cells, causing superficial ulcers and a milder form of the disease known as Cutaneous Leishmaniasis. Other species are capable of causing similar ulcers in mucous membranes such as lips and nasal cartilage, resulting in the more severe Mucocutaneous Leishmaniasis. A minority of *Leishmania* species, notably *Leishmania donovani* and *Leishmania infantum* (also known as *Leishmania chagasi*), are capable of infecting the spleen, liver, and bone marrow, as well as other internal organs in some cases. This is the most severe form of the disease, called Visceral Leishmaniasis, and is responsible for the vast majority of human leishmaniasis fatalities(38).

Amastigotes residing in macrophages may be ingested by sandflies as they seek out a blood meal, where the macrophage membrane is digested by midgut enzymes and the cells are released. In the sandfly midgut, amastigotes transform into procyclic promastigotes. Procyclic promastigotes, like their metacyclic counterparts, also possess a flagellum and are highly mobile; unlike metacyclic promastigotes, however, procyclic promastigotes actively divide as they migrate upward. Once they reach the proboscis, they become metacyclic and cease dividing until they once again infect a mammalian host(38). Most *Leishmania* species reproduce in a predominantly asexual way, although there is some evidence of sexual reproduction in the sandfly midgut in some species(39).

Patients may develop the more severe Visceral Leishmaniasis; however, the vast majority of Leishmaniasis cases are from the less severe Cutaneous and Mucocutaneous forms, and may clear on their own even without treatment, though they can leave extensive scarring(38). Amphotericin B, an antifungal drug isolated from the bacterium *Streptomyces nodosus*, is available in a lipid-encased ("liposomal") form for intravenous administration, and has been shown to be up to 95% effective in clearing Visceral Leishmaniasis(40). It has become the new standard treatment, replacing therapy with pentavalent antimonial compounds, which can have detrimental cardiac and renal side-effects, and to which many *Leishmania* species, particularly in India, are becoming resistant(40). Thus, Leishmaniasis is only responsible for approximately 20 000-30 000 worldwide deaths annually; however, this MID is the second most fatal parasitic infection in humans, following malaria(41). Figure 5 shows the worldwide distribution of the most severe form of the disease, Visceral Leishmaniasis.

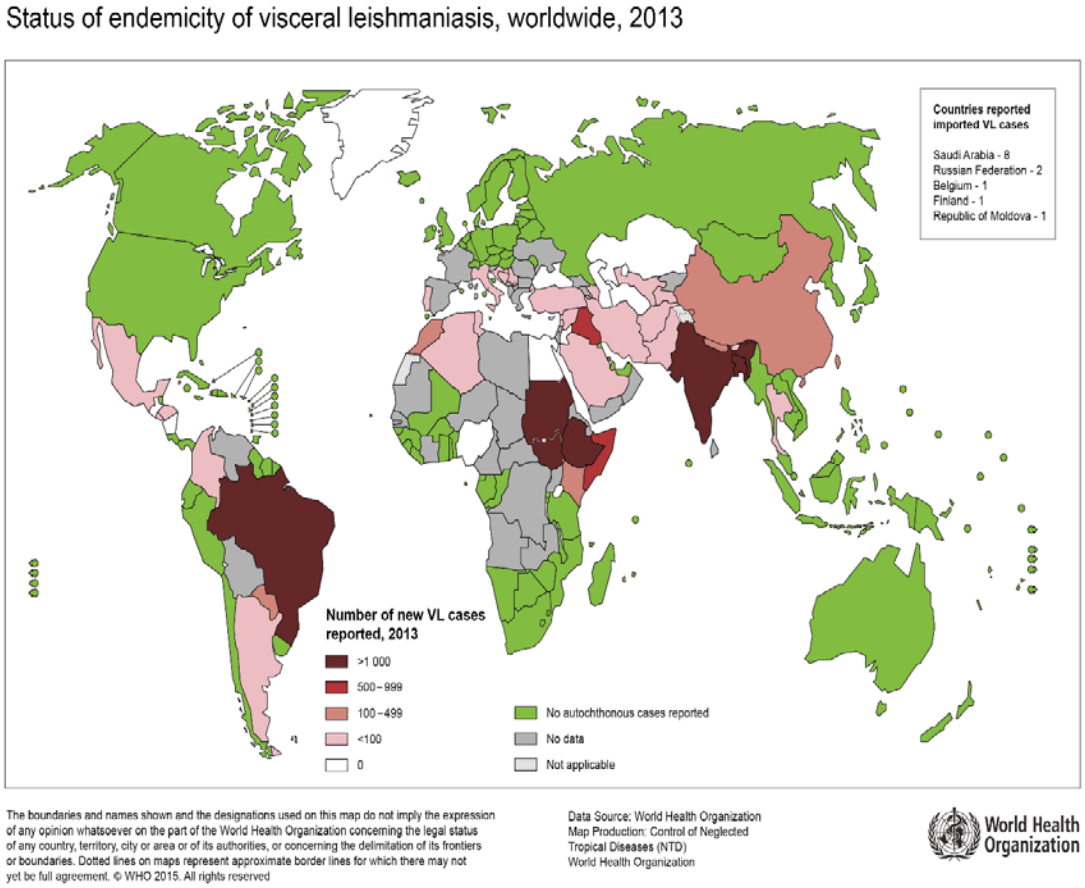

FIGURE 5: Global incidence of new Visceral Leishmaniasis cases in 2013, as estimated by the WHO[5].

1.f Microscopic and Protein-Based Molecular Diagnostics

Both malaria and leishmaniasis are currently diagnosed microscopically as a gold-standard(42,43). Similarly to clinical symptom-based diagnosis, this is done by a highly-trained health-care professional. Patients must have blood drawn in a clean environment, typically a hospital or clinic, using proper sterile technique in order to avoid exacerbating infection or causing additional ones. Care must be taken to ensure blood does not coagulate. Samples must then be processed through proper blood smearing on sterile glass, and carefully dried and stained (differently, depending on which disease is being investigated) as they are prepared into slides for microscopic evaluation(44). The microscopic evaluation itself is done by trained microscopists or doctors of pathology, who have been educated to correctly identify the particular stained parasites themselves, visually, within infected cells, as both parasites are rarely found extracellularly(42,43). Medical grade light microscopes themselves, of course, can be elaborate technologies that may cost over $1500USD(45). All of this adds significant materials and labor costs to the process. In addition, depending on the efficiency of the particular institution performing the diagnosis, obtaining and communicating the results can take several days. For patients suffering from more severe *Plasmodium falciparum m*alaria or *Leishmania donovani* visceral leishmaniasis, this delay in itself can spell a death sentence. It has already been discussed at length how both malaria and leishmaniasis are largely endemic to tropical regions of the globe, which also happen to be abundant in resource-poor LMICs.

Microscopic methods using light microscopes are ineffective at diagnosing HIV infection, as with all viruses, since the virion particles themselves are simply too small to visualize, and do not even exist in assembled virion forms for very long. Taking a cue from the body's own immune system, HIV diagnosis is therefore done using protein-based molecular diagnostics, which may also provide some limited benefits for malaria and leishmaniasis detection.

Antibody-based assessments can be done by drawing patient blood and testing for the presence of particular targeting antibodies, for example, when evaluating the success of a vaccination. Testing blood for circulating antibodies is also an indirect protein-based molecular diagnostic tool, as it often correlates well with the presence of the pathogen itself, and a diseased state. However, there is often a significant delay between the onset of infection and the production of antibodies. In cases such as HIV/AIDS, this can be very undesirable – particularly as some patients take very long to produce antibodies, or "sero-convert"(46). Not only can this delay shorten an infected patient's life expectancy, but it can also introduce viral contamination to donated blood if the routine testing is performed before sero-conversion.

Although antibody-based tests represent the earliest protein-based molecular diagnostics, and are still very effective for many diseases, they are giving way to more direct diagnostic assays in many other cases, which test for proteins produced by the pathogens themselves, using very similar methods.

Taking a cue from the immune system, alternative diagnostic methods for MIDs have been focusing on targeting proteins produced by the infectious agent. HIV is a good example of this, where alternatives such as microscopic diagnosis by light microscopy are ineffective, diagnosis by electron-microscopy would also be extremely difficult (any such diagnosis would have to catch the virus at stages in its life-cycle where virions are fully assembled, and even then they may be difficult to distinguish from other cellular components), not to mention impractically resource-draining, and antibody-based molecular diagnosis or symptom-based clinical diagnosis may come too late. For a long time, the standard for diagnosing HIV infection was a protein-based method called Enzyme-Linked Immunosorbent Assay (ELISA), wherein antibodies cloned in a laboratory setting are raised against an HIV protein produced by the cells it infects, called “p24”. One set of laboratory-raised antibodies are linked to an enzyme that produces easily-detectable results, typically a color change(47). Another set have been immobilized on a solid support. Patient blood-sample isolates are exposed to the solid support, and p24 proteins bind to the immobilized antibodies, if present. After a wash, the setup is exposed to the enzyme-linked antibodies. If any antibodies have bound, they will typically resist the wash step and still be present for the final step, wherein the enzyme's substrate is added and the reaction allowed to proceed. Areas containing the protein being sought after will then typically appear in a different color, making detection simple(47). Of course, samples must be safely drawn from patients in clinical settings, as for malaria and leishmaniasis, and the ELISA assay also necessitates a full functional laboratory for preparing isolates and properly caring for perishable biological components. As well, this test lacks significant amplification, and relies on relatively high levels of circulating HIV

p24 antigen in the blood. This means that the test is only effective, on average, within 2 months after the initial HIV infection, after which antibody-based ELISA tests are preferable(48). For reference, a schematic illustration of two commonly used general ELISA embodiments are shown in Figure 6.

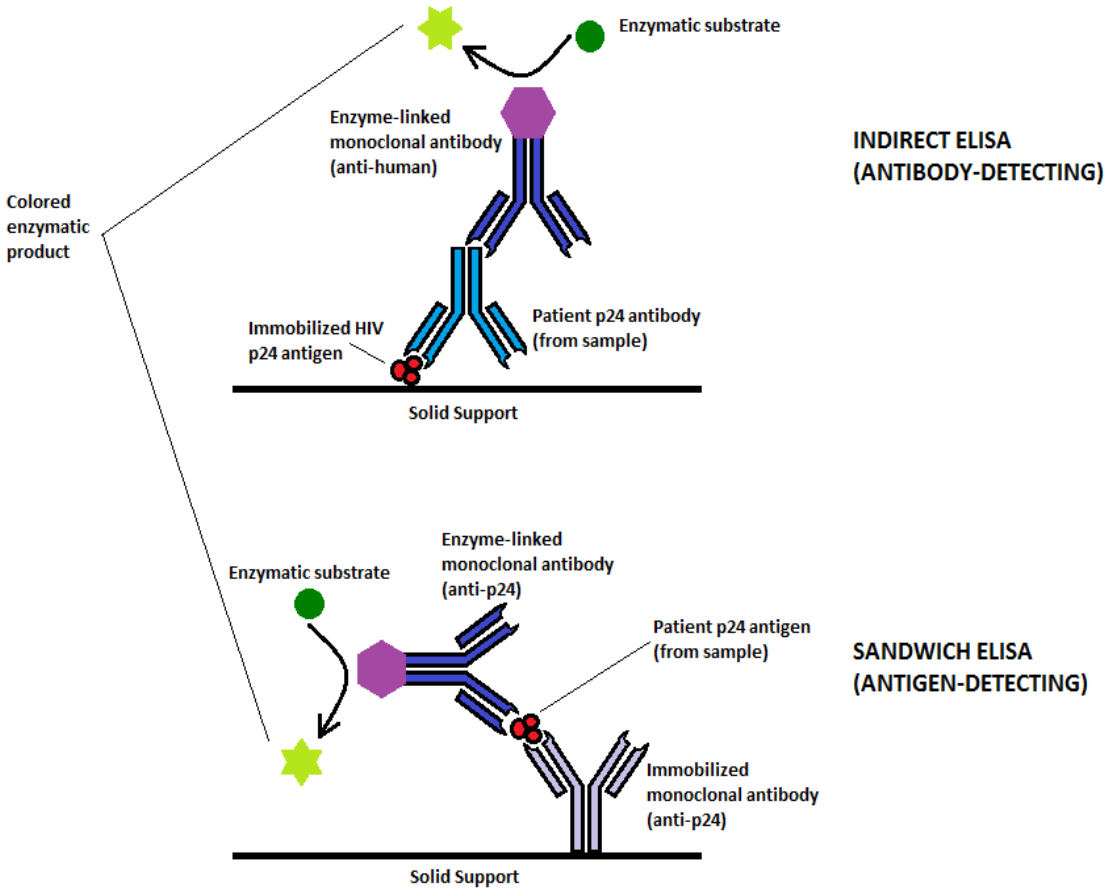

FIGURE 6: General schematic of two common ELISA embodiments. Earlier HIV testing using the top approach detected circulating antibodies against HIV's p24 protein; later methods such as the bottom approach have made it possible to test directly for the protein itself.

Protein-based diagnostic tests exist for a wide range of diseases, including some bacterial infections, but they are gaining particular momentum in the diagnosis of certain infections by eukaryotic parasites. A prime example are the Rapid Diagnostic Tests (RDTs) often used for malaria. These tests rely on detection of proteins expressed by the Plasmodium parasites as part of its normal metabolism through antibodies immobilized in a matrix. The proteins detected are not found abundantly in blood under normal conditions, as mature erythrocytes (red blood cells) do not perform many metabolic functions(49). However, some of these RDTs are limited by the potential for false-positive readings if other endogenous blood components such as Rheumatoid Factor are present in the tested sample, thus introducing ambiguities, particularly in arthritic patients(50). Some RDTs for malaria have been developed in recent years for proteins more specific to Plasmodia; however, the proteins have a tendency to persist long after an infection has been cleared(51). No malaria RDTs currently have the potential for a quantitative read-out to determine the patient's parasitic load. Many of these tests are also perishable and must be stored chilled in order to remain functional. As an indicator of proper function, many of these tests have a section for patient sample read-out, and a control section to confirm that the RDT is working properly. These tests are also limited by a 20-fold decrease in sensitivity as compared to microscopic methods, and are not widely accepted clinically(52). Typically, they are regarded as a "quick-and-dirty" first-pass methods, which require professional validation by microscopy to confirm the diagnosis, if positive. They are also one-time use tests, and while they may cost as little as $0.55USD in some cases, a new test needs to be purchased for every patient or if

confirmation is required in a single patient(53). RDTs have also been developed for Leishmaniasis, but only quite recently, and are still in the process of validation(54). There are currently no accepted alternatives to the laborious ELISA-based diagnostic tests for HIV, which require fully functional laboratories, expensive and perishable reagents that need to be stored under special conditions, and highly-trained personnel to perform the assays.

1.g Diagnosis by Nucleic-Acid-Amplification-Tests: Polymerase Chain Reaction

The other identifiable component to any pathogen, other than its unique proteins, is its nucleic acid genome that encodes them. For the majority, including bacteria, fungi, and protozoa, this genome is DNA-based; however, as in the case of HIV and many other viruses, it may be an RNA genome. Faced with the limitations of protein-based approaches to MID diagnostics, scientists have recently begun to explore diagnostic tests based on nucleic acids instead – and, indeed, some have already become the state-of-the-art gold standards for certain diseases(55). Often, multiple loci of the genome are targeted in separate assays that are later correlated, in order to increase the statistical power of the test and reduce ambiguities.

Although protein encoding can be regarded as a primary function of all nucleic acid genomes, significant portions, if not majorities, of many organisms' genomes does not actually code for proteins. Because these portions do not have a strict protein structure to

translate in order to achieve a specific function, they often have a much higher variability from species to species, compared to coding regions that may display lower variability between species, in order to preserve a crucial protein function. In contrast, we have seen how protein-based RDTs for malaria can be confounded by proteins expressed endogenously by metabolically active human cells. Differentiating between the five species of Plasmodia that can cause malaria in humans is even more difficult. The ELISA tests for HIV target a protein expressed by all HIV subtypes; however, one of the major challenges facing HIV research is its high variability, which may potentially affect protein assays(56). Nucleic acid-based diagnostics, however, can be designed to target highly variable regions of the genome, and can thus easily distinguish causative agents from the patient themselves, as well as potentially offer higher specificity between different species or subtypes of a single disease-causing agent(57).

Nucleic acid-based diagnostic tests are a recent development, and have been made possible by the advent of Polymerase Chain Reaction (PCR). HIV testing for antibodies to the p24 antigen is only effective after a lag of ~2 months, as some time is necessary for the antibody production to reach detectable levels(58). However, because many proteins are produced from a single genomic template copy, pathogenic genomes rarely reach detectable levels along with their protein counterparts and must be amplified in order to be assessed. Thus, nucleic-acid-based molecular diagnostics take the form of Nucleic-Acid-Amplification-Tests (NAATs), and have traditionally been based on PCR.
PCR was originally developed as a tool to aid molecular biologists in acquiring high copy numbers of genes or genomic regions they wished to further study. Though short

sequences of DNA can be synthesized chemically (so-called “oligonucleotides”), this process is quite unstable and non-specific after approximately 100 bases, resulting in mixtures of DNA fragments with similar but not identical sequences(59). Since most genes are considerably longer, it became necessary to employ a natural DNA Polymerase enzyme to acquire a full gene. “Taq” DNA polymerase, isolated from the bacterium *Thermus aquaticus* has become the standard for PCR, because it does not require coenzymes, additional scaffold proteins, or many cofactors(60). In addition, this enzyme, isolated from a bacterium that thrives in natural hot-springs, is highly thermostable. This not only means that it will remain in a properly folded state at room temperatures such as those found in most laboratories, but that, with an optimal functioning temperature of 72°C, scientists performing PCR can be fairly certain that nucleic acid amplification from outside contaminants in the PCR reaction tubes will be insignificant, as the vast majority of DNA polymerases operate at or below 37°C. As well, this eliminates the need for coenzymes such as helicases and topoisomerases to separate DNA strands prior to polymerization; strand separation can be achieved simply by incubating the template DNA at 95°C, without damaging the enzyme(60). Other thermostable DNA polymerases used in PCR include Pfu Polymerase, isolated from the archaeon *Pyrococcus furiosus*, and Vent Polymerase, from the archaeon *Thermococcus literalis*(61). Both Pfu and Vent are more thermostable than Taq, and also boast higher fidelity, due to a 3'->5' proofreading function that can correct any mismatched bases in the synthesized strand, in addition to their 5'->3' polymerase function, but are considerably slower to produce DNA(61).

In order to initiate DNA polymerization, all DNA polymerases require a partially double-stranded starting sequence. In most organisms, after the DNA strands have been pulled apart by helicase or topoisomerase enzymes in the target region, single-stranded mRNA fragments are recruited, which hybridize with the complementary DNA strand they were once synthesized from and form an RNA-DNA hybrid that can “prime” the DNA polymerization(62). The mRNA eventually dissociates, and the empty space is filled in later if necessary(62). In PCR, this can be accomplished using the short chemically-synthesized “oligonucleotide” sequences alluded to earlier, which can be made in a laboratory, but generally do not exceed 100 base-pairs (bp)(63). As long as the sequence of the target DNA (i.e. “template”) is known, oligonucleotide “primers” can be synthesized to hybridize specifically with the genomic region of interest. In order to balance sequence fidelity in the primers, which decreases as a function of oligonucleotide length, with specificity of hybridization to the template (since a sequence of 3bp, for example, is likely to be found in many places throughout the template), PCR primers are typically required to be 18-30bp in length(62). Their specific length, as well as their Guanosine/Cytosine vs. Adenine/Thymine content, affects the temperature at which they will hybridize most efficiently to the template DNA to prime polymerization. Typical PCR primers are designed to have target annealing temperatures of 55-65°C(62). A PCR reaction, then, becomes a cycle of three steps: “Melting” at 95°C to separate the two DNA strands, “Annealing” at 55-65°C (depending on the nature of the primers) to allow the primers to bind their targets, and “Elongation” at 72°C to allow the DNA polymerase to function(62). Each step in the cycle is allotted between 30 and 90 seconds, and the

whole cycle is repeated 30-40 times to generate amplification of the target region on the order of 10^6(62). A schematic overview of the PCR cycle is shown in Figure 7.

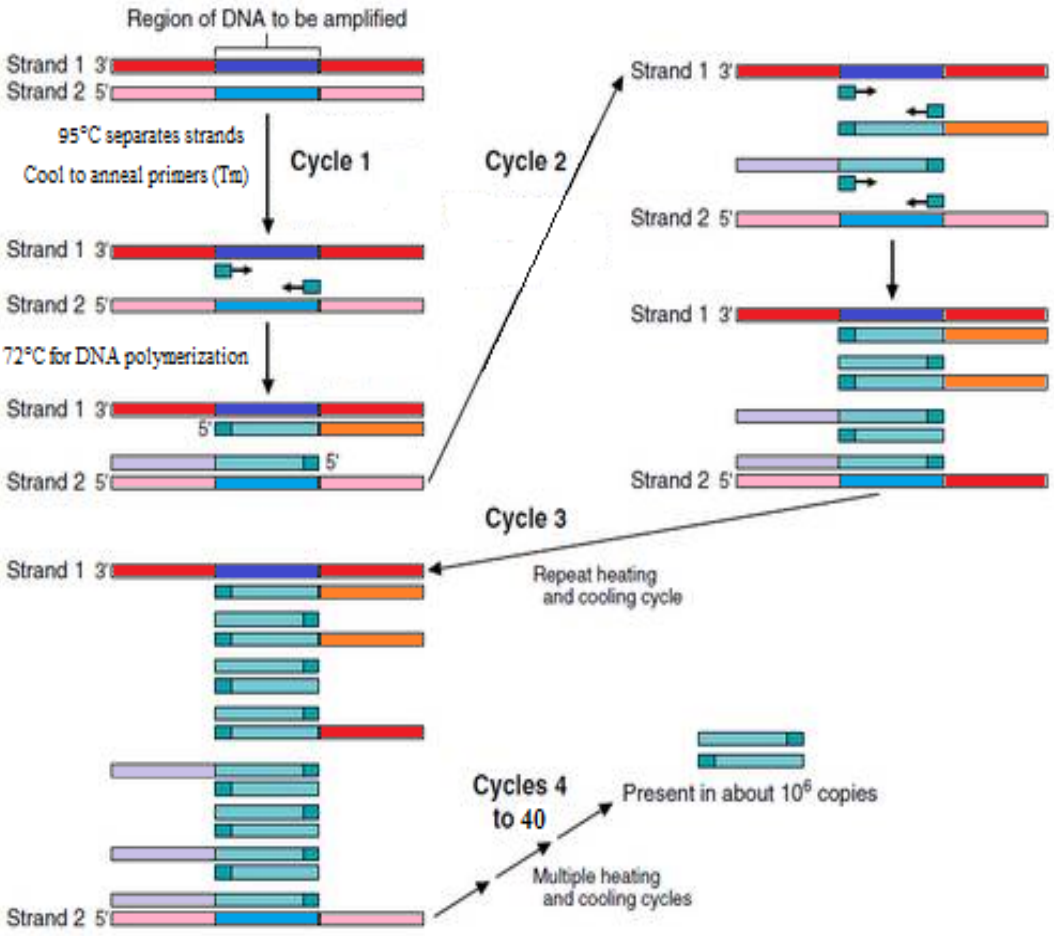

FIGURE 7: Schematic overview of the Polymerase Chain Reaction.

Early PCR was a laborious task. Three separate water baths or heat-blocks would be prepared, at 95°C, 72°C, and the primer annealing temperature, and researchers would have to be vigilant of the process for hours in order to manually transfer samples from one bath to the next(63). With the rise of microprocessors, PCR became a much more

widespread and accessible process after the invention of the so-called “PCR Machine” (also “thermal cycler”, or “thermocycler”): a computer-controlled thermal cycling device capable of rapidly changing the temperature of an aluminum block designed to hold PCR reaction tubes, through the three cycle temperatures, as well as a storing temperature of 4-12°C post-reaction, to minimize heat-catalyzed degradation of the amplified DNA(62).

The heating elements in current PCR Machines are usually Peltier Thermoelectric Coolers (PTCs). These compact pads exploit the Peltier Effect in order to pump heat in one direction, depending on the direction of electrical current flow. The Peltier Effect is a phenomenon whereby thermal energy will be pumped in one direction at a junction of two different electrical conductors, when a direct current (DC) is applied across the junction. The Peltier Effect is governed by the equation:

$\dot{Q} = (\Pi_A - \Pi_B)I$

Where $\dot{Q}$ is heat generated on the heat-rejecting side per unit time (usually Joules per second, or J/s), Π_A is the Peltier coefficient of conductor A, Π_B is the Peltier coefficient of conductor B, and I is the current in Amperes flowing across the junction(64). Peltier coefficients of the conductors are determined by their specific conductivities and thermodynamic properties. Usually, one conductor has a very high conductivity, while the other is a semiconductor. If the current flows in one direction, heat will be rejected at the side of one conductor, and it will heat up. Conversely, heat will be absorbed at the side of the other conductor, and that side will cool down. If the direction of the current is reversed, the thermal properties of the two sides will reverse as well; this effect is what allows PCR machines to cycle both above and below room temperatures during and after

a PCR reaction, respectively, using the same thermodynamic system(64). The opposite phenomenon, whereby a temperature gradient across a junction of two different conductors produces a voltage, is called the Seebeck Effect(64).

The significant separation of heat on two sides of a single compact pad of two conductors is an unstable process, and can quickly reach a maximum beyond which increasing the current through the junction may damage the materials(64). To provide greater stability, PCR Machines employ very elaborate heat-sink setups. Large aluminum blocks are located underneath the PTC, cut in narrow strips designed to maximally contact the many Peltier junctions in the coolers and conduct the flow of heat vertically, while allowing air flow to carry off unwanted heat as well. Underneath the aluminum block is a powerful fan that draws in outside ambient air. If more heat is required for the PCR experiment, the fan can draw warm ambient air up through the aluminum to be absorbed by the heat-absorbing side of the PTCs and finally rejected at the heat-rejecting side and allow the PCR reaction tubes to be heated without an excessive amount of current. Conversely, if the reaction tubes are to be cooled, the fan can be switched to dissipate heat radiating down the aluminum block from the bottoms of the PTCs, which must be operating in heat-rejecting mode. The interface between the PTCs and the aluminum heat-sink block is firmly adhered using silicone-based thermal grease, otherwise known as heat-sink-compound, which is not only designed to provide a powerful bond between the materials and an additional highly conductive surface for heat flow, but also to exclude air, which is a thermal insulator(65). A diagram of the heating and heat-sinking system found in a typical PCR Machine is shown in Figure 8.

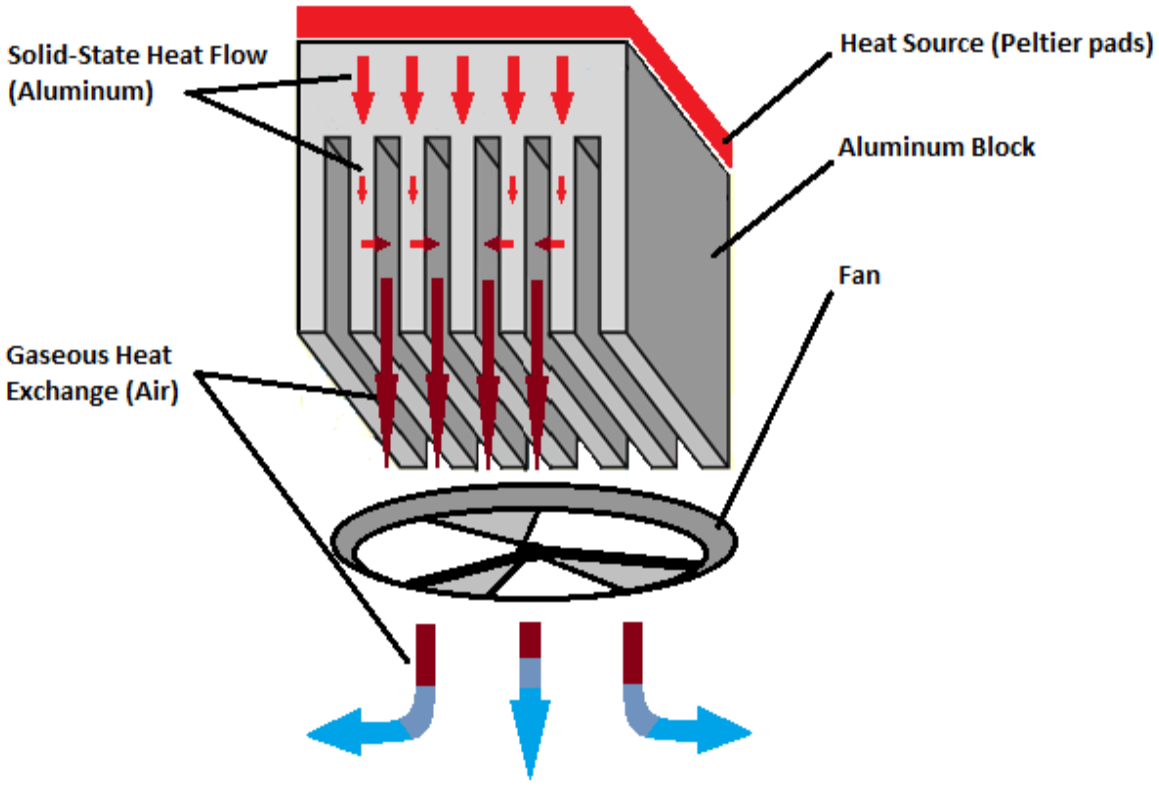

FIGURE 8: Schematic diagram of the heat-sinking apparatus and heat exchange patterns found in a typical PCR machine/thermocycler, during a cooling cycle (heat pumped away from samples).

In order to maintain function of a PCR Machine, then, several processes need to be under strict control. Firstly, if the device is to be powered by an outlet, Alternating Current (AC) from the grid must be converted to Direct Current (DC) through a system of Voltage Rectifiers. Though the Peltier Effect will certainly proceed under AC, the frequent change in direction of the current will cause the heat-absorbing and heat-rejecting sides of the PTCs to switch with such rapidity that the alternating effects will average out to a

practically indiscernible thermal change. Not only would this be ineffective for any heating/cooling application, but the strain on the PTCs would quickly damage them. The high voltages found in typical AC sources – 120V in North America and 240V in most other regions of the world – would also damage PTCs of the sizes and conductivities required in most PCR applications; thus, the second major consideration in PCR Machines is the stepping-down of source voltage to a range suitable for the PTCs in the desired temperature range. Typical PCR machine PTCs operate in the range of 2-5V DC in order to generate temperatures between 4-95°C. This DC voltage fed to the PTCs must be precisely controlled and sometimes reversed in order to achieve the full temperature range. It is therefore insufficient to have just one large step-down transformer for the voltage source, but a sophisticated array of different step-down transformers, as well as voltage rectifiers of both directions, which must all be precisely coordinated by a robust microprocessor. Finally, it isn't enough to simply control the electrical properties of this sort of device – the thermodynamic properties of heat flow must be addressed as well. The fan underneath the aluminum heat-sink is of an adjustable speed as well, and can work at various intensities to pump heat to or away from the PTCs, depending on the range in which they are operating. Temperatures closer to the ambient room temperature require milder fan speeds to dissipate thermal energy, while more extreme temperatures require rapid and intensive heat conduction. This, in turn, also requires the fan to be controllable by a range of DC voltage. It also necessitates continual monitoring of both the temperature of the working side of the PTCs, as well as the ambient temperature – and, indeed, PCR Machines are rated for operation within a certain ambient temperature range.

All of these control considerations for achieving such rapid and dramatic thermal cycling drive up the costs of PCR Machines considerably. Depending on its capacity and complexity, a PCR Machine, even previously used, can cost anywhere between $2 000-$20 000USD or more(66,67). As well, they have a very high and variable power draw, as heat generation in itself requires much power, and the computerized control system must be fed as well. This presents a very significant limitation to the application of PCR for nucleic-acid-based diagnostic tests, especially for their application to MIDs, which, as has been discussed, are more problematic in resource-limited areas.

1.h Diagnosis by Nucleic-Acid-Amplification-Tests: Loop-Mediated Isothermal Amplification

The current hardware requirements for PCR have created considerable attention for Loop-Mediated Isothermal Amplification (LAMP), a recently developed NAAT that may be able to reduce the cost of nucleic-acid-based diagnostics by over 90% compared to PCR, and be reusable for years(68).

In LAMP reactions, a DNA polymerase isolated from the bacterium *Bacillus stearothermophilus* is used to make new DNA. *B. stearothermophilus* is a thermophilic bacterium, though not quite an extremophile, as it typically grows between temperatures of 30-75°C(69).

B. stearothermophilus is interesting for its DNA polymerase, which is the chosen enzyme in LAMP reactions. *B. stearothermophilus* DNA polymerase (Bst) possesses a strong helicase activity, meaning it is capable of efficiently unwinding complementary DNA strands, and thus opening DNA for base-pairing, without the need for a denaturing step at 95°C(73). The enzyme functions optimally between 60 and 65°C. At these temperatures, it also “loads” the primers onto itself and “scans” along the template DNA for their complementary binding sites, where it allows them to hybridize with the template, and thus eliminates the need for thermal cycling to precise primer-annealing temperatures. Thus, Bst is theoretically capable of replicating DNA at a single temperature, between 60 and 65°C(74). Bst is also a robust enzyme, as far as DNA polymerases go. Most DNA polymerases operate in a sort of narrow range of tolerance with regard to buffer components, and concentrations must be carefully accounted for in order to successfully produce DNA. Indeed, even small changes in local concentrations may have pronounced effects on PCR protocols, with polymerization failing if the buffer concentrate isn't mixed thoroughly prior to being dispensed in the reaction tube. PCR is only performed using purified DNA in water or a mildly basic solution as a template, and most additional contaminants from biological sources almost always have detrimental effects on the reaction's performance. PCR-based diagnostics, as a result, cannot be performed on freshly collected “dirty” biological samples (e.g. blood, urine), and thus carry the additional costs of DNA purification which must be performed in a laboratory by highly-trained personnel and can take hours(68). In contrast, Bst is more forgiving in several aspects. It has been shown to have a much more robust tolerance of salt concentrations

than Taq, for example – a property that New England Biolabs (Boston, MA, USA) have further enhanced in their engineered “Bst2.0” recombinant enzyme, which performs similarly to Bst under normal conditions, but has a significantly higher tolerance to salts(75). Bst has also been found to perform with varying degrees of blood, urine, and fecal contaminants introduced to the reaction mixture, making it a perfect candidate for diagnostics on freshly-collected or only partially purified biological samples(76).

The problem with a typical PCR-like approach to DNA synthesis using Bst is, however, precisely the lack of cycling. Without a 95°C step to detach primers and re-open the template DNA, fully complementary primers such as those found in PCR reactions will remain tightly bound to the template DNA after Bst synthesizes the first strands. Although Bst possesses helicase activity, otherwise known as “strand-displacement” capability, and can peel away older primers to insert newer ones, this process is inefficient, and only typically used to displace a complementary DNA strand ahead of a replication fork. The development of LAMP solved this issue, in an exquisite example of biomedical engineering in molecular biology. Developed by the Eiken Chemical Company of Japan, LAMP uses a specially designed set of four primers that bind a total of six unique sequences on the template, in order to achieve continual DNA replication by allowing primers to extend into sequences that are self-complementary, and exploiting DNA's capacity to form secondary structures(74).

The procedure was first detailed by Notomi, et al, in 2000 when the technique was first described in publication(74). LAMP is first initiated by the partial binding of the

Forward-Inner-Primer (FIP) to the negative strand of the template, after Bst peels away the positive strand. FIP is a hybrid primer consisting of two separate sequences, often linked by an intermediate sequence of four thymines, which is unlikely to initiate productive binding on its own. The second FIP sequence, dubbed F2, binds its complement on the template, which is dubbed F2c, while the TTTT linker, if present, and the first sequence, dubbed F1c, remain free and unbound. On the template, the F2c sequence to which FIP is partially bound, is followed downstream by the same F1c sequence also found on FIP, before the TTTT linker. Thus, when the primer is extended and new DNA is synthesized, a new sequence called F1 is made. F1 is complementary to F1c (or rather, vice-versa, as the c stands for “complementary”), meaning it has the capacity to loop back around and bind the newly synthesized sequence – if only F1 weren't still bound to the template. To deal with this, another LAMP primer, dubbed “F3”, has been designed similarly to a PCR primer, to fully bind a sequence on the template, “F3c”, upstream of the F2c sequence where FIP initially bound. F3 then initiates a second round of DNA polymerization, which soon meets the first and displaces the nascent sequence from the template. The displaced sequence made by Bst from extension of the FIP primer allows the F1 and F1c sequences to bind each other, forming a stem-loop structure, while the FIP polymerization extends all the way to the end of the template on the other end, followed by polymerization of F3 displacing it constantly(74). The initiation of LAMP is shown schematically in Figure 9.

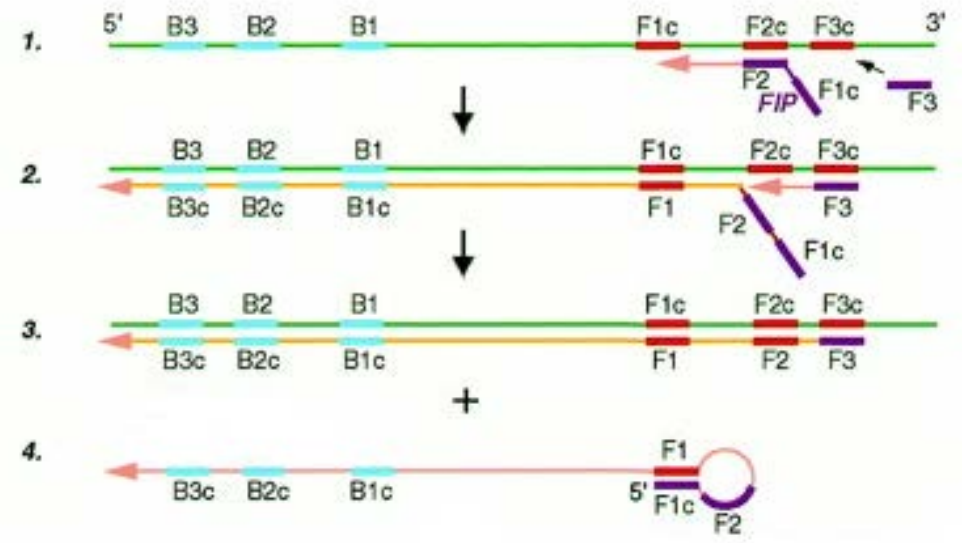

FIGURE 9: Schematic representation of the first steps in Loop-Mediated Isothermal Amplification(74)[6]. Initial polymerization from partial binding of the FIP primer is displaced by a second polymerization event from the F3 primer behind. The displacement allows the F1c sequence on the FIP primer to hybridize to its downstream complementary F1 sequence, synthesized in the first polymerization event, forming a loop.

The positive strand stem-loop strand then synthesized from FIP can serve as template for the binding of the Back-Inner-Primer (BIP) and B3 primer, as shown in Figure 10. Although at this point the reaction is already technically independent of the original template, the FIP or BIP steps can occur in reverse order to that described herein, depending on which primer Bst grabs first. Juxtaposed to the F3, F2, and F1 sequences on the positive strand of the template are the B1c, B2c, and B3c sequences on the minus strand, mirroring them after an interval. BIP contains a B2 sequence, similar to F2 on FIP,

which binds the B2c sequence and initiates another replication, which synthesizes the B1 sequence downstream. Similarly to F1 on FIP, the second part of BIP following the TTTT linker and unbound to the template, the so-called B1c, can bind the newly synthesized B1 sequence as a loop. Once again, to make this happen, a displacement is necessary, which is achieved through extension of the “B3” LAMP primer, which binds upstream of BIP and dislodges it from the template soon after it is extended itself. Because this round uses DNA made in the first round as a template, the polymerization no longer proceeds until the end of the whole template molecule, but only to the loop formed by F1 and F1c binding. Bst is capable of opening up this short double-stranded portion and replicating all the sequences at that end as well. The result of this third replication event, after the fourth replication event initiated by B3 displaces it, is a “dumbbell” DNA structure with loops on both ends(74). The formation of this structure is shown schematically in Figure 10.

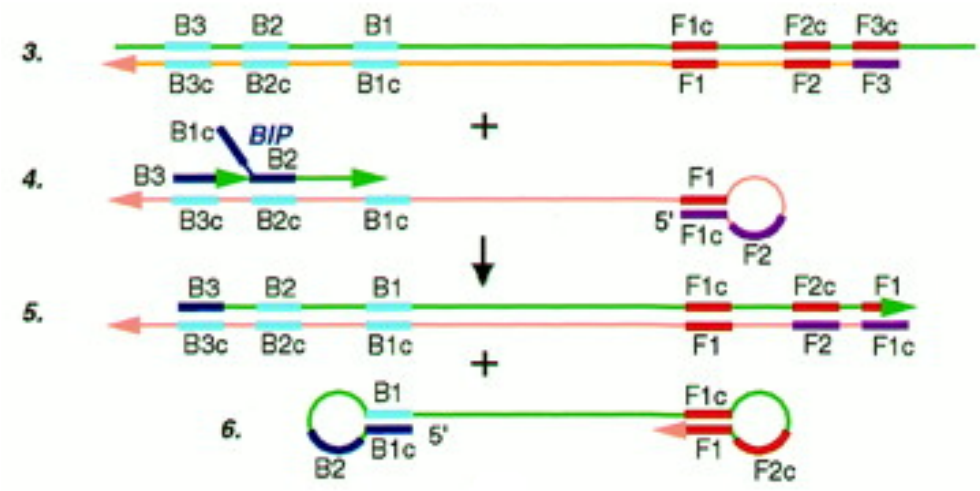

FIGURE 10: Schematic representation of the formation of the "dumbbell" intermediary template structure during Loop-Mediated Isothermal Amplification(74)[6]. After formation of the stem-loop structure during the first two polymerization events (see Figure 9), two similar polymerization events take place, using the synthesized stem-loop structure as a template, and the BIP/B3 primers. Following displacement, a structure has been formed with loops on either end, giving it a "dumbbell" shape.

The dumbbell structure then serves as the template for all further downstream polymerization events, and the reaction becomes completely independent of the original template. Due to the design of the LAMP primers, and their capacity to form partial double-stranded regions, Bst can initiate polymerization in many different spots. For example, one loop end is already a primed site for polymerization, as it contains a short double-stranded DNA portion followed by a single-stranded one. Bst's strand-displacement activity allows it to unravel these same loops on the ends, once it reaches them, so the sequences are copied again and can continue binding each other. Every time

a new loop is formed, a new Bst enzyme can swoop in to extend the double-stranded portion, and loops can be unraveled whenever they are in the way of a replication fork. Because the initiation was from a loop and not two unique bound strands, this results in a variety of interesting secondary structures, often containing multiple stem-loops all contacting each other from the same strand, affectionately dubbed “cauliflower structures”. New FIP and BIP primers also bind to the loops, most notably on the F2 and B2 sequences on the ends of the loops, to initiate more strand synthesis and even more varieties of secondary structure. The resulting DNA of LAMP cycling is thus largely non-functional for downstream applications, as it isn't made in a simple form. It may be used for molecular cloning, however, if it is subsequently treated with restriction enzymes that cut somewhere between the F and B sequences – a property that would have to be taken into account during the laborious task of LAMP primer design. For this reason, LAMP has been gaining widespread popularity as a diagnostic tool, rather than a tool purely for laboratory DNA synthesis. To further speed up LAMP cycling in some applications, additional “Loop-Primers” may be used, which bind to the short intervening sequences between F1 and F2 and between B1 and B2, on proximal regions of the loops, to serve as further starting points for LAMP cycling, though they may confound results in other ways, as will be discussed further(77). Some examples of post-dumbbell LAMP cycling are shown schematically in Figure 11a, while the positioning of Loop-Primers and more possible polymerization outcomes are shown in Figure 11b.

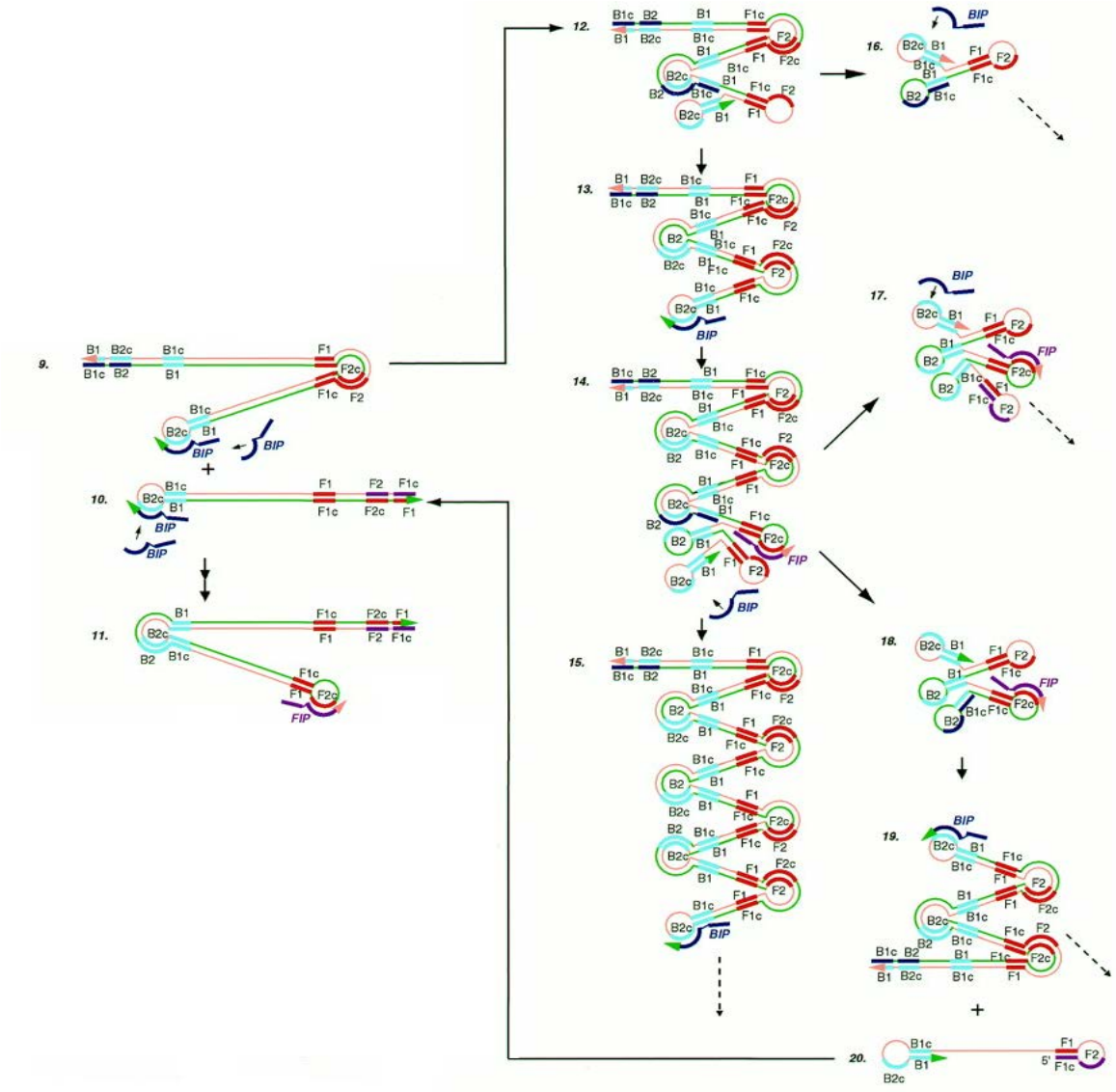

FIGURE 11a: Examples of polymerization outcomes during the final stages of Loop-Mediated Isothermal Amplification, where dashed arrows indicate potential for further polymerization events(74)[6]. New polymerization events are initiated by Bst wherever it recognizes a partially double-stranded DNA fragment, such as those formed by any loop, or through more primer binding events. The strand displacement activity of the Bst enzyme allows it to resolve secondary structures such as loops as it encounters them, and continue polymerization without being hindered.

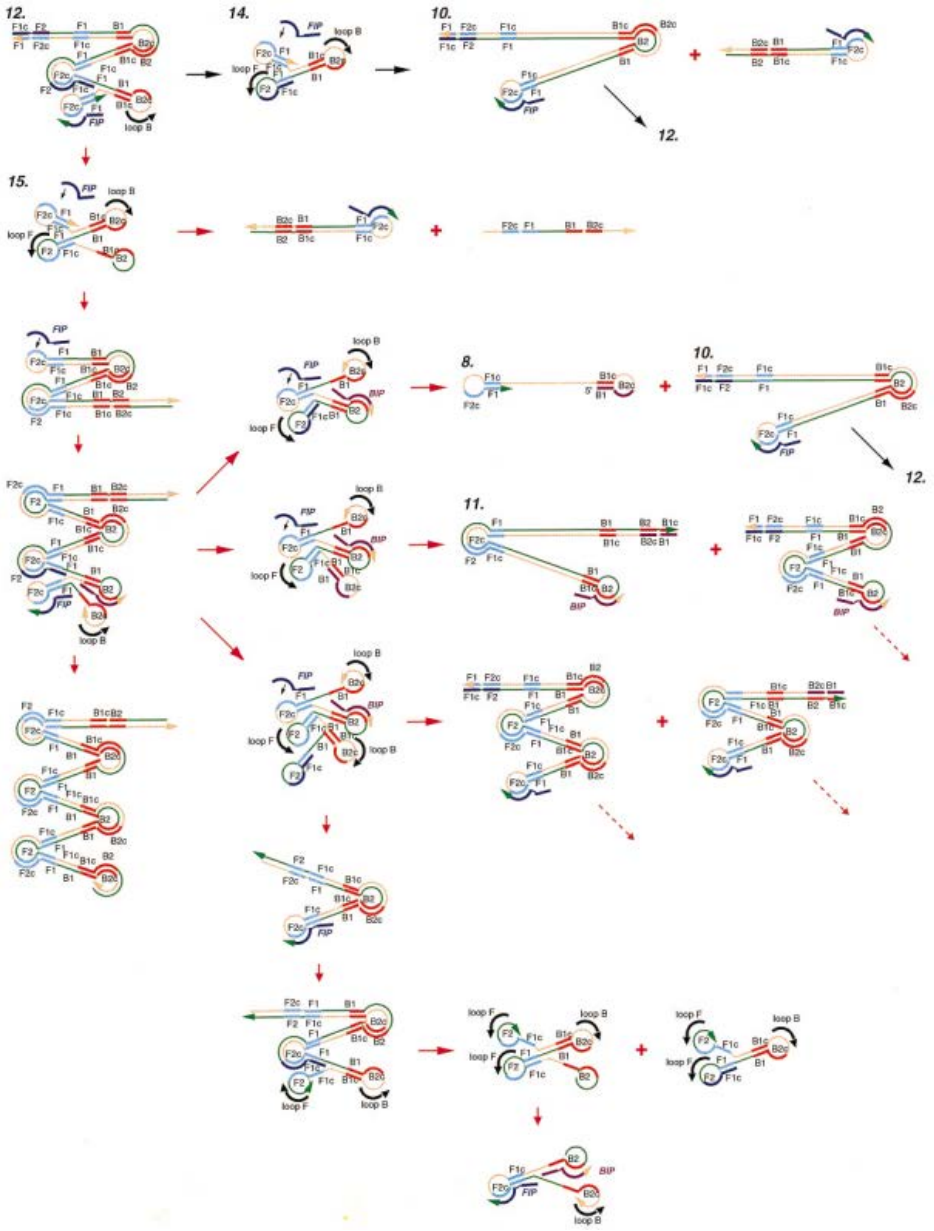

FIGURE 11b: Positioning of Loop Primers ("loop F" and "loop B") on the intermediary template structure, and more possible polymerization outcomes, during the final stages of Loop-Mediated Isothermal Amplification(77)[7]. Loop primers bind along the loops formed through the hybridization of F1/F1c and B1/B1c sequences, between F1 and F1c or B1 and B1c, in order to create more partially double-stranded starting points for Bst to initiate new polymerization events.

LAMP reaction mixtures are similar to PCR mixes, but have several differences. Firstly, while PCR reactions can be done in total volumes of 25-50μL, a 25μL reaction volume is preferred for LAMP, to promote more molecular collisions for DNA synthesis. For PCR's Taq polymerase, Tris-HCl, at a concentration of 10mM, serves to effectively mimic normal cellular membrane/lipid components that it would be surrounded with under endogenous conditions. For Bst, Tris is additionally joined by the amphiphile Polysorbate 20, which has significantly longer non-polar chains. Both reaction mixtures use potassium chloride (KCl) at 50mM as an electrolyte in the mixture; however, Bst also responds well to ammonium sulfate ($(NH_4)_2SO_4$) at low concentrations of 10mM. The sulfate ion seems to be favorable for Bst in general, as Bst prefers magnesium sulfate ($MgSO_4$) as a source of magnesium ion cofactors over the magnesium chloride ($MgCl_2$) used for Taq. Finally, a rather high 400mM supplement of betaine, or trimethylglycine, is added(74). This molecule coordinates with DNA secondary structures and stabilizes them, helping to facilitate multiple amplification loops. For comparison, a quantitative list of components in a typical PCR mixture is shown in Table I, while those for a LAMP reaction are shown in Table II.

TABLE I: Optimized (50µL) PCR reaction mixture.

CHEMICAL	**CONCENTRATION – "Standard Taq Buffer" (New England Biolabs)**	**Concentration (PCR reaction mixture)**
Tris-HCl	10mM	1mM
KCl	50mM	5mM
$MgCl_2$	1.5mM	0.15mM
$MgCl_2$	-	2mM
dNTP mixture	-	0.2mM
Forward Primer	-	0.4µM
Reverse Primer	-	0.4µM
Purified Template DNA	-	Variable by experiment
Taq polymerase (in buffered 50% glycerol solution)	-	5 units Taq; 1% glycerol

TABLE II: Optimized (25µL) LAMP reaction mixture.

CHEMICAL	**CONCENTRATION – "Isothermal Buffer" (New England Biolabs)**	**Concentration (LAMP reaction mixture)**
Tris-HCl	20mM	2mM
$(NH_4)SO_4$	10mM	1mM
KCl	50mM	5mM
$MgSO_4$	2mM	0.2mM
Polysorbate 20	0.10%	0.0025µL
$MgSO_4$	-	6.0mM
Betaine/trimethylglycine	-	400mM
Bst (in a buffered 50% glycerol solution)	-	8 units Bst; 2% glycerol
dNTP mixture	-	1.4mM
FIP (primer)	-	0.0016mM (1.6µM)
BIP (primer)	-	0.0016mM (1.6µM)
F3 (primer)	-	0.0002mM (0.2µM)
B3 (primer)	-	0.0002mM (0.2µM)
Template DNA	-	Variable by experiment

The extensive thermal cycling in PCR makes the reaction quite lengthy, with many protocols taking over 3 hours. By contrast, LAMP reactions can be completed in 45-60 minutes at Bst's optimal temperature range of 60-65°C, after which 10 minutes at 80°C can denature the enzyme so as to completely terminate any further amplification(74). This speed of amplification is also very beneficial, as it suggests the LAMP technique may be used as a bedside point-of-care technique to determine the nature of a patient's disease quickly, while they have access to medical equipment and health-care practitioners close at hand.

A final alluring feature of the LAMP reaction, is one of the byproducts it produces. As seen in Tables I and II, deoxynucleoside triphosphates (dNTPs) are used as building materials for DNA polymerization in both LAMP and PCR reactions. This is because the cleavage of two out of the three phosphate groups attached to each nucleoside releases a lot of energy that can be exploited by the DNA polymerase enzyme. The two terminal phosphates are released as an inorganic molecule of “pyrophosphate”, which carries a charge of -4, and is written as PPi^{4-}. Because of the higher concentration of magnesium ions, which carry a charge of +2, in LAMP reaction mixtures, pyrophosphate complexes with two magnesium ions, forming magnesium pyrophosphate ($Mg_2P_2O_7$)(78). Magnesium pyrophosphate is weakly soluble in water, and thus the newly formed compound precipitates from the reaction mixture. The compound absorbs light just on the edge of the visible spectrum for humans, making a successful LAMP reaction visible to a well-trained eye as slightly cloudier, or more “turbid”, and sparking possibilities for potential low-cost optical detection methods for the reaction, as well as the potential for

quantification of LAMP reactions. If quantitative measurements of precipitate can be related to starting template concentration, the LAMP technique has the potential to assess viral/parasitic loads in patients.

Previous work has exploited this precipitate formation to some degree; however, other studies have used additional reagents, such as the fluorescent DNA-binding Malachite Green, as LAMP assay reporters(79).

2. OBJECTIVES

Our group identified the LAMP technique as having the potential to bring rapid, robust, and direct nucleic-acid-based molecular diagnostics for the problematic MIDs HIV/AIDS, malaria, and leishmaniasis, to resource-limited settings such as those found in many tropical LMICs.

Although LAMP has been done by other groups for all three of our target diseases, and commercial kits exist for some of them, these LAMP-based diagnostics are not currently accepted by clinicians as offering definitive diagnoses. Our first goal, then, was to explore why the performance of LAMP is more disputed. We chose to identify published LAMP primer sets for malaria-causing *Plasmodium* species, leishmaniasis-causing *Leishmania* species, and as many subtypes of HIV as possible. We then proceeded to validate these LAMP assays in ideal laboratory conditions, to assess their efficacy for diagnosis, and determine whether we could make recommendations for an optimized standard LAMP protocol for diagnostics that could bring the assay closer to becoming clinically accepted.

Along with these validation and optimization tests, we explored the main quantifiable parameters of LAMP. We set out to investigate the lower limit of detection of the various primer sets, in terms of initial concentration of template DNA. We also developed real-time LAMP methods to quantitatively measure the reaction progress and see what

information, such as initial template DNA concentration, could be extracted after a reaction had completed.

We explored various reporting systems for the LAMP assay, to explore which methods could give robust and reliable read-outs of LAMP results, and at what cost.
Finally, our main objective was to use this information to design a portable, low-cost, low-power device for performing LAMP-based diagnostics in resource limited settings, using a self-developed optimal LAMP protocol designed to optimize the performance of the assay. This device, we decided should be versatile in terms of power consumption, to exploit a range of available energy sources in LMICs. It was also to be built using as many low-cost or recycled materials as possible, so as to be reproducible in resource-limited areas, rather than being so specialized that additional dependencies on developed nations would be created in LMICs for its import and repair. Finally, we wanted the device to interface with widely available signal processing hardware and software platforms, for similar reasons, and to be reusable for as long as possible, to keep its costs to a minimum.

The ultimate goal of this research is to bring the prototype to a LMIC setting, to assess its performance in the field and determine whether it could function as a clinical tool in resource-limited areas.

3. METHODS

3.a Validation of LAMP: Malaria, Troubleshooting

For malaria, LAMP regions were selected from the DNA encoding the 18s rRNA ribosomal subunit. This region is generally highly conserved across *Plasmodium* species, allowing for general diagnosis, but also contains several regions of higher variability between species, allowing for species-specific diagnoses as well. Since the primary objective was validation and optimization, LAMP primer sequences were taken from previous work by Han et al., and are shown in Table III(80).

TABLE III: LAMP Primers for Genus and Species-Specific *Plasmodium* Detection in 18s rRNA Region. FIP, Forward-Inner-Primer; BIP, Back-Inner-Primer; LPF, Loop-Primer-Forward; LPB, Loop-Primer-Back.

Target	Primer	Sequence (5'-3')
Plasmodium (genus)	F3	GTATCAATCGAGTTTCTGACC
	B3	CTTGTCACTACCTCTCTTCT
	FIP	TCGAACTCTAATTCCCCGTTACCTATCAGCTTTTGATGTTAGGGT
	BIP	CGGAGAGGGAGCCTGAGAAATAGAATTGGGTAATTTACGCG
	LPF	CGTCATAGCCATGTTAGGCC
	LPB	AGCTACCACATCTAAGGAAGGCAG
P. falciparum	F3	TGTAATTGGAATGATAGGAATTTA
	B3	GAAAACCTTATTTTGAACAAAGC
	FIP	AGCTGGAATTACCGCGGCTG GGTTCCTAGAGAAACAATTGG
	BIP	TGTTGCAGTTAAAACGTTCGTAGCCCAAACCAGTTTAAATGAAAC
	LPF	GCACCAGACTTGCCCT
	LPB	TTGAATATTAAAGAA
P. vivax	F3	GGAATGATGGGAATTTAAAACCT
	B3	ACGAAGTATCAGTTATGTGGAT

	FIP	CTATTGGAGCTGGAATTACCGCTCCCAAAACTCAATTGGAGG
	BIP	AATTGTTGCAGTTAAAACGCTCGTAAGCTAGAAGCGTTGCT
	LPF	GCTGCTGGCACCAGACTT
	LPB	AGTTGAATTTCAAAGAATCG
P. malariae	F3	CAAGGCCAAATTTTGGTT
	B3	CGGTTATTCTTAACGTACA
	FIP	TATTGGAGCTGGAATTACCGCGATGATGGGAATTTAAAACCT
	BIP	AATTGTTGCAGTTAAAACGCCTATGTTATAAATATACAAAGCATT
	LPF	GCCCTCCAATTGCCTTCTG
	LPB	TCGTAGTTGAATTTCAAGGAATCA
P. ovale	F3	GGAATGATGGGAATTTAAAACC
	B3	GAATGCAAAGAACAGATACGT
	FIP	TATTGGAGCTGGAATTACCGCGTTCCCAAAATTCAATTGGAGG
	BIP	GTTGCAGTTAAAACGCTCGTAGTGTATTGTCTAAGCATCTTATAGCA
	LPF	TGCTGGCACCAGACTTGC
	LPB	TGAATTTCAAAGAATCAA

All oligonucleotide primers were synthesized in the University of Calgary DNA Services Lab (AB, Canada) or by Eurofins MWG Operon Inc. (ON, Canada). The majority were done on a 50nmol scale, purified by a standard low-cost desalination procedure, which uses solvent chemistry to separate oligonucleotides from byproducts of chemical synthesis, at a cost of $10-$25 per primer. In some later experiments, FIP and BIP primers were ordered purified from agarose gel. This procedure runs the synthesized DNA in an agarose gel electrophoresis protocol, and subsequently purifies the primers from the agarose. Gel purification yields a higher purity of primers with less contamination from chemicals involved in synthesis, at an increased cost of ~$5-10 per primer. The reasons for this alternate purification will be discussed in Section 4.

Using Genbank and Basic Local Alignment Search Tool (BLAST) from the National Center for Biotechnology Information ("NCBI": MD, USA), these primer sequences were digitally mapped to the genomic template. Using this information, PCR primers were designed to amplify region containing the LAMP target sequences for genus-specific *Plasmodium* LAMP, and about 200 base-pairs (bp) upstream and downstream, dubbed the "Plasmodium LAMPflank" primers. Figure 12 shows the mapping and LAMPflank primer design for genus-specific *Plasmodium* LAMP.

P.falciparum (isolate "SF4") 18S rRNA Partial Sequence (Genbank JQ627152):

TCAAAGATTAAGCCATGCAAGTGAAAGTATATATATATTTTATATGTAGAAACTGCGAACGGCTCATTAAAACAGT
TATAGTCTACTTGACATTTTTATTATAAGGATAACTACGGAAAAGCTGTAGCTAATACTTGCTTTATTATCCTTGATT
TTTATCTTTGGATAAGTATTTGTTAGGCCTTATAAGAAAAAAGTTATTAACTTAAGGAATTATAACAAAGAA
GTAACACGTAATAAATTTATTTTATTTAGTGTGTATCAATCGAGTTTCTGACCTATCAGCTTTTGATGTT
AGGGTATTGGCCTAACATGGCTATGACGGGTAACGGGGAATTAGAGTTCGATTCCGGAGAGGGAGCCTGAGAA
ATAGCTACCACATCTAAGGAAGGCAGCAGGCGCGTAAATTACCCAATTCTAAAGAAGAGAGGTAGTG
ACAAGAAATAACAATGCAAGGCCAATTTTTGGTTTTGTAATTGGAATGGTGGGAATTTAAAACCTTCCCAGAGTA
ACAATTGGAGGGCAAGTCTGGTGCCAGCAGCCGCGGTAATTCCAGCTCCAATAGCGTATATTAAAATTGTTGCAG
TTAAAACGCTCGTAGTTGAATTTCAAAGAATCGATATTTTATTGTAACTATTCTAGGGGAACTATTTTAGCTTTTC
GCTTTAATACGCTTCCTCTATTATTATGTTCTTTAAATAACAAAGATTCTTTTTAAAATCCCCACTTTTGCTTTTGC
TTTTTGGGGATTTTGTTACTTTGAGTAAATTAGAGTGTTCAAAGCAAACAGTTAAAGCATTTACTGTGTTTGAATAC
TATAGCATGGAATAACAAAATTGAACAAGCTAAAATTTTTTGTTCTTTTTTCTTATTTTGGCTTAGTTACGATTAATA
GGAGTAGCTTGGGGACATTCGTATTCAGATGTCAGAGGTGAAATTCTTAGATTTTCTGGAGACGAACAACTGCGA
AAGCATTTGTCTAAAATACTTCCATTAATCAAGAACGAAAGTTAAGGGAGTGAAGACGATCAGATACCGTCGTAAT
CTTAACCATAAACTATGCCGACTAGGTGTTGGATGAAAGTGTTAAAAATAAAAGTCATCTTTCGAGGTGACTTTTA
GATTGCTTCCTTCAGTACCTTATGAGAAATCAAAGTCTTTGGGTTCTGGGGCGAGTATTCGCGCAAGCGAGAAAGT
TAAAAGAATTGACGGAAGGGCACCACCAGGCGTGGAGCTTGCGGCTTAATTTGACTCAACACGGGGAAACTCACT
AGTTTAAGACAAGAGTAGGATTGACAGATTAATAGCTCTTTCTTGATTTCTTGGATGGTGATGCATGGCCGTTTTTA
GTTCGTGAATATGATTTGTCTGGTTAATTCCGATAACGAACGAGATCTTAACCTGCTAATTAGCGGCGAGTACACT
ATATTCTTATTTGAAATTGAACATAGGTAACTATACATTTATTCAGTAATCAAATTAGGATATTTTTATTAAAATATC
CTTTTCCCTGTTCTACTAATAATTTGTTTTTTACTCTATTTCTCTCTTCTTTTAAGAATGTACTTGCTTGATTGAAAAGC
TTCTTAGAGGAACATTGTGTGTCTAACACAAGGAAGTTTAAGGCAACAACAGGTCTGTGATGTCCTTAGATGAACT
AGGCTGCACGCGTGCTACAATGATATATATAACGAGTTTTTAAAAATATGCTTATATTTGTATCTTTGATGCTTATAT
TTTGCATACTTTTCCTCCGCCGAAAGGCGTA

ALL SEQUENCES BELOW WRITTEN 5'->3':

GTATCAATCGAGTTTCTGACC = Plasmodium F3 LAMP primer;
CTTGTCACTACCTCTCTTCT = Plasmodium B3 LAMP primer
(AGAAGAGAGGTAGTGACAAG = complementary binding sequence on positive strand);
TCGAACTCTAATTCCCCGTTACCTATCAGCTTTTGATGTTAGGGT = Plasmodium FIP LAMP primer (dark purple indicates template-binding portion);
CGGAGAGGGAGCCTGAGAAATAGAATTGGGTAATTTACGCG = Plasmodium BIP LAMP primer
(CGCGTAAATTACCCAATTCTATTTCTCAGGCTCCCTCTCCG = complementary binding sequence on positive strand/purple indicates template-binding portion)

ATCTTTGGATAAGTATTTGTTAGGC = Plasmodium LAMPflank-F primer (PCR) for template region
AGCGTATTAAAGCGAAAAGC = Plasmodium LAMPflank-R primer (PCR) for template region
(GCTTTTCGCTTTAATACGCT = complementary binding sequence on positive strand)

FIGURE 12: Mapping of *Plasmodium* LAMP primers to genomic template region and design of "Plasmodium LAMPflank" PCR primers for downstream applications.

After successful PCR of Plasmodium LAMPflank sequence from *P. falciparum* genomic DNA, it was ligated using T4 DNA Ligase (Promega, Inc.: WI, USA) into a plasmid containing the amp^R selection gene (pGEM T-Easy from Promega, Inc.: WI, USA) for bacterial expression in *Escherichia coli* strain DH10β ("Top10"; Invitrogen, Inc.: CA, USA). Following heat-shock transformation, 20μL cell samples were spread onto Lysogeny Broth (LB) Agar doped with 100μg/mL ampicillin, at 37°C overnight. As this protocol ensures that colonies are formed overnight from individual cells, colonies with little genetic variability were then selected and streaked onto new ampicillin-doped LB-Agar plates, as well as grown overnight in 2mL liquid LB cultures doped with 100μg/mL ampicillin, at 37°C. Plasmid DNA was purified form overnight cultures (Miniprep Plasmid Purification Kit; Sigma-Aldrich: MO, USA), and the purified DNA screened for presence of the correct sequence by Restriction Assay and 1% agarose gel electrophoresis using SYBR Green stain (SafeView™; Applied Biological Materials, Inc.: BC, Canada). Colonies expressing the constructed LAMPflank plasmids were then re-selected from streaked LB-Agar plates and regrown overnight in 5mL of ampicillin-doped liquid LB. Plasmid DNA subsequently purified from these 5mL cultures was then used as template for downstream LAMP experiments. LAMPflank PCR primers were also used in later experiments to carry out PCR experiments in parallel with LAMP, as a basis for comparison. Similar methods were used to prepare a "Falciparum LAMPflank" PCR fragment, which was simply confirmed to be successful using agarose gel electrophoresis and used as template in downstream LAMP experiments, without cloning, for reasons that will become apparent in Section 4. Unfortunately, due to funding restrictions, genomic DNA containing species-specific LAMP target regions for *P. vivax*, *P. malariae*,

and *P. ovale* could not be obtained, so validation of LAMP primer specificity was simply done between genus-specific *Plasmodium* primers and *P. falciparum* primers.

LAMP reactions were carried out in the same 0.5mL plastic tubes used for PCR reactions, which have little DNA-binding properties. 25μL LAMP reaction mixtures were prepared as described in Table II, with the remaining volume made up using DNase and RNAse-free molecular grade distilled water. Reaction mixtures were prepared in a separate clean-room facility detached from the main lab, with additional desktop clean-air chambers specifically for PCR applications (AirClean 6000; AirClean Inc.: CA, USA) that use High Efficiency Particle Arrestance (HEPA) filtration to minimize sample contamination. Template DNA was strictly excluded from this room, and was added to the reaction tubes in the main laboratory, in a second desktop clean-air chamber (AirClean 6000; AirClean Inc.: CA, USA). Bst polymerase used was “Bst2.0”, an engineered recombinant protein from New England Biolabs (MA, USA) with all the functionality of Bst and an improved tolerance to impurities, particularly higher salt concentrations. LAMP assays using LAMPflank plasmid DNA templates were initially carried out using a protocol of 5 minute incubation of LAMP mixtures lacking the Bst enzyme, at 95°C, to separate template DNA strands, followed by addition of Bst and incubation at 65°C for 60 minutes of polymerization, and a final 10 minute incubation at 80°C to denature the enzyme and terminate the reaction. This initial 95°C step has been described to improve LAMP efficacy in some previous work(81). Subsequent experiments without the initial 95°C denaturing step showed that there wasn't an appreciable difference in successful versus unsuccessful LAMPs with and without this

step ($p<0.05$, $n=30$) for our applications, and it was dropped from the incubation protocol. All incubations were done in a conventional PCR Thermocycler (Bio-Rad T100™; Bio-Rad, Inc.: CA, USA). LAMP reactions were then analyzed through agarose gel electrophoresis. Agarose gel electrophoresis allows for the separation of DNA fragments based on size, by forcing them to migrate through the pores of the gel toward a positive cathode, since the phosphate backbone of DNA makes the molecule quite negatively charged. The sizes of these pores can be manipulated by the concentration of the gel, with fragments ≥1kb generally run on a 1% agarose gel, and smaller fragments run on a 2% agarose gel. LAMP fragments proved to be tricky immediately, as it was first hypothesized that the extended contactomers of stem-loop structures would increase the total sizes of LAMP products to a range more appropriate for 1% gels, although the LAMP regions themselves were often <100bp. Subsequent experiments, however, showed that secondary contactomers do detach significantly from one another producing fragments of varying small lengths, and protocols were adjusted to 2% agarose gels. Electrophoresis was carried out with a voltage gradient of 100V and running time of 70 minutes. DNA within the gels was visualized using SYBR Green fluorescent DNA-binding dye (“SafeView”; ABV Inc.: BC, Canada) and was imaged using a VersaDoc 1D Imaging chamber (Bio-Rad, Inc.: CA, USA).

Being our first LAMP validation, we used the malaria assays as a basis for trouble-shooting the LAMP technique, and experimenting with various small variations in the protocol, so as to attempt recommendations for the protocol's optimization. Many different alternatives were tried, as the assay proved to be quite difficult to reproduce, and

these minute variations would be exhaustive and largely irrelevant to fully detail herein; however, final conclusions as to optimal methods for LAMP-based diagnostic tests will be expounded in Section 4.

3.b Validation of LAMP: HIV, Optics

Previous work has developed a technique for direct detection of retroviral virions such as HIV using the reverse-transcriptase enzyme, dubbed “RT-LAMP”. This method, however, increases the cost of the process with additional perishable reagents, and necessitates additional reverse-transcriptase protocols prior to LAMP, involving some thermocycling(82). To keep the cost of our assay and device to a minimum, we chose to do classical LAMP on DNA templates for HIV, and thus test for the integrated provirus rather than infectious virion particles themselves.

Once again, with the focus being on validation rather than the complex task of *de novo* LAMP primer design, we identified two previously published primer sets to perform our experiments with. The first set targets the genes encoding HIV's p24 antigen, from work published by Curtis, et al.(83). As has been discussed, this is the protein antigen that can be tested for with ELISA-based early protein diagnostics, as it is one of the earliest detectable HIV antigens in circulation, before sero-conversion. Thus, the region was selected as one that would have a nice correlation to current clinical testing, as a solid

basis for comparison. The second primer set targets HIV's integrase gene, from work by Zhao, et al.(84). Genetic variation is a very important consideration in any nucleic-acid-based test for viral pathogens, as viral polymerases are often extremely error-prone, and mutation rates are generally much higher than those found in eukaryotic parasites such as *Plasmodium* and *Leishmania.* The integrase region was chosen because a properly functioning integrase enzyme is absolutely crucial to the virus' proliferation, and thus there is minimal genetic variability in this gene across HIV subtypes(84). With this primer set, we hoped to provide a maximally robust HIV test that would be reliable for many different subtypes of HIV-1 across many different regions, whereas it is possible that p24 tests may need to be optimized and updated for different regions, as well as every few years. The two primer sets are detailed in Table IV.

TABLE IV: LAMP Primers for Clinically-Correlated and Robust HIV Provirus Detection from P24 and Integrase Genes. FIP, Forward-Inner-Primer; BIP, Back-Inner-Primer; LPF, Loop-Primer-Forward; LPB, Loop-Primer-Back.

Target	Primer	Sequence (5'-3')
Integrase (Robust)	F3	ATGGAATAGATAAGGCCCAA
	B3	CTTTTCCTTCTAAATGTGTACAATC
	FIP	AGGTGGCAGGTTAAAATCACTAGTTTTGATGAACATGAGAAATATCAC AGT
	BIP	GCAAAAGAAATAGTAGCCAGCTGTTTTTACTACAGTCTACTTGTCCATG
	LPF	AGAGACTGAAAACCTGTTTGGC
	LPB	AAATGGCTGACATCCTACATGAC
P24 (Clinically-Correlated)	F3	ATTATCAGAAGGAGCCACC
	B3	CATCCTATTTGTTCCTGAAGG
	FIP	CAGCTTCCTCATTGATGGTTTCTTTTTAACACCATGCTAAACACAGT
	BIP	TGTTGCACCAGGCCAGATAATTTTGTACTGGTAGTTCCTGCTATG
	LPF	TTTAACATTTGCATGGCTGCTTGAT
	LPB	GAGATCCAAGGGGAAGTGA

Similarly to the case in *Plasmodium*, these primers were digitally mapped onto the HIV genome so as to gain a solid grasp of the process, and conventional PCR primers were designed to amplify a region flanking the LAMP area for downstream template use, as well as for correlative experiments using PCR amplification. HIV tests focused primarily on the integrase-targeting primer sets; their mapping and PCR primer design of “HIVint LAMPflank” primers is detailed in Figure 13.

HIV clone pNL4-3, subclone 4.20 (Genbank: U26942) – integrase region only:

GGGCAAGGCCAATGGACATATCAAATTTATCAAGAGCCATTTAGAAATCTGAAAACAGGAAAGTATGCAAGAATG
AAGGGTG**CCCACACTAATGATGTGAAAC**AATTAACAGAGGCAGTACAAAAAATAGCCACAGAAAGCATAG
TAATATGGGGAAAGACTCCTAAATTTAAATTACCCATACAAAAGGAAACATGGGAAGCATGGTGGACAGAGTATT
GGCAAGCCACCTGGATTCCTGAGTGGGAGTTTGTCAATACCCCTCCCTTAGTGAAGTTATGGTACCAGTTAGAGAA
AGAACCCATAATAGGAGCAGAAACTTTCTATGTAGATGGGGCAGCCAATAGGGAAACTAAATTAGGAAAAGCAG
GATATGTAACTGACAGAGGAAGACAAAAAGTTGTCCCCCTAACGGACACAACAAATCAGAAGACTGAGTTACAAG
CAATTCATCTAGCTTTGCAGGATTCGGGATTAGAAGTAAACATAGTGACAGACTCACAATATGCATTGGGAATCAT
TCAAGCACAACCAGATAAGAGTGAATCAGAGTTAGTCAGTCAAATAATAGAGCAGTTAATAAAAAAGGAAAAAGT
CTACCTGGCATGGGTACCAGCACACAAAGGAATTGGAGGAAATGAACAAGTAGATAAATTGGTCAGTGCTGGAA
TCAGGAAAGTACTATTTTTAG**ATGGAATAGATAAGGCCCAAGATGAACATGAGAAATATCACAGT**A
ATTGGAGAGCAATGGCTAGTGATTTTAACCTACCACCTGTAGTAGCAAAAGAAATAGTAGCCAGCTGTGATAAAT
GTCAGCTAAAAGGGGAAGCCATG**CATGGACAAGTAGACTGTAG**CCCAGGAATATGGCAGCTA**GATTGTA**
CACATTTAGAAGGAAAAGTTATCTTGGTGGCAGTTCATGTAGCCAGTGGATATATAGAAGCAGAAGTAATT
CCAGCAGAGACAGGGCAAGAAACAGCATACTTCCTCTTAAAATTAGCAGGAAGATGGCCAGTAAAAACAGTACAT
ACAGACAATGGCAGCAATTTCACCAGTACTACAGTTAAGGCCGCCTGTTGGTGGGCGGGAATCAAGCAGGAATTT
GGCATTCCCTACAATCCCCAAAGTCAAGGAGTAATAGAATCTATGAATAAAGAATTAAAGAAAATTATAGGACAG
GTAAGAGATCAGGCTGAACATCTTAAGACAGCAGTACAAATGGCAGTATTCATCCACAATTTTAAAAGAAAAGGG
GGGATTGGGGGGTACAGTGCAGGGGAAAGAATAGTAGACATAATAGCAACAGACATACAAACTAAAGAATTACA
AAAACAAATTACAAAAATTCAAAATTTTCGGGTTTATTACAGGGACAGCAGAGATCCAGTTTGGAAAGGACCAGC
AAAGCTCCTCTGGAAAGGTGAAGGGGCAGTAGTAATACAAGATAATAGTGACATAAAAGTAGTGCCAAGAAGAA
AAGCAAAGATCATCAGGGATTATGGAAAACAGATGGCAGGTGATGATTGTGTGGCAAGTAGACAGGATGAGGAT
TAACACATGGAAAAGATTAGTAAAACACCATATGTATATTTCAAGGAAAGCTAAGGACTGGTTTTATAGACATCAC
TATGAAAGTACTAATCCAAAAATAAGTTCAGAAGTACACATCCCACTAGGGGATGCTAAATTAGTAATAACAACAT
ATTGGGGTCTG**CATACAGGAGAAAGAGACTGG**CATTTGGGTCAGGGAGTCTCCATAGAATGGAGGAAAA
AGAGATATAGCACACAAGTAGACCCTGAC

ALL SEQUENCES BELOW WRITTEN 5'->3':

ATGGAATAGATAAGGCCCAA = HIV Integrase F3 LAMP primer;
CTTTTCCTTCTAAATGTGTACAATC = HIV integrase B3 LAMP primer
(GATTGTACACATTTAGAAGGAAAAG = complementary binding sequence on positive strand);
AGGTGGCAGGTTAAAATCACTAGTTTTGATGAACATGAGAAATATCACAGT = HIV integrase FIP LAMP primer (dark purple indicates template-binding portion);
GCAAAAGAAATAGTAGCCAGCTGTTTTTACTACAGTCTACTTGTCCATG = HIV integrase BIP LAMP primer
(CATGGACAAGTAGACTGTAGTAAAAACAGCTGGCTACTATTTCTTTTGC = complementary binding sequence on positive strand/purple indicates template-binding portion)

CCCACACTAATGATGTGAAAC = HIVint LAMPflank-F primer (PCR) for template region
CCAGTCTCTTTCTCCTGTATG = HIVint LAMPflank-R primer (PCR) for Template region
(CATACAGGAGAAAGAGACTGG = complementary binding sequence on positive strand)

FIGURE 13: Mapping of HIV Integrase (Robust) LAMP primers to genomic template region and design of "HIVint LAMPflank" PCR primers for downstream applications.

For HIV LAMP tests, it was decided to use PCR-amplified template regions only, rather than perform molecular cloning and plasmid purification as in *Plasmodium*, for reasons that will be discussed in Section 4. An engineered *E.coli* DH10β strain, constructed in earlier research and containing the full HIV genome of strain pNL4-3, subclone 4.20, within a pUC19 plasmid alongside the amp^R selection gene, was revived from glycerol stocks and grown on an ampicillin-doped LB-Agar plate. This strain was taken to be a representative strain for North American HIV; its genome is available from Genbank at the Accession Number U26942.1. Colonies from this plate were selected and grown overnight in 2mL liquid LB cultures doped with 100μg/mL ampicillin, at 37°C, as well as streaked onto ampicillin-doped LB-Agar plates and grown overnight at 37°C for re-selection later. Plasmid DNA was purified from overnight cultures (Miniprep Plasmid Purification Kit; Sigma-Aldrich: MO, USA), and the purified DNA screened for presence of the correct sequence by 1% agarose gel electrophoresis using SYBR Green stain (SafeView™; Applied Biological Materials, Inc.: BC, Canada), where size of bands correlated with a DNA molecular ruler ("1kb DNA Ladder" from New England Biolabs: MA, USA) was used to indicate appropriate plasmid, since it was considered highly unlikely that an insert of the large size of the HIV genome could be incorporated from other sources. Colonies positive for the HIV genome insert were re-selected from streak plates and used as template for HIVint LAMPflank PCR. Successful PCR was confirmed through another round of 1% agarose gel electrophoresis using the same protocol, and size correlation as a responding variable to indicate success. Confirmed HIVint LAMPflank PCR samples were analyzed spectrophotometrically using a Nanodrop 1000 spectrophotometer (Thermo Scientific: DE, USA) to quantify the DNA concentration.

These PCR samples were then used for downstream LAMP experiments, including evaluation of the LAMP method's lower limit of detection, which was done by preparing tenfold serial dilutions of the quantified PCR samples.

Finally, HIV LAMPs were also evaluated spectrophotometrically, based on the magnesium pyrophosphate precipitate. Absorbance values were measured in the visible and near-UV spectra of light using 2μL post-reaction aliquots in a Nanodrop 1000 spectrophotometer (Thermo Scientific: DE, USA), and were correlated with 2% agarose gel electrophoresis results to evaluate the potential for low-cost optical readouts of LAMP reactions.

3.c Validation of LAMP: Leishmaniasis, Real-Time, Quantification

For Leishmaniasis, we elected not to pursue extensive species-specific LAMP, as the condition is cause by over 20 species of *Leishmania*. We instead chose a genus-specific set of primers based, as in our *Plasmodium* primers, on the highly conserved 18s rRNA region. This served our purposes for our validation of the LAMP approach in this application and for our proof of concept. However, we also identified and ordered LAMP primers specific to the kinetoplast minicircle DNA region of *Leishmania donovani*, as this species typically has the worst prognosis and is often the one responsible for Visceral Leishmaniasis. Primer sets were found from previous work by Nzelu, et al. and Takagi, et al.(79,85). Both primer sets are detailed in Table V. For this last validation, we purposely

chose primer sets that excluded the loop primers, which as has been discussed are not strictly necessary for the reaction, for reasons that will be expounded upon in Section 4.

TABLE V: LAMP Primers for Genus-specific Leishmania Detection from 18S rRNA Gene, and Species-Specific Detection of *Leishmania* donovani. FIP, Forward-Inner-Primer; BIP, Back-Inner-Primer.

Target	**Primer Name**	**Sequence (5'-3')**
Genus (*Leishmania*)	F3	GGGTGTTCTCCACTCCAGA
	B3	CCATGGCAGTCCACTACAC
	FIP	TACTGCCAGTGAAGGCATTGGTGGCAACCATCGTCGTGAG
	BIP	TGCGAAAGCCGGCTTGTTCCCATCACCAGCTGATAGGGC
Leishmania donovani	F3	GAAAAATGGGTGCAGAAATCC
	B3	CAAGCCAGGTCCAAAACC
	FIP	TACACCAACCCCCAGTTTCCCAAAAAATAGCCAAAAATGCCA
	BIP	GCTCGGACGTGTGTGGATATCCATACAAGTACAACCCACTC

LAMP tests for leishmaniasis focused primarily on the genus-specific *Leishmania* primer set, which was digitally mapped to the organism's genome similarly to mapping done for *Plasmodium* and HIV, before flanking PCR primers dubbed “Leish18S LAMPflank” were designed for downstream template applications and PCR correlation. The mapping and design is shown in Figure 14.

Leishmania donovani 18S rRNA Gene (Genbank: GQ332356.1) – minus strand:

ACTTGTCGCACAGCTCCATAATCTCCAATAGACCTTTAAAACCAACAAAAGCCGAAACGGTAGCCTAGAGGCTGCT
CCTTTGTTATCCCATGCTTTCTAATTCAAGTCAAATGACTGCTTTAGTCACGCTTCTTTAGTCACAGTAAAAAATCAC
GGACGCCCCCTGGCATGCATGACATGCGTAAATCAGGAAAGGAACCACTCCCGTGTTTCTTGTTTCTTTGAATGTT
CACGGGCTGCAAGGGCCTGGGTCACCAAATCCGACATGGACGGGACG**ACCAGGAACAAACCTGCACA**GCC
CACAGTTCAACTACGAACCCTTTAACAGCAACAGCATTAATATACGCTTTTGGAGCTGGAATTACCGCGGGTGCTG
GCACCAGACTTGTCCTCCAATTGTTACTCGATATTGGATGGGTTTAAATATCCCCCATTGAAATGACAATCCAAATG
GACTGACAACTCTATTTCTTTTCGCTGCCTCATCGTTTTGTTTTGACATTGGGCAATTTGCGCGCCTGCTGCCCTCCG
TAGAAGTGGTAGCTATTTCTCAGGCTCCCTCTCCGGAATCGAACCCTAATCCCCCGCTCCCGTCAACG**CCATGGC**
AGTCCACTACACGG**CCATCACCAGCTGATAGGGC**AGTTGTTCGTCAAAAGACGCCGGAACAAGCCGGCT
TTCGCACGGAATGAATTGAGTCAACACTGCTGGGTGTTACTGCCAGTGAAGGCATTGGTTTTACTGTCATTCATTC
GCTGGGCGT**CTCACGACGATGGTTGCC**CACCG**TCTGGAGTGGAGAACACCC**GGTTGGTTCATGTATTA
GCTTGGCGTTTCGCCAAGTTATCCAATTTTGCGGAAACCGCAAGATTTTTGCGGCAGATTACGTCTGATGTAATGA
GCCATGCGCAGATTCCTGCAAATGCAGTGATTCTGAGGCATGCATGGCTAAGTCCTTGAAACAAGCATATGACTAC
TGGCAGAATCAACCAGATCTCAATTGTGTGACAACGTGAGTCGTGTGTGTGTGCGCCACGTGCGTCCTAAAAGGA
GA**AACGTAAGCACACAACACGC**GCACATTGCGCATTGATGATCAGTGTTGTATTTTGTTGTATTTTTCGTGA
ATTGCATCTGTAGGAGCTGCGCGCATGTTACTATAAAAAATATGTCACACACAGCAGCAGCAGCACATCTGACAAC
TCAGCTTTTTGGGTGGTAACAAAACAAACGCATATATACATACACATGGTGTGTGGTGTATATGTGTACACGCGGC
TTGGTTGTTGACCTCTTGTTTGGCTGAAATTCCTCGAAATGCAGCAACAATCAAGTTCTGTTTCTGGTTCAACCGAG
TTTCCGCTGCAAACGTGTAGACACGGCAGCACACACAAAACATGTTCTGCACG

ALL SEQUENCES BELOW WRITTEN 5'->3':

GGGTGTTCTCCACTCCAGA = Leishmania 18S rRNA F3 LAMP primer
(**TCTGGAGTGGAGAACACCC** = complementary binding sequence on minus strand);
CCATGGCAGTCCACTACAC = Leishmania 18S rRNA B3 LAMP primer;
TACTGCCAGTGAAGGCATTGGTGGCAACCATCGTCGTGAG = Leishmania 18S rRNA FIP LAMP primer
(**CTCACGACGATGGTTGCC**ACCAATGCCTTCACTGGCAGTA = complementary binding sequence on minus strand/dark purple indicates template-binding portion)
TGCGAAAGCCGGCTTGTTCCCATCACCAGCTGATAGGGC = Leishmania 18S rRNA BIP LAMP primer (dark purple indicates template-binding portion);

GCGTGTTGTGTGCTTACGTT = Leish18S rRNA LAMPflank-F primer (PCR) for template region;
(**AACGTAAGCACACAACACGC** = complementary binding sequence on minus strand)
ACCAGGAACAAACCTGCACA = Leish18S rRNA LAMPflank-R primer (PCR) for template region

FIGURE 14: Mapping of Leishmania 18S rRNA (genus-specific) LAMP primers to genomic template region (*L. donovani*) and design of "Leish18S LAMPflank" PCR primers for downstream applications.

For leishmaniasis tests, an additional focus on the potential for quantitative LAMP was introduced. Visualization of LAMP results by 2% agarose gel electrophoresis was gradually phased out for reasons that will be detailed in Section 4, and reactions were performed primarily in a “CFX96 Touch™ Real-Time PCR Detection System/C1000 Touch™ Thermal Cycler” real-time PCR system (Bio-Rad, Inc.: CA, USA). 6.5µL of water in the standard LAMP reaction mixture shown in Table II was replaced with a 1/50 000 dilution of SYBR Green dye (Invitrogen: CA, USA). SYBR Green is a fluorescent dye that binds to double-stranded DNA molecules, whereupon its fluorescence properties increase in intensity by ten-thousandfold. It is commonly used in real-time and quantitative PCR protocols to evaluate DNA amplification as the reaction proceeds, when visualization of total DNA concentration is a goal. Though we are not aware of any previous work using SYBR Green in LAMP applications to monitor the reaction in real-time, the principle is simple and easily-translated, and thus our group developed a “real-time LAMP” protocol for monitoring the amplification as it occurred. The real-time PCR machine was programmed in 30 second intervals, with 30 seconds of simple incubation at 65°C followed by 30 seconds of 65°C incubation accompanied by fluorescence detection. These cycles were repeated 60 times initially, to give a one hour incubation as in previous experiments, but the protocol was later shortened to a total 45 minutes (45 cycles) for reasons that will be discussed in Section 4. As this machine uses an overhead optics system to excite the SYBR Green fluorophore within the mixtures and detect its emitted fluorescence, experiments were initially performed in 96-well micro-plates, with each well resembling an open 0.5mL PCR tube. An optically transparent adhesive covering was used over the micro-plate in lieu of PCR tube lids, to facilitate optical detection in

the device. Later on, different styles of PCR tubes with lids were also experimented with, for reasons that will become apparent in Section 4. The device gives an output of fluorescence traces in “Relative Fluorescence Units” (rfu) compared to a threshold detection level based on initial conditions, the values of which can be directly correlated to the amount of DNA present within each sample tube.

3.d Design of a Low-Cost Device for LAMP-based Diagnostics in Resource-Limited Settings

After validation of LAMP in our three target diseases, our next aim was to set about designing a platform for carrying out LAMP reactions that could be implemented in LMICs and resource-limited settings. Such areas have limited, intermittent, or non-existent access to a stable electrical power grid, so the consideration of whether the device would need to be powered electrically was one of the first major considerations. Though there have been recent initiatives aimed at designing electricity-free LAMP devices, which we found very innovative and intriguing, we eventually chose to pursue a solid-state electrical device, for reasons that will be discussed in Section 5.

With this approach in mind, the first and most crucial part of the device was the heating of samples. Heat is unfortunately a relatively high power goal, electrically speaking, so we were challenged to see whether the feat could be accomplished in a battery-powered

device. Indeed, it is difficult to find an example of a battery-powered product for generating heat that can operate for very long. However, with the relatively quick reaction time of LAMP, 45-60 minutes, we hypothesized that a suitable rechargeable battery could be obtained for at least one reaction before it would need to be recharged. With regard to power requirements, we also strove to be as versatile as possible, in order to exploit whatever available resources in our challenging target settings. With a rechargeable battery as power supply, we have an extremely versatile platform to work with. In the simplest embodiment, we can use an appropriate voltage rectifier and current regulator to recharge the battery from outlet power, in between diagnostic runs to rural/resource-limited settings.Similarly, recharging of the battery could be done by drawing current from a 12V automobile battery. Other embodiments could include solar panels, small wind turbines, or manually-powered dynamo cranks to recharge the device's battery. Of course, we would also ideally like to retain the options of powering the device using 120 or 240V AC power, depending on the region, from a grid source as well, when available, without adding too many additional costs to the device's circuitry.

In order to keep the power requirements low, efficient heat transfer is a necessity. We decided that the most ideal course of action would be to use the aluminum heat-blocks from a Thermocycler/PCR machine, as these are designed in precisely cut wells to hold the 0.5mL plastic reaction tubes used in PCR (and LAMP) with maximum surface are contact, to transfer the most heat possible while dissipating very little.
Of course, unwanted heat transfer to other parts of the device, and heat escape out into the ambient environment would have to be addressed as well. Several ideas were

formulated based on the heat-sink methods used in PCR Thermocyclers (see Background) and also on insulating methods used in heat-generating laboratory devices; however, it was decided that this issue would be addressed at the time of device testing, when we would attempt to solve it the most minimally-invasive and cost-effective way.

Finally, we wanted to design a device with an output as well. In order to keep costs down for LMIC applications, we decided to work as much as possible strictly with the precipitate formation from successful LAMPs, which had been extensively evaluated in both HIV and leishmaniasis validation assays, without adding additional fluorescent reagents. We decided, moreover, to attempt to integrate the output with one or more reaction chambers as well, in order to have the potential for real-time reaction monitoring if possible. A general schematic was designed, shown in Figure 15, in which a well of the aluminum heating block for the reaction tubes could be minimally modified to allow a small beam of light to pass horizontally through the reaction tube.

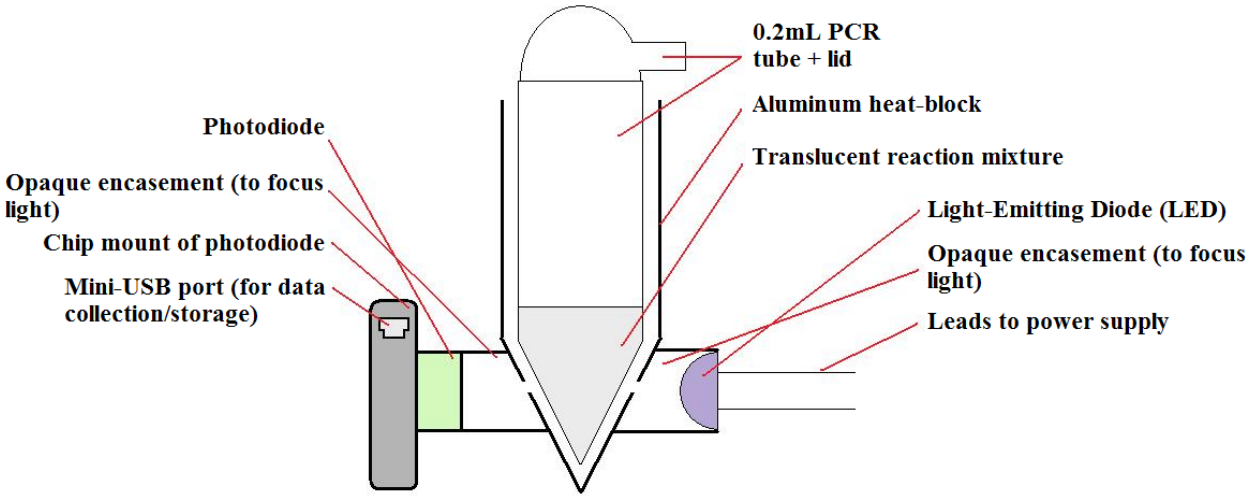

FIGURE 15: Cross-sectional schematic diagram of an optical detection/real-time monitoring system for Loop-Mediated Isothermal Amplification reactions.

By positioning this chosen LED on one side of the modified reaction well with the horizontal opening, and a photodiode capable of absorbing the LED's output light and converting it to a noticeable change in either current or voltage, we reasoned that we would be able to determine whether the reaction took place, as well as potentially measure its progress in real-time. A precipitate formation would theoretically absorb the LED's light efficiently, attenuating much of it, resulting in less photons striking the juxtaposed photodiode, and thus a lower current or voltage reading as an output.

Although having an integrated device with a unique user-interface is attractive, we eventually decided against pursuing this. In the age of smart-phones and abundant portable computers, it is easier than ever to integrate many user interfaces on one mobile device, with the capability of communicating with many forms of hardware. As their costs continue to fall, smart-phones are becoming more and more popular as the preferred

method of communication in LMICs, where the land-line generation has almost been skipped entirely. Many initiatives are currently focusing on integrating much needed health-care tools with widely available smart-phones. By making the LAMP device interface with standard mobile computing platforms, and by potentially using a free open-source software for image/signal processing from the device's photodiode, we further eliminate instrumentation costs for display hardware and custom-programmed user interface software.

3.e Construction of a Low-Cost Device for LAMP-based Diagnostics in Resource-Limited Settings: Heat-Transfer

As mentioned, it was important to the desired application of this project to build a device incurring minimal cost, and built from as many recycled materials as possible, so as to make it maximally translatable to LMIC settings, where locals could replicate the process in a straightforward and cost-effective manner.

An old and malfunctioning PCR thermocycler (Applied Biosystems® GeneAmp® PCR System 9700 from Life Technologies, Inc.: CA, USA) was obtained, and its four 4cm x 6cm Peltier heating pads were tested for function. As we were unable to gain access to manufacturers' specifications specific to only the device's pads, this proved to be a more laborious task than anticipated and ended up permanently damaging two of the pads

before it was found that a high current (~4A) DC voltage of 1.5-10V was their operating range.

The first power-supplying embodiment that was chosen to be built was the simplest: outlet/grid AC power. A power supply was extracted from an old and malfunctioning Dell computer and tested for function. The supply was capable of delivering power at a constant voltage of either 5.0 or 3.3V, as well as exploiting both 120V and 240V outlet sources, which is crucial to any application outside of North America. As this power supply employs a fan to prevent overheating (and other Dell computer power supplies were readily available...), it was left running in an overnight test to investigate how long it could operate. When it was found that the unit was only mildly warmed after >12 hours of continual operation, it was hypothesized that the fan was only minimally necessary if the power unit was taken out of the metal-filled enclosed plastic shell of the computer, where stagnant heat could indeed build up quickly to dangerous levels. Thus, the heating apparatus of the prototype was initially assembled such that the fan could be doubly exploited in a similar manner to the fan used for the heat-sink function in the PCR thermocycler, so that power requirements could be kept to a minimum. The two functional Peltier pads were removed from the broken PCR machine, along with the aluminum heat-transfer block with wells for holding 0.2mL PCR tubes situated above them, and the large aluminum block underneath them, used for heat-sink purposes. The PCR machine's fan underneath the heat-sink was discarded. Both aluminum blocks were cut in half, since only two of the Peltier pads were to be used in the LAMP prototype, which would still allow the prototype to perform 48 simultaneous reactions. Noting that the heat-absorbing side of the Peltier pads was facing the heat-sink block, and that the

power supply's fan was designed to reject heat built up within the unit and radiate it outward, the power unit was initially positioned underneath the heat-sink block, with the fan pointing upward toward the pads on top of it. It was thought that this exchange could benefit not only the pads, but the power unit as well, by recycling its radiated heat for the heat-absorbing faces of the pads, so that it could be transferred to the heat-rejecting side and help heat the reaction tubes on the other face. A schematic of the assembly is shown in Figure 16.

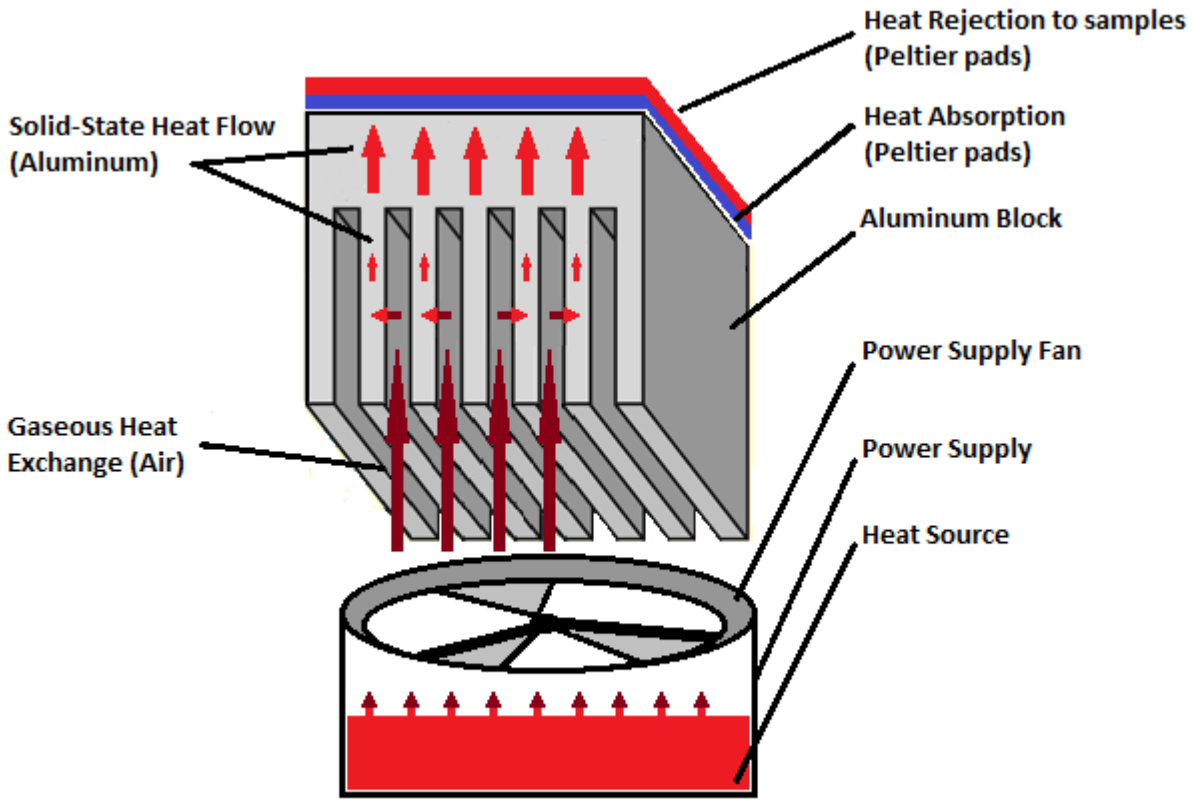

FIGURE 16: Schematic diagram of initial heat-exchange system for LAMP prototype.

Unfortunately, it was found that this arrangement added a lot of time to the heat-transfer process, and resulted in inconsistent and non-linear heating of samples. This is likely due to a two-stage heating process that took place, with the solid top of the aluminum heat-sink block being heated first by the Peltier pads, followed by heating of the thinner aluminum strips underneath, and the air interspersed between them. Around the same time, a typical laboratory ceramic hot-plate was also dissected in order to investigate what use it could be to the project. Its thermodynamic assembly is to an extent fundamentally opposite to that of the PCR machine, with the underside of its nichrome heating pad packed with fiberglass insulation, in order to *prevent* any heat transfer in the opposite direction. The assembly holding this amorphous insulation in a stable compacted state was somewhat elaborate and deemed extraneous, but the insulating principle was adopted for the prototype. Fiberglass was clearly chosen for the hot-plate because its nichrome pads heated on both sides, and thus there was a risk of igniting any flammable insulator underneath. However, noting that the underlying insulator would contact only the cold heat-absorbing faces of the Peltier pads in the prototype and thus there would be no risk of ignition, several new options became available. Taking a cue from insulating sleeves for coffee cups, it was decided that a corrugated cardboard insulator would perhaps suffice, as its interplay of fibrous mesh and pockets of air allow it to have insulating properties comparable to those of fiberglass, at a minute fraction of the cost. This alternative insulating design was experimented with, and found to be very favorable for rapid heating in the prototype. Thus, the assembly was reworked such that the heat-sink was discarded, and the Peltier pads were re-positioned away from the power supply's

fan, on a rectangular platform of corrugated cardboard further insulated by a pocket of air underneath.

At this point, the maximum temperature of the device was, however, still too high for the LAMP reaction. It was found that by reducing the voltage of the DC power supply to the device, the temperature could be dropped. The relationship between the voltage supplied to the pads, at the same current, was quantified and a drop in voltage that would lower the temperature to the optimal 65°C was estimated. Applying Ohm's Law – $V = I*R$, where V is voltage in Volts (V), I is current in Amperes (A), and R is resistance in Ohms (Ω) – the resistance necessary to achieve this drop was calculated. It was found to be an extremely low resistance that would typically be quite cheap to produce, for most low-power applications in which it would be required. However, the high power draw of the circuit complicated matters further, as it was found through power calculation using the formula $P = I^2R$, where P is power in Watts (W) and the other conventions are as previous described, that the resistor would have to have a power rating significantly higher than what would be typical for resistors of this resistance range. Appropriate low-ohmage high-power resistors were eventually found and purchased; however, these resistors were designed for printed-circuit-board applications, where they would be machine-mounted. Being awkward to solder into the device's circuitry, and having access only to low-power solder which risked softening under the heat that was dissipated by these resistors, the resistors were eventually discarded in favor of an even more cost-effective approach using simple copper wiring. It was found that 22awg stranded copper wire could certainly take the power of the circuit without melting, and that the necessary resistance could be

achieved with 21', or 6.4m. The wire was coiled in a spool attached to the device away from the aluminum block, so that the heat dissipated in the wire would not affect the sample heating, and the heat-transferring component to the prototype was completed. A full quantitative disclosure of the various heat-transfer embodiments tried for the prototype, and their corresponding thermodynamic effects, both with respect to maximum temperature and the time taken to reach this maximum, will follow in Section 4.

Finally, after notes were made as to the final power requirements of the device, an alternative power source was selected and purchased. It was important to the intended device application to have a rechargeable battery alternative, which could be later adapted to draw power for recharging from a variety of energy sources. The Ampere-hours (Ah) of the battery was also an important consideration, as the high current draw excluded many more readily-available commercial battery packs. A Nickel-Metal-Hydride battery pack was settled on, “HR-DF3” from FDK America, Inc. (CA, USA), with a voltage of 3.6V (in practice, likely 3.3V to the circuit after losses within the cells), and a capacity of 6.5Ah, which would allow for one full one-hour LAMP reaction and would hopefully sustain at least a dozen more reactions after recharging, conservatively assuming a drop in capacity of 0.1Ah per recharge cycle. It is rechargeable in 1.7 hours with a DC current of 5A. The dimensions of the pack are 3.4cm x 6.0cm, and it weighs less than 0.2kg, making it extremely portable, and able to be housed in the same container as the Dell power supply. It is the second most costly component of the prototype, at $73.10CAD, though this cost is quite low given that most of the device was assembled using recycled materials, and it is rechargeable. Full technical specifications are available in the

component's data-sheet, in Appendix I, along with the data-sheets for the optical components of the device. The circuitry of the device was left so that it could be disconnected at crucial junctions and re-attached from the Dell power supply to this battery, though this was not attempted in practice, due to a lack of infrastructure for its recharge.

3.f Construction of a Low-Cost Device for LAMP-based Diagnostics in Resource-Limited Settings: Optics

Finally, an optical component was integrated into the device in order to allow for the detection of diagnostic results, as well as for potential monitoring of the reactions in real-time, to determine viral/parasitic load. It was decided that a Light Emitting Diode (LED) would serve as a light source, as these are inexpensive and robust, with long life-spans and low power requirements. An LED with a peak emission of 405nm, to correlate with the wavelengths absorbed by the magnesium pyrophosphate precipitate byproduct of LAMP reactions, was eventually selected and purchased, model “SSL-LXTO46UV2C” from Lumex, Inc. (IL, USA), as it was less costly than other Ultraviolet-emitting LEDs of shorter wavelengths within the range of magnesium pyrophosphate's absorbance spectrum. As the prototype's Dell AC power supply has more than one 3.3V outlet, it was not necessary to redesign the heat-transfer circuitry to account for this new load. Since the photodetector system also relied on its own separate circuitry, as will be discussed

shortly, it was not necessary to factor it into any power considerations when wiring the LED. A data-sheet detailing technical specifications of the LED is available in Appendix I. A circuit diagram of the final home-built prototype circuitry is shown in Figure 17, including a hypothesized circuit for the conversion of rectification of 120V AC current to 3.3V DC current within the computer power supply.

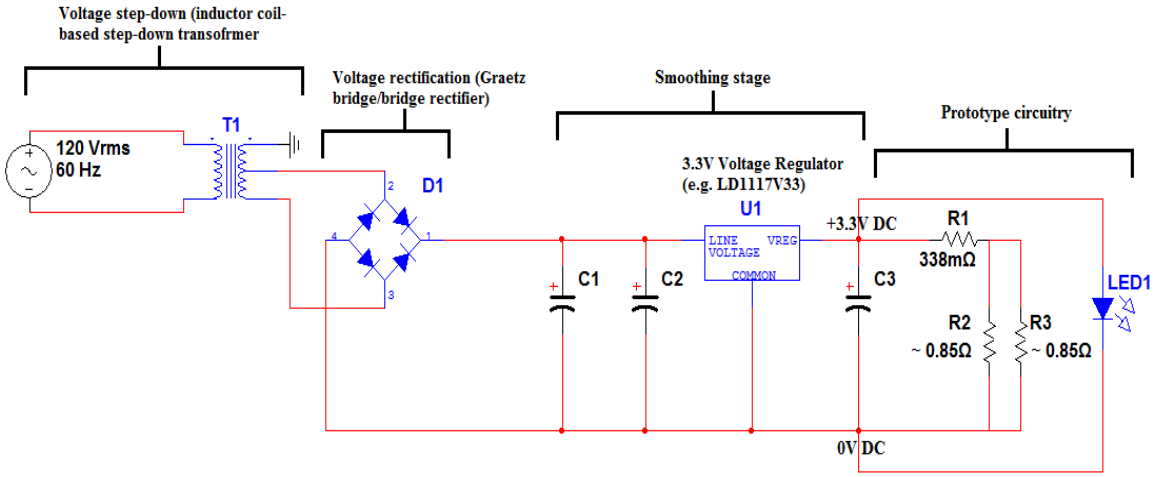

FIGURE 17: Circuit diagram of prototype circuitry, including hypothesized circuitry of the power supply. T1, step-down voltage transformer 110V AC to 3.3V DC; D1, Graetz bridge for AC to DC conversion; C1/C2/C3, smoothing capacitors on the order of 0.1µF capacitance; R1, 21’ coil of wire; R2/R3, Peltier heating pads; LED1, 405nm.

Next, two holes, approximately 0.3cm in diameter were drilled horizontally through one corner well of the aluminum block designed to house and heat the reaction tubes. The holes were located toward the bottom of the well, with its center approximately 0.6cm up from the very bottom, where the resulting opening would be sure to pass light through the liquid samples within the reaction tubes. The LED was positioned adjacent to one hole,

facing inward to shine into the well, and affixed in place using an opaque epoxy putty so as to minimize light scattering. The other hole opened to the outer edge of the aluminum block, being drilled through a corner well.

It was decided that a *de novo* instrumentation system for the light signal would be undesirable, as there would be many components to engineer and the end result would be a highly specialized proprietary system for obtaining results. We wanted our device to interface as seamlessly as possible with other instrumentation infrastructure, in either computer or smart-phone-based systems, so as to be more accessible. Thus, it was decided that detection could be done by an already assembled camera apparatus. This would eliminate the need to investigate the light signal's dynamics in order to determine what sort of analog amplification and/or filtration of the signal might be appropriate, analog-to-digital conversion of the signal would come implemented in such a way as to maximize information retention while rejecting noise, and the signal's output would already be engineered so as to interface with a digital user-interface program.

The camera selected in the end was model “UI-1222LE-M-GL” from 1stVision, Inc. (MA, USA); a data-sheet detailing its full technical specifications is available in Appendix I. It is a core-component camera on a single printed-circuit-board, without a shutter or casing, for industrial applications such as integration with the optics of other devices. It is assembled around a Complementary Metal-Oxide Semiconductor (CMOS) photodiode array called model “MT9V032” from Aptina Imaging/ON Semiconductor, Inc. (AZ, USA), which contains an integrated circuit with built in amplification for every individual photodiode. Briefly, a CMOS image sensor was selected because its digital

logic functions use low power Metal-Oxide-Semiconductor Field-Effect Transistors (MOSFETs). In contrast to regular transistors, MOSFETs can be activated by extremely low currents (<1mA), yet deliver much higher currents to a load (>10A), provided there is a substantial voltage (>3V) to draw on(86). They generally draw very low currents, as they are composed of two circuits containing complementary p-n-p and n-p-n transistors, which means that one circuit branch will always be off when the other is on. As the UI-1222LE-M-GL camera model contains a mini-USB output port for both data acquisition and powering of the device through its interface with a USB-enabled microprocessor (e.g. computer, smart-phone, tablet), and this same power source is not needed for the higher-power heat-transfer components of the device, this was not seen as a problematic energy draw that might exhaust the microprocessor and harm data acquisition. In practice, this MOSFET-based integration of signal amplification with digital logic functions not only simplifies the overall circuitry, but allows for detection of very low levels of light. We felt that this would be best for the device, as we were unsure how much the LED would need to be dimmed in order to provide a measurable contrast between positive and negative LAMP samples. Although CMOS sensors generally produce lower-resolution images than their Charge-Coupled Device (CCD) image-capturing counterparts, which are actually the typical standard used in most medical applications, our particular application necessitates only a simple distinguishing of light intensity, and the substantially lower cost of CMOS sensors plus their much lower power consumption tipped the scale heavily in their favor when we selected our components. In addition, as CMOS image sensors have become the standard in digital cameras and phone cameras, this allows for more readily available sources of parts that are designed to interface with more microprocessor

platforms; a CCD image sensor would almost certainly require a uniquely engineered proprietary software for interfacing with the user.

Although this camera component of our prototype proved to be by far the most costly, the principle of using a CMOS image sensor for this device opens up a wealth of possibilities for the recycling of old digital cameras and smart-phones, as long as their CMOS photodiode arrays are in-tact. Due to time constraints on this project, we chose to purchase a brand new camera; however, with some knowledge of electrical instrumentation design, a CMOS sensor from any discarded source could be engineered to output with a mini-USB port, and interface with a plethora of available image-processing software. The software we chose for our prototype, for example, is an open-source program available for free download online called μEye, from Imaging Development Systems (IDS), GmbH (Obersulm, Germany; https://en.ids-imaging.com/download-ueye.html), a major worldwide manufacturer of CMOS-based cameras. The software interfaces with all current and many previous IDS cameras using USB, USB2.0, and USB3.0 ports.

A square plastic mount for the UI-1222LE-M-GL's circuit board was 3D-printed such that it could fit against the aluminum heat-block containing LAMP reaction tubes, on the corner. It was designed to cover the outer edges of the 0.3mm hole in the side of the well, and channel the light onto the photodiode array, allowing for efficient light capture with minimal scattering and loss of light. It was affixed in place using opaque epoxy putty, and the camera was mounted to it with screws, so that it could be dismounted if needed. The

prototype was tested with various positive and negative LAMP samples, and it was found that light from the LED shone through the sample tube and was successfully detected by the photodetector and the μEye software on two different laptop computers, as a bright circle with a slight cut-off on the bottom right-hand side (owing to a small misalignment of the hole in the well relative to the sensor), for 100% of samples tested (n=10).

Finally, the prototype was encased in a custom-built acrylic shell. This component was also excessively costly, but we decided on this durable transparent shell for the purposes of showcasing the device in an academic setting, where the various components could be pointed out by the researchers. This also reduced any risk of damage due to any electrical fire that might take place. This risk was not negligible, as the prototype's circuitry was not permanently fixed in place in order to preserve the possibility of switching it to battery power without having to purchase new components, and loose connections occasionally produced small sparks. Owing to the considerable drop in weight that would accompany a switch from the AC power supply to battery power, however, and assuming a new permanently fixed and insulated circuitry system, the device could theoretically be housed in a typical shoe-box.

A labeled photograph of the final assembled prototype is shown in Figure 18.

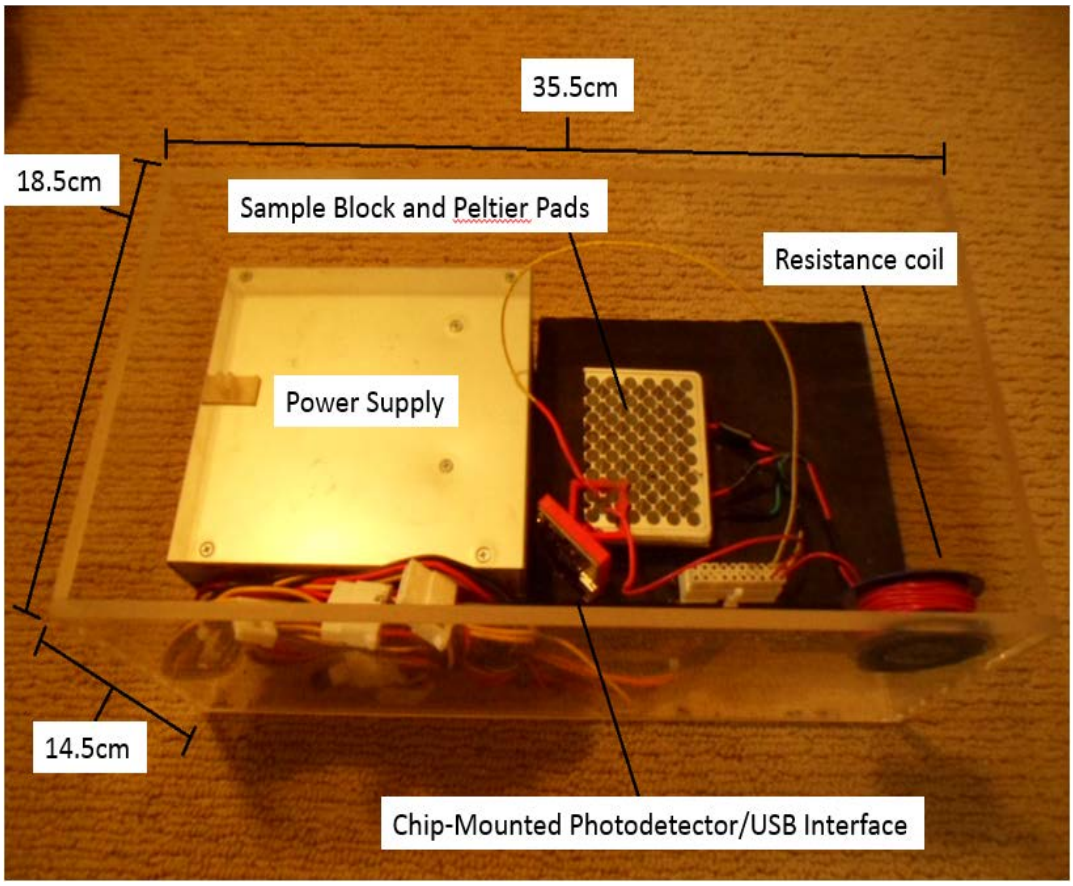

FIGURE 18: LAMP prototype for use in resource-limited settings.

4. RESULTS

4.a HIV and Lower Limit of Detection

The LAMP primers for HIV's integrase gene were designed and synthesized as described in Section 3. Successful HIV LAMPflank PCR fragments were simply used directly or in aqueous dilutions as template in LAMP experiments for HIV, after they were confirmed as present and of the appropriate length, through visualization by 1% agarose gel electrophoresis. The lower limit of detection for the LAMP reaction was assessed, through LAMP experiments using serial ten-fold dilutions of HIV LAMPflank PCR samples. Because the length of the sequence was known, DNA copy numbers could be calculated from absorbance ratios of visible light, obtained through spectrophotometry, indicating the mass of DNA present per microlitre. A sample calculation is shown below:

HIV LAMPflank PCR#1: 9.3ng/μL (nanograms per mictrolitre) [spectrophotometry data]

Sequence length: 1650bp

Average mass of a double-stranded DNA bp: 650g/mol (62)

650g/mol/bp * 1650bp = 1072500g/mol of HIV LAMPflank sequence

$9.3ng = 9.3*10^{-9}g$

$9.3*10^{-9}$g / 1072500g/mol = $8.7*10^{-15}$mol of HIV LAMPflank/μL [of PCR#1]

$8.7*10^{-15}$mol * $6.02*10^{23}$molecules/mol =

$5.2*10^{9}$ molecules (copy numbers) HIV LAMPflank sequence per μL of PCR#1 solution

Based on these calculations, ten-fold serial dilutions were prepared sequentially, until the copy numbers of the sequence were down to the order of 10^0 (i.e. less than ten) per microlitre. LAMP assays were performed in triplicate across the decreasing template concentrations to evaluate the lower detection limit. It was found that template with a concentration as low as the 10^1 order could occasionally be detected, though this was quite rare. 10^2 copy numbers frequently gave successful LAMPs and, this was initially thought to be the lower limit of detection (and, indeed, has been reported as such by other groups); however, it was found that on rare occasions LAMP wouldn't be successful at this low concentration, so the fully reliable lower limit of detection for the LAMP reaction was taken to be on the order of 10^3, or ~1000 copy numbers(87). Representative data is given in Figure 19, showing faint bands even at the order of 10^1 copy numbers.

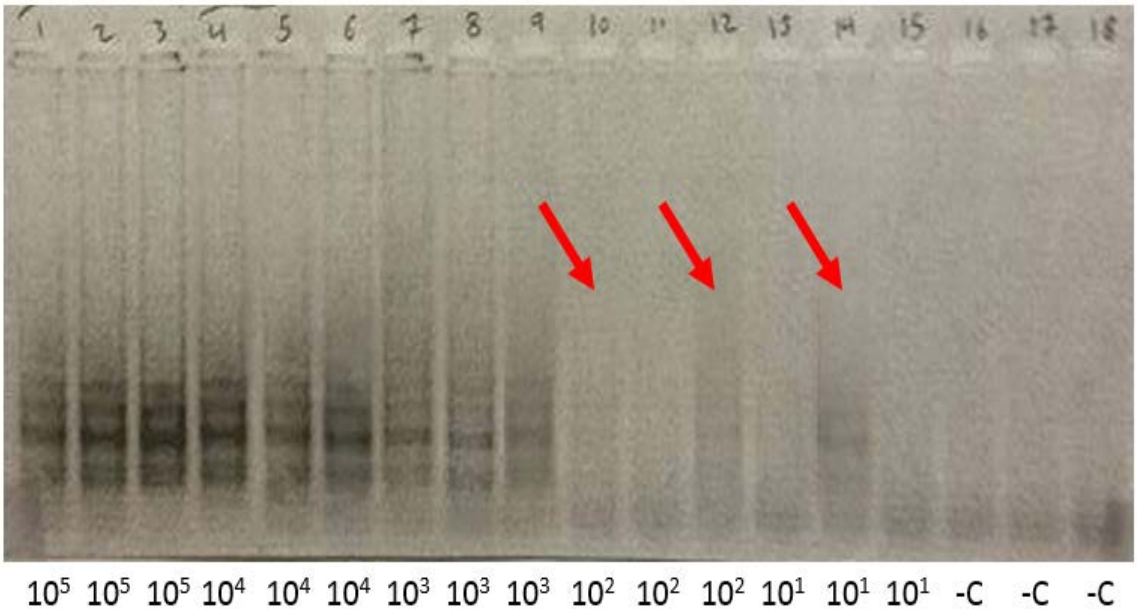

FIGURE 19: Lower detection limit of LAMP reaction, as visualized on 2% agarose gel**,** using HIV Integrase primer set and tenfold serial dilutions of template. Lanes 1-3, 10^5 copy numbers; lanes 4-6, 10^4 copy numbers; lanes 7-9, 10^3 copy numbers; lanes 10-12, 10^2 copy numbers; lanes 13-15, 10 copy numbers; lanes 16-18, negative controls. Less prominent LAMPs (i.e. lower concentration of amplified DNA) in lanes with template concentrations lower than the lower detection limit are indicated with red arrows in lanes 10, 12, and 14 to showcase the sensitivity of the assay.

After this evaluation, results began to take on an inconsistent nature due to major difficulties encountered in LAMP reactions, and, more specifically, the methods used to visualize them, as will be discussed in Section 4c. Thus, it became necessary to continue LAMP evaluation for leishmaniasis, where a real-time optical detection system was used, and detection limit evaluations were confirmed.

4.b Leishmaniasis and Real-Time LAMP

The merits of LAMP for leishmaniasis diagnosis were explored with a focus on the potential for quantification. Genomic DNA of *Leishmania donovani* was obtained, and the chosen primers were mapped to their target region on the genome, as was done for malaria and HIV. PCR primers were designed and synthesized for a region flanking the target region of the 18S rRNA gene, dubbed the “Leish18SLAMPflank” primers, and used to produce template in known concentrations for downstream LAMP experiments as was described in Section 3. At this point, we asked ourselves what sort of quantitative information we might extract from the LAMP reaction, and thus began to look at the optics of magnesium pyrophosphate formation more closely.

Using a Nanodrop 1000 spectrophotometer, it was found that the precipitate absorbed 300-400nm light effectively enough to be distinguished. As other components of the reaction mixture also absorbed in the 300nm range even if LAMP hadn't occurred (e.g. Oligonucleotide DNA, free dNTPs), and in order to maximize the safety and reduce the cost of the eventual prototype, we chose to work with 400nm absorbance, on the lower end of the visible light spectrum. It was found that successful LAMP reactions had a significant range of absorbance at 400nm as measured by the spectrometer, ranging between 0.011 and 0.400. We were able to demonstrate that 400nm absorbance >0.011 as measured by the spectrophotometer had a direct statistically-significant correlation with visible DNA bands on agarose gels ($p<0.01$, $n=50$).

Figure 20 shows a representative correlation of LAMP results as measured by gel electrophoresis and 400nm absorbance in 8 samples.

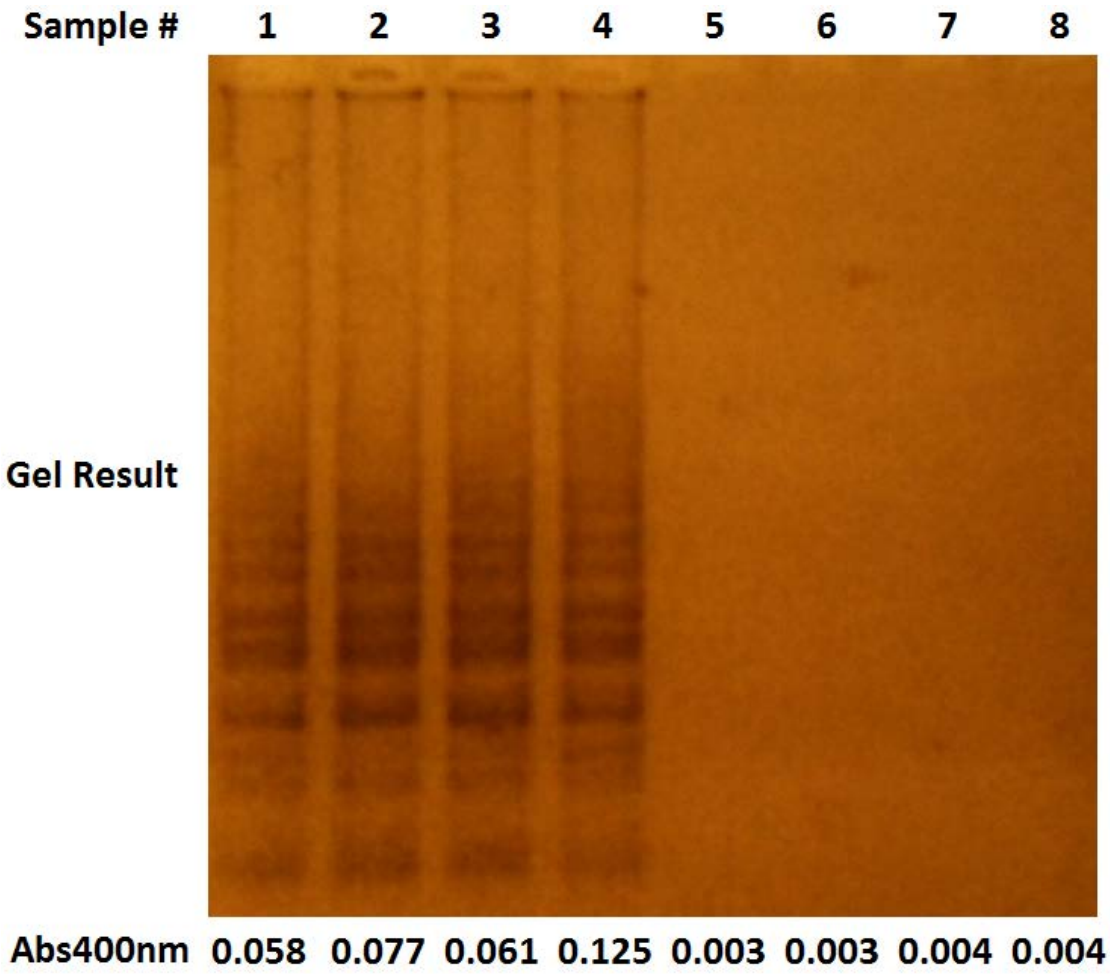

FIGURE 20: Correlation between presence of visible bands following gel electrophoresis, and an absorbance measurement of >0.011 (Nanodrop 1000 Spectrophotometer) for 8 LAMP samples.

Unfortunately, we found no correlation between the concentration of initial template in the LAMP mixtures and the final spectrometer absorbance values, suggesting that all

LAMP polymerization eventually reached similar maximums, and no quantitative data as to original template concentration, or viral/parasitic load in a patient, could be extracted from the assay after the fact.

In order to investigate whether quantitative information could be extracted from the reaction during polymerization, we took a cue from quantitative PCR (qPCR), and asked whether the time at which LAMP began, or reached a certain threshold, could be used to retroactively quantify initial template concentration. A “real-time LAMP” protocol was designed as described in Section 2 and implemented.

A trend was indeed observed in the fluorescence curves, with a tendency for reactions with higher initial template concentration to cluster earlier, while more dilute reactions clustered later. However, these trends were general and not without significant outliers, such that their statistical significance was questionable ($p>0.15$, $n=12$). This clustering became more and more erratic after repeated experiments, as the sensitivity of the assay began to return more false-positives, as will be discussed in section 4.c. In the early stages of this degeneration, one noteworthy observation was the tendency for samples containing template within the established detection limit of $\geq 10^3$ copy numbers to LAMP within the first 45 minutes of incubation, while false-positive negative controls and samples with extremely dilute template would suddenly spike in the last 5-15 minutes. Also noteworthy was the observation that the contamination issues with this evaluation seemed to arise even earlier than in the case of HIV and malaria, despite an even more vigilant dedication to bleaching and sterility, and a decreased number of primers, with very few possible primer-dimer combinations.

A sample trace of real-time LAMP performed for decreasing concentrations of “Leish LAMPflank” DNA fragments is shown in Figure 21.

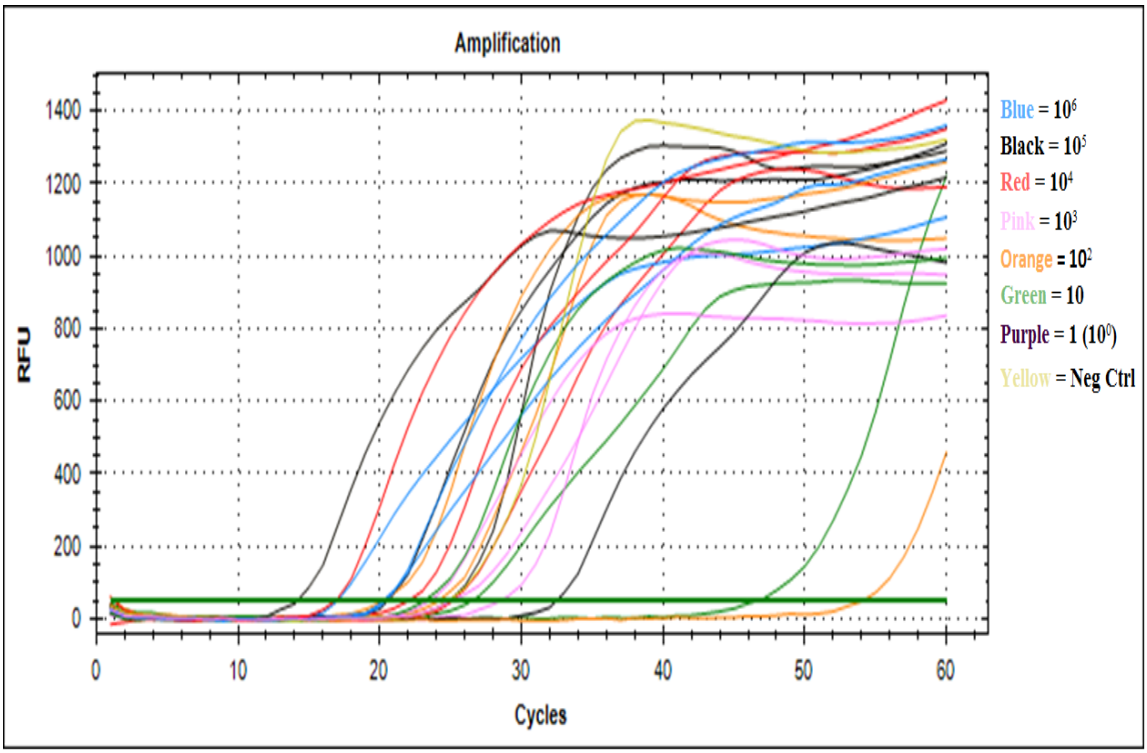

FIGURE 21: Real-time trace of triplicate LAMP runs with genus-specific Leishmania 18S rRNA primers for color-coded dilutions of template DNA. Color legend refers to approximate copy numbers of template DNA added. Some clustered results and some erroneous ones, particularly in the last 15 minutes, prompting the decision to shorten the protocol to 45 minutes.

4.c Malaria and LAMP Contamination Issues

Evaluation first began with the genus-specific *Plasmodium* LAMP primers. Successful PCR amplification of the Plasmodium LAMPflank region was confirmed using 2% agarose gel electrophoresis before it was ligated into the pGEM T-Easy vector and transformed into *E. coli*. A similar confirmation was done on the Falciparum LAMPflank sequence PCR, though this second PCR fragment was not cloned, for reasons that will be discussed shortly. Plasmid DNA from selected colonies of the Plasmodium LAMPflank clones was confirmed to be the desired sequence using Restriction Assay and 1% agarose gel electrophoresis, before it was used as template in downstream LAMP experiments. Agarose gel confirmations of Plasmodium LAMPflank PCRs (based on size alone), and purified plasmid DNA from selected *E. coli* colonies following molecular cloning (based on Restriction Assay) are shown in Figure 22.

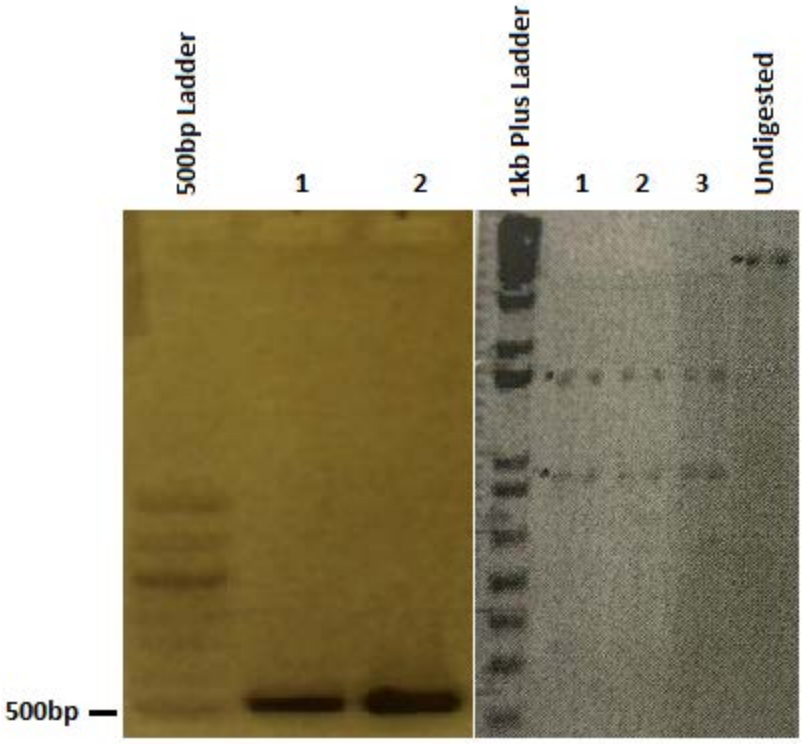

FIGURE 22: Confirmation of "Plasmodium LAMPflank" cloning. Left, 2 successful PCRs of the 518bp sequence. Right, 3 restriction digests confirming correct sequence on 3 transformations of "Plasmodium LAMPflank" sequence into "pGEM T-Easy" vector with a fourth lane showing an undigested plasmid for reference.

Initially, it was thought that the connectivity between stem-loop DNA structures in LAMP would effectively render them much larger fragments, and LAMP reactions were visualized by 1% agarose gel electrophoresis (SafeView stain) at 100V for 60 minutes. This was quickly shown to be ineffective, since LAMP products appeared as smears using this protocol. The protocol was changed to run LAMP reactions in 2% agarose for 65 minutes at 105V, which allowed the products to be visualized as the ladder-like bands characteristic of LAMP. This first trial-and-error heavily foreshadowed the many

difficulties later encountered with LAMP, as it suggested LAMP stem-loop structures do in fact detach from one another into smaller fragments in a range of sizes, to form the ladder-like image. For comparison, LAMP products on a 1% and a 2% agarose gel are both shown in Figure 23.

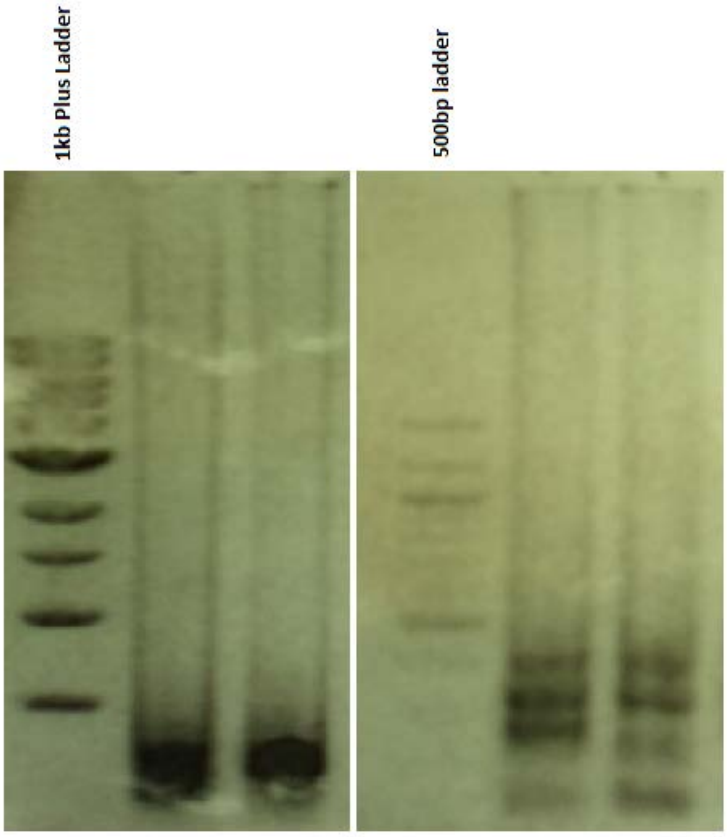

FIGURE 23: Representative LAMP visualizations on different agarose gels. Left, 1% agarose gel showing a continuous “smear” for LAMP reactions. Right, 2% agarose gel resolving the characteristic ladder-like bands of LAMP, suggesting full detachment of DNA contactomers from one another.

.

It quickly became apparent that small fragments of LAMP products were indeed highly mobile and likely airborne, as repeated LAMP experiments in the same laboratory soon became almost nonsensical. DNA capable of serving as LAMP template contaminated the laboratory increasingly, even though measures such as the separate room for preparation of reactions, with lab attire and gloves discarded by staff between the two rooms, and the desktop HEPA-filtered hood for template addition were strictly followed. Only filtered pipet tips were used, and pipets were regularly exchanged for new ones whenever contamination issues were encountered. Even within the template hood, repeated thorough cleansing with 10%, and later 20%, aqueous bleach solutions, as well as 3% Virkon solution, and UV radiation could not completely eliminate contamination issues; LAMP reactions often occurred in negative controls, regardless. Eventually, experiments of up to 30 replicates were prepared in the separate clean room and brought into the main laboratory, where they were simply opened for 10 seconds in the freshly bleached and UV-irradiated HEPA-filtered desktop hood, without any explicit template addition, and it was found that even this was enough to set off LAMP reactions. Reaction tubes prepared in the separate clean room and never opened in the main laboratory at all were also shown to sustain LAMP reactions. Although this was observed at a much lower rate than in tubes that were opened in the main lab, it was still enough to call LAMP into question as a consistent indicator. Genomic DNA fragments in the 18s rRNA region for *P. vivax, P. malariae, and P. ovale*, were used with LAMP primers specific for *P. falciparum* to evaluate cross-species specificity. The first two experiments of this kind showed no cross-

LAMPing; however, agarose gel electrophoresis of later experiments showed significant erroneous LAMPs. Figure 24 shows an early malaria LAMP experiment of this type beside a later one, as a basis for comparison.

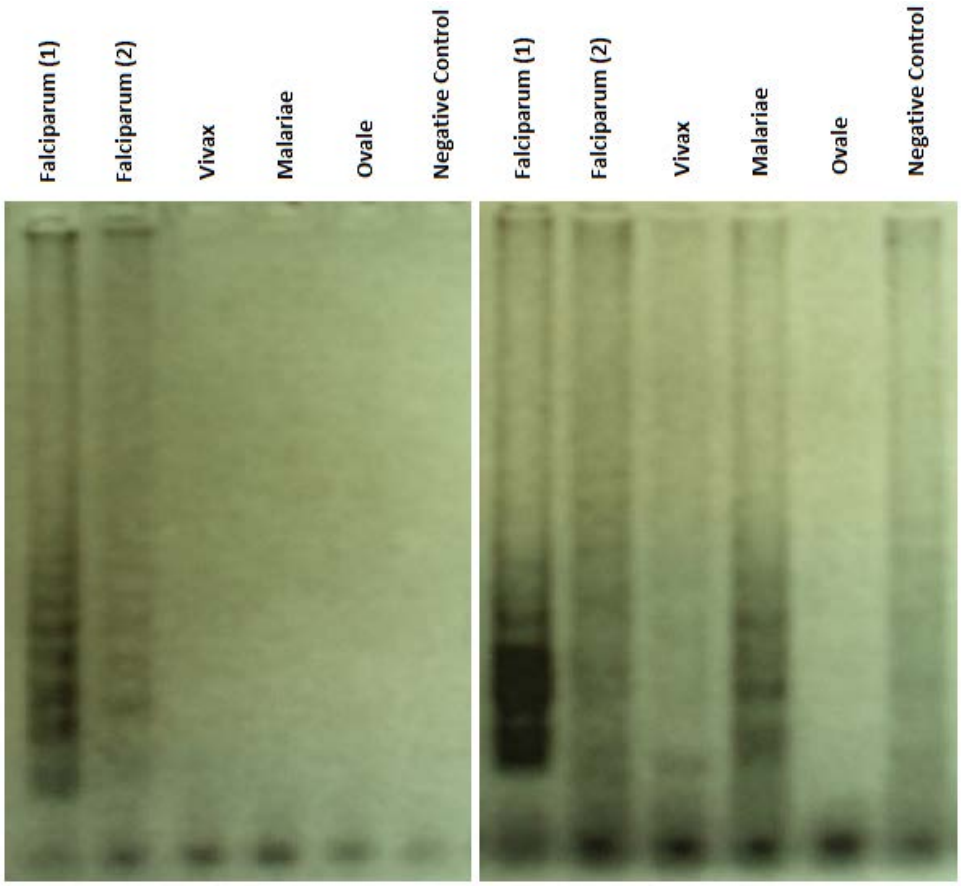

FIGURE 24: Contamination of LAMP reactions over time. Left, an early evaluation of *Falciparum* species-specific LAMP primers for cross-reactivity with genomic DNA fragments of other malaria-causing *Plasmodium* species. Right, the same evaluation done later, after some airborne template contamination had built up in the laboratory, showing extensive cross-reactivity.

It was found that LAMP contamination issues could be minimized by changing settings entirely and mixing up the reaction tubes in different areas, preferably in HEPA-filtered desktop hoods, fume-hoods, or Bio-Safety-Cabinets (BSCs). This solution was highly temporary, however, and often served for the first two or three experiments in one location, before it would also become contaminated to a point where vigorous cleaning did little to salvage the situation. Decreasing the concentrations of added templates was effective in extending a location's lifespan by a maximum of two additional experiments, raising questions about LAMP's lower detection limit. In the end, the most effective method for dealing with LAMP contamination in *Plasmodium* experiments was to move on to evaluation of LAMP for HIV diagnosis, where investigating the lower detection limit became an early priority.

After a literature review, we discovered that some groups working on LAMP reported a need for higher purity in the FIP and BIP primers for more reproducible results(88). However, our problems stemmed from the LAMP reaction working too well, rather than beginning to fail over time as might be expected from simple primer degradation. Noting that the FIP and BIP primers consisted of two separate sequences linked by a spacer, we wondered whether degradation in this region could contribute to the problem, as it might liberate the two shorter sequences. We theorized that this might increase the chances of primer dimerization across all the primers and potentially trigger erroneous LAMPs. We inputted LAMP primer sequences into an online tool for calculating primer dimerization possibilities (Multiple Primer Analyzer: Invitrogen, Inc.; available from: http://www.lifetechnologies.com/ca/en/home/brands/thermo-scientific/molecular-

biology/molecular-biology-learning-center/molecular-biology-resource-library/thermo-scientific-web-tools/multiple-primer-analyzer.html) and indeed found that there was a qualitative correlation between the number of primer-dimer combinations that could be found by the software, and the LAMP assay's propensity to begin returning false-positives earlier; this relationship, however, was too complex and dependent on too many other variables to be meaningfully quantified. Although it was recognized that these dimers might not form spontaneously in solution at the 65°C LAMP reaction temperature, it is important to note that Bst's strand displacement activity includes hybridizing complementary sequences, and these dimers could have thus been formed by the enzyme itself.

For this reason, it was decided that the loop primers would be omitted from HIV LAMP protocols, though this did not improve false-positives from already established contamination. It was decided, however, that the remaining LAMP assays for leishmaniasis would be done using a primer set that excluded the loop-primers, as this could help minimize false positives due to primer-dimerization. A sample primer-dimerization check for HIV primers versus *Plasmodium* genus-specific primers, where results confirmed the increased propensity for erroneous LAMPs in the former set, is shown in Figure 25.

FIGURE 25: Results of primer-dimerization prediction using “Multiple Primer Analyzer” (Life Technologies, Inc.), confirming a higher probability of erroneous LAMP results due to primer-dimerization for *Plasmodum* primers over HIV integrase primers, which showed no significant dimers.

4.d Engineered Prototype for LAMP-based Diagnostics in Resource-Limited Settings: Heat-Transfer

When the components for the LAMP prototype were selected and its construction began, the 5V output of the Dell power supply was initially used. This voltage was found to produce heat in the aluminum sample block well in excess of 100°C. A reduction of the voltage to the 3.3V output also heated the Peltier pads excessively, though only to an 82°C maximum.

At this point, however, a different problem arose, in the form of the kinetics with which this maximum was attained. The initial prototype, making use of the aluminum heat-sink apparatus of the PCR machine, took 53 minutes to reach its 82°C maximum operating temperature. Because of the high current draw of the circuit, at ~4A, this was highly undesirable, as it meant an extremely limited choice of rechargeable batteries that could be used for an eventual portable device. A battery pack would need to sustain a constant current output of ~4A for almost an hour just to heat the device, then maintain that current output for at least another 45 minutes for a LAMP experiment. Taking a conservative approach, and totaling this to 2 hours, the battery pack would need to have a minimum current output of 8Ah. Allowing for losses, especially once recharging of the battery began, 10Ah would be a safer bet. Unfortunately, battery packs with this high of a current output in the low operating voltage of the device, 3.3V, are expensive and difficult to find. As well, the heating of the prototype under this embodiment did not appear to be

linear. Two noticeable regions of slowed heating were observed when the temperature of the aluminum sample block was plotted against time.

The heat-sink embodiment was then replaced with an insulating mechanism as mentioned in Section 3, and the time taken for the device to reach the same maximum operating temperature was reduced to 25 minutes, following a linear relationship. Figure 26 below shows superimposed heating curves for the heat-sink and insulating embodiments, for comparison.

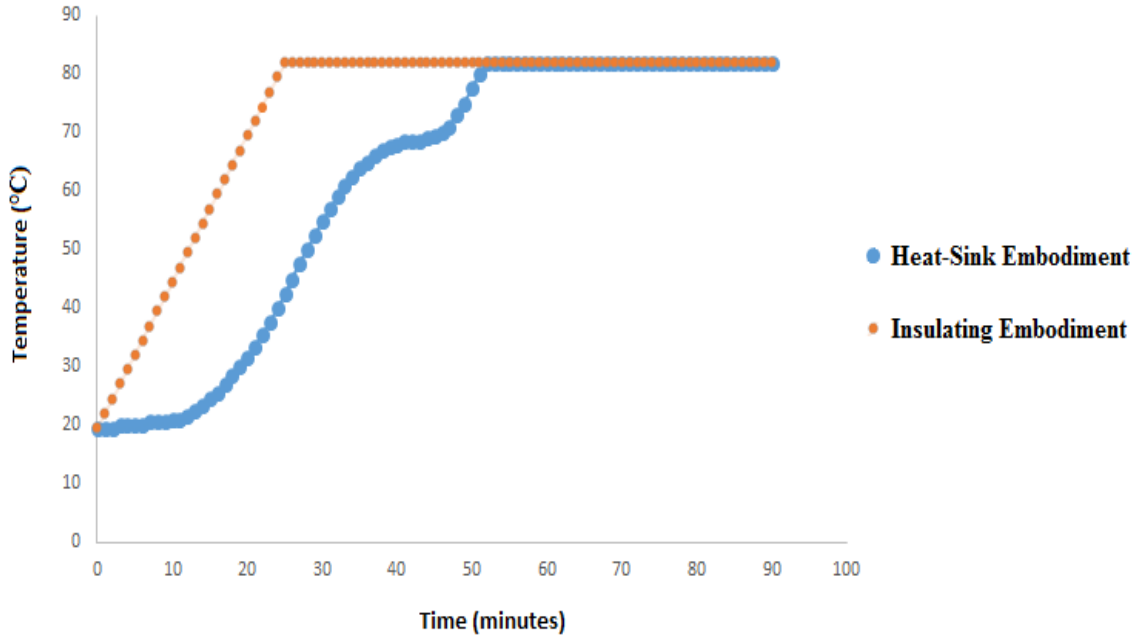

FIGURE 26: Heating kinetics to a maximum (82°C) temperature, from a 19.5°C starting ambient room temperature, over a 90-minute period, for heat-sinking versus insulating embodiments of LAMP prototype's heat-transfer system.

After the speed of heating was dealt with, the next major thermodynamic challenge was to adjust the circuitry in order to lower the maximum temperature to Bst's optimal range of 60-65°C.

As mentioned, the 5V output of the Dell power supply allowed the device to heat in excess of 100°C. The final maximum at this voltage was never observed, as this would have damaged our lower operating-range thermometer. The principle, however, was applied using an adjustable DC power supply. With a 2.7V input, the maximum temperature reached by the device was 31°C, which was too low. In both cases, current was measured at an initial 3.98A, which eventually dropped to a stable 3.84A, suggesting a highly variable nature to the resistance of the Peltier pads that increases slightly over time. Factoring in the maximum 82°C at 3.3V, it was thus estimated that a reduction in the voltage of 0.2V, to ~3.1V, would lower the temperature sufficiently, after temperature was plotted as a function of the input voltage of a 3.84A DC current and the linear relationship was established, as well as extrapolated up to 5V – shown in Figure 27.

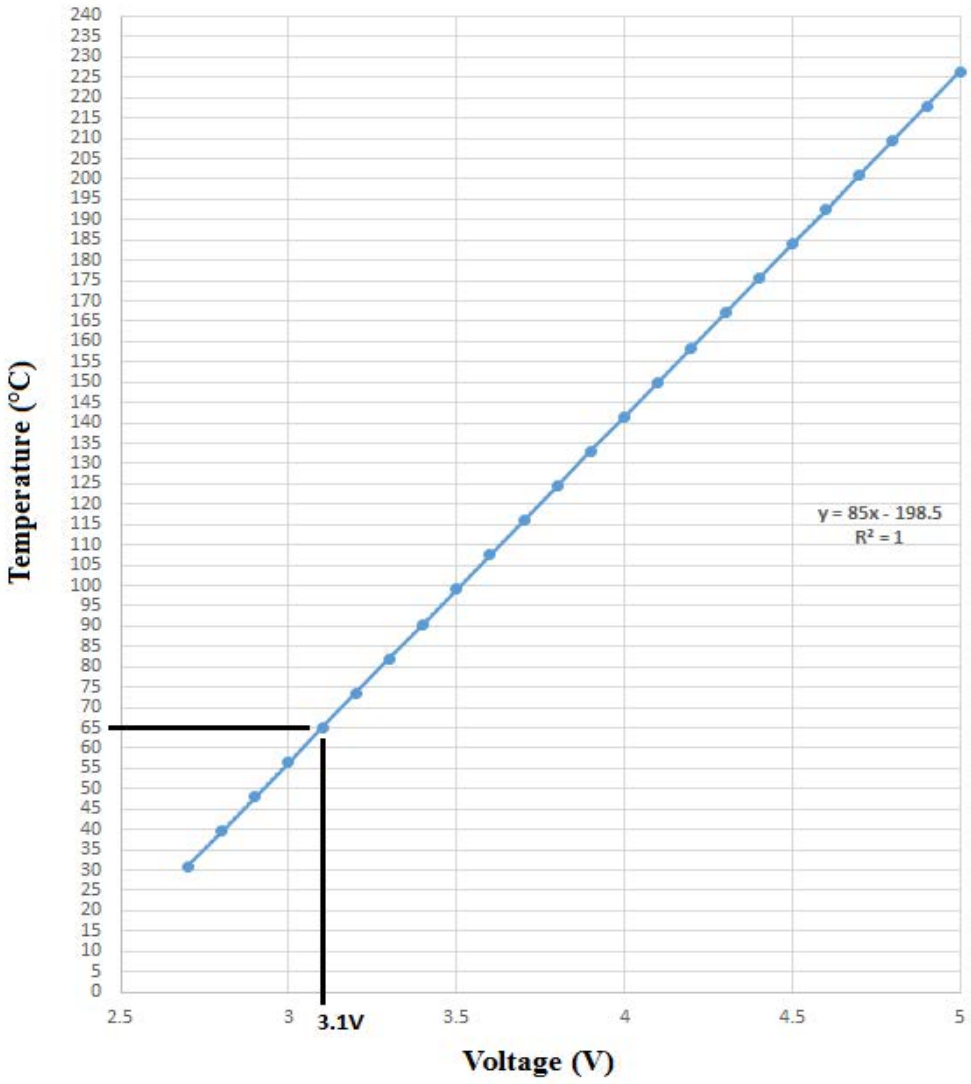

FIGURE 27: Established linear relationship of maximum temperature (°C) reached by Peltier Pads as a function of voltage (V) supplied at a current of 3.84A

Ohm's Law (see Section 3.e) was then used to calculate the value of an appropriate resistor which, when wired in series with the Peltier pads (which both had the same voltage drop of ~3.3V, as they were wired in parallel with respect to one another), would

effectively reduce the voltage from 3.3 to 3.1V. It was thus found that this would correspond to a resistor of approximately 0.052Ω, or 52mΩ; by the methodology shown below.

3.3V = 3.84A * XΩ

X = 0.86Ω (the total resistance of the circuit, including the Peltier pads)

0.2V (voltage-drop across the needed resistor) = 3.84A * XΩ

X = 0.052Ω (52mΩ)

This, as mentioned in Section 3, is an extremely low ohmage, especially relative to the voltage and current values in this circuit. Thus, the power of the circuit became a focus point, so as not to select a resistor that would burn out or melt under the strain of the current. The power of the circuit was calculating using the formula $P = I^2R$ (see Section 3.e), it was found that the resistor would have to have a power rating of at least 0.8W, as shown below.

$P = 3.84A^2 * 0.052\Omega$

P = 0.77W

0.8W being an uncommon power rating for such a low ohmage resistor, 2W resistors in the range of 30-120mΩ were eventually selected and purchased. This also factored in the recommendations of a consulting electrical engineer, who observed that the alligator clips being used for the circuit while it was still being troubleshooted had significant

resistances as well, and the actual power the resistor would need to take in a finalized circuit would likely be significantly higher.

As mentioned in Section 3.e, these resistors proved to be awkward for the application, however, as they were intended for printed circuit boards, and dissipated enough heat to melt a widely-available soldering alloy. The low-ohmage resistance needed to drop the sample temperature was thus achieved simply using wire. Initially, using a table of wire resistance for standard American Wire Gauge (awg) wires, it was calculated that 3.2 feet (3.2') of 22awg bundled copper wire would achieve the necessary 0.052Ω resistance; for reference, the table used in this calculation, which also shows resistance per foot of various other awg wire options, is available in Appendix II. However, this once again raised the prototype's maximum temperature to well above 65°C. In the end, the alligator clips used for easy restructuring of the circuit in the early stages were measured using an ohmmeter and found to have a combined resistance of 0.286Ω. This gave a total resistance of 0.338Ω, or 338mΩ. The wire approach was thus adjusted, and eventually 21' of 22awg bundled copper wire, which was coiled around a spool and attached to a face of the prototype away from the aluminum sample-block, so as not to interfere with the thermodynamics, gave the prototype a final maximum temperature of 63°C while maintaining similar heating kinetics, taking 25 minutes to reach this maximum. This resistance method added very little to the total cost of the prototype, as 100' of 22awg insulated bundled copper wire can be purchased for <$20CAD(89).The final power of the circuit was calculated to be 4.98W – considerably higher than the initial <2W that was anticipated. The discrepancy was accounted for by the difference in resistance of the wire

versus the alligator clips used in the earlier stages of the circuit design, which were observed to heat up considerably.

Lastly, the device was encased in a solid acrylic shell, which, as alluded to in Section 3.e, proved to carry a significant cost, at $150CAD, but was chosen for demonstrative purposes in an academic setting, and could be done in many much more cost-effective ways, including a simple shoe-box.

4.e Engineered Prototype for LAMP-based Diagnostics in Resource-Limited Settings: Optics

The final component of the device to be implemented was the optical detection system, consisting of the SSL-LXTO46UV2C LED and the UI-1222LE-M-GL, juxtaposed across a modified sample well in the aluminum sample-block, as described in Section 3.e. As alluded to therein, the camera was by far the most costly component of the device, at $312CAD. The LED, as anticipated, was quite low in cost, at $13.29CAD. The total cost of the prototype's construction, then, was $479.29CAD, though we estimate that it can be built for under $100CAD, as will be discussed in Section 5.

The suitability of the 400nm for this application was confirmed by spectral analysis of positive and negative LAMP samples post-incubation, using a Nanodrop 1000 spectrophotometer. Representative traces in the range of 220-740nm are shown in Figure

28, giving an indication of the absorbance spectrum for the magnesium pyrophosphate precipitate.

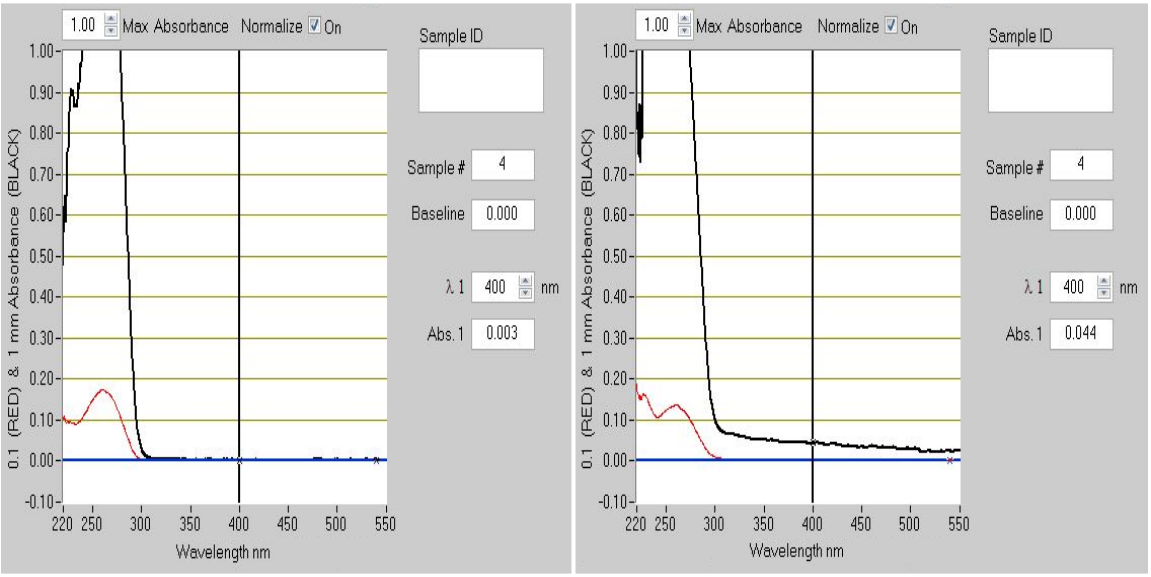

FIGURE 28: Absorbance spectra of LAMP reaction mixtures post-incubation over the range of 220-550nm, as measured by a Nanodrop 1000 Spectrophotometer (Thermo Scientific: DE, USA). Left, a negative reaction with no DNA amplification. Right, a positive reaction with DNA amplification (confirmed by agarose gel electrophoresis). λ1, measurement at 400nm: 0.003 in the left (negative) sample, and 0.044 in the right (positive) sample.

Testing was performed on a laptop computer with the µEye software downloaded free of charge (https://en.ids-imaging.com/download-ueye.html). LAMP reaction mixtures were evaluated after LAMP performed in a conventional PCR thermocycler (BioRad, Inc.: CA, USA), a real-time PCR thermocycler (BioRad, Inc.: CA, USA), and in the prototype's

own heated sample-block, after the incubation. It was found that light detected by the camera was clearly visible in the software interface in a circular area corresponding to the hole drilled through the sample well, distinct from other areas of light capture by the camera. The μEye software was capable of distinguishing pixels within this circle, and analyzing them selectively for light intensity.

The software was not able to distinguish pixel intensities between successful and unsuccessful LAMP reactions with statistical significance ($p>0.3$). Several hypotheses as to why this is have been postulated and will be discussed in the following section, along with recommendations for trouble-shooting in Section 6. Unfortunately, budgetary constraints restricted the implementation of these recommendations within the time-frame of this project. Therefore, while the recommendations for functional optimization could not be tested, the concept of simple low-cost optical detection of magnesium pyrophosphate precipitate as an indicator of LAMP reactions has been demonstrated, as well as an ability to distinguish the presence of a reaction tube.

A final summary of the components of the point-of-care LAMP device, and their respective costs, are given in Table VI.

TABLE VI: Summary of Device Components and Costs

COMPONENT	RECYCLABLE?	COST (CAD)
Computer Power Supply	Yes	$60-$75 (www.atxpowersupplies.com)
HR-DF3 Battery Pack	No	$73.10 (www.digikey.com)
21’ (6.4m) 22awg copper wire	Yes	$14.71 (www. canada.newark.com)
4A Peltier Tiles (2)	Yes	$18.13CAD each (www.digikey.com)
Cardboard-Air Insulator	Yes	Negligible
SSL-LXTO46UV2C 405nm LED	No	$13.29 (www.digikey.com)
Photodetector (e.g. UI-1222LE-M-GL camera)	Yes	$312.00 (www.1stvision.com)
Opaque Epoxy Putty	No	$6.96 (www.homedepot.ca)
Aluminum Sample Block	Yes	$5.00 (estimated – University of Calgary Faculty of Engineering Machine-Shop)
3D Photodetector Mount	No	$1.00 (estimated – University of Calgary Faculty of Engineering Machine-Shop)
Outer Casing	Yes	Variable - $0-200
TOTAL COST	$94.35 (recycled)	$522.32

5. DISCUSSION/CONCLUSIONS

5.a LAMP Protocol Recommendations

LAMP is a robust new NAAT that offers a wealth of potential for use as a diagnostic tool in areas that have traditionally had very limited access to basic health-care, if it can be developed into a clinically accepted method. Currently there are a few obstacles preventing this, most notably the test's tendency toward false-positives and low repeatability.

The latter issue with LAMP actually stems from one of its benefits: a very low lower limit of detection and thus, a higher sensitivity compared to PCR-based NAATs. Previous studies have found improvements in sensitivity up to one-hundredfold in LAMP, compared to PCR, with LAMP tests capable of detecting as low at 10^2 colony-forming-units of template where PCR tests could only detect 10^5(90). We came up with similar figures in our experiments, with a lower detection limit of 10^3 copy numbers of template DNA, which corresponded to a hundredfold increase in sensitivity over PCR's lower limit of 10^5 copy numbers. Unfortunately, this higher sensitivity is what causes problems in LAMP's specificity, and leads to a greater propensity to be confounded by contamination issues.

Quantitative specificity tests for LAMP were difficult to perform in a laboratory setting, owing to the difficulties with contamination that began almost immediately, after as little as two experiments with the same template. As mentioned, this project was done under an extremely restricted time-frame; much of this time was spent simply attempting to combat the contamination problems in LAMP experiments so as to have more repeatable replicate results on a single target. Though elaborate measures for separating template from other LAMP reagents and frequent cleaning for DNA contaminants using bleach solutions, detergents, and UV radiation were employed, the tendency of LAMP to occur even where no template had been added presented a constant challenge to the researchers. Indeed, LAMP tests were done in which tubes lacking template were simply left open for several seconds, without any template addition, and still showed DNA amplification following incubation.

Eventually, it was hypothesized that the practice of performing agarose gel electrophoresis on LAMP experiments was one of the most detrimental practices to repeated LAMP tests. Specifically, simply opening the amplified reaction tubes after incubation at all, was likely releasing so much aerosolized DNA that the laboratory air itself became a ripe template for the highly sensitive assay. This idea is supported by the pattern of LAMP DNA on agarose gels. As mentioned, it was initially hypothesized that the extended contactomers formed during LAMP would remain more connected and form larger fragments that would be visible on 1% agarose gels with electrophoresis. The fact that LAMP reactions were much more visible as many discreet bands of smaller sizes on 2% agarose gels suggests that they do detach from one another significantly, forming fragments of varying sizes, many of which are quite small. Such tiny fragments, when

aerosolized by the opening of a sample tube, can travel great distances to contaminate every corner of a contained room. As most laboratories are kept pressurized under a negative air pressure, so that outside air flows in rather than vice-versa, and potentially undesirable airborne elements are kept contained, this could further exacerbate the problem. Without an efficient system for purging laboratory air and exchanging it for fresh uncontaminated air, it is reasonable to assume that this invisible hurdle stood before our research efforts for months.

Yet, if this were the only issue, we may still have been able to work out an inexpensive method for dealing with this difficulty. Unfortunately, it became apparent that the template contamination had ways of spreading even further. Our team kept a second clean room facility set up solely for the preparation of LAMP and PCR reaction mixtures, from which template DNA and laboratory wear were strictly prohibited, and all work was done within additional HEPA-filtered tabletop hoods. When LAMP began to occur even in reaction mixtures that had never been opened outside of this facility, it became clear that contamination could spread in ways we could barely even fathom. All manners of air-currents, for example, and even researcher respiration, could eventually expel template contaminants into fresh LAMP reaction tubes as they are being prepared. This hypothesis was supported by a careful examination of the three enclosures used during temple addition. Though fume-hoods, HEPA-filtered tabletop hoods, and BSCs all have quite different internal air circulations, all three could be theoretically susceptible to aerosolized LAMP contaminants. The common factor observed in all three was their interface with the researcher, which was done through an opening on the front, around chest-level for a seated adult, through which arms could be introduced. Unfortunately,

this opening also seems to be at just a level where a researcher's exhalations would be introduced into the container. Though BSCs and HEPA-filtered tabletop hoods meet incoming air through this frontal opening with a downward air current from above, this is primarily designed for lower-pressure air flow from the ambient air in the room, and may not be robust enough to overcome the higher pressure of an exhalation.

Of course, many other possibilities for contamination spread exist, such as adhesion of airborne DNA to a researcher's hair, pants, face, and wrists between gloves and lab-coat sleeves. All in all, it is thought that nothing short of a fully-contained glove-box apparatus for preparing LAMP reaction mixtures, and a sterility protocol for researchers comparable to that of surgeons preparing to enter an operating-room, complete with a full change of clothes and scrubbing of any exposed skin, could overcome an established LAMP contamination. While doable, this is fundamentally counter-productive to the main objectives of LAMP-based assays: to perform crucial diagnoses at very low costs, to patients who cannot afford to support expensive resources, in regions that do not possess them.

When it became clear that opening amplified LAMP tubes to run the products on agarose gels was a major setback to reliable results, we switched to real-time LAMP as our primary output source, and observed some improvement, which led to some key design features of our prototype. It was interesting to note, however, that in several real-time LAMP experiments, some tubes that were not expected to amplify did so, rapidly, only during the last 15 minutes of the incubation. We thus recommend that anyone performing

LAMP experiments who is worried about contamination issues from previous experiments may try shortening their protocol to an incubation time of only 45 minutes, to give less time for Bst to find trace amounts of contaminant template.

In addition, we have also explored the possibilities of false positives arising by other means, such as primer degradation and primer-primer interactions. We first pursued this course upon a literature review wherein one group had recommended High Performance Liquid Chromatography (HPLC) purification of just the FIP and BIP primers(85). The latter method is more expensive, and typically yields a higher purity product of >85%(91). Thus, it was hypothesized that the FIP and BIP primers have the highest effect on proper LAMP reactions, and it must be ensured that they are of the highest fidelity to the desired sequences as possible, and that they are kept from degrading into degenerate fragments with reduced specificity for template binding sites as much as possible..

Furthering this concept, we used an online primer-dimerization tool to calculate possible primer-dimers that could form in our LAMP primer sets. We found a qualitatively apparent correlation between primer sets with more primer-dimer combinations and their tendencies to give false-positive LAMP reactions in laboratory experiments. We attempted to quantify this relationship statistically; however, it was extremely difficult to describe a binary relationship between the two, owing to the myriad of other confounding variables involved, such as the inconsistent LAMP results we were experiencing, and the apparent carry-over contamination issues from previous experiments where amplified tubes had been opened. Nevertheless, we adopted primer-dimer evaluation of LAMP

primer sets into our protocols, and began to use it as a general predictor of LAMP success before new LAMP experiments were started. Though we consider this a relatively minor factor in LAMP ambiguity next to aerosolized contamination from previous amplifications, it did also lead us to begin performing our LAMP assays without the use of loop-primers, which we felt just added more primer-dimerization possibilities while contributing little to LAMP efficiency.

It is interesting to note that, while it seems evident through browsing of several large discussion forums online that many other researchers exploring the LAMP technique have encountered the same frustrations, there is little formal research published on the subject. Some groups have employed a technique used in PCR protocols to prevent carry-over contamination called the “dUTP-UNG” method. In this protocol, the dNTP mixture used for LAMP reactions is modified, replacing some or all, of the dTTP (deoxyribose-Thymine-triphosphate) with dUTP (deoxyribose-Uracil-triphosphate). As several DNA polymerases, including Bst and engineered versions of Taq, can use dUTP to incorporate Uracil into the DNA the replicate, this would mean all amplified DNA would contain Uracil bases replacing Thymine, while the original template would still retain its Thymines. New sample tubes are then incubated with Uracil-DNA-Glycosylase (UNG) at its optimal functioning temperature of 37°C for 10 minutes, prior to regular incubation/thermocycling protocols. Uracil-DNA-Glycosylase cuts the backbone of DNA when it encounters a Uracil residue, as this enzyme's physiological function is to ensure no Uracil, which is a nucleotide base specific to RNA, is incorporated into nascent DNA, as this could introduce other mutations in subsequent replication events. When used in

the dUTP-UNG protocol, it fragments any Uracil-containing DNA that may be present in the reaction mixture from previous amplifications, rendering it unusable as a template for the polymerase, while leaving the Thymine-containing template DNA intact(92).
This method has been used successfully in PCR protocols for years, and has recently made the jump to LAMP in some recent attempts to overcome contamination issues. Several groups have used different fractions of dTTP replacement by dUTP, from 5/8 to 100%, with mixed results, as LAMP efficiency was sometimes found to decrease with the protocol(93).

While the dUTP-UNG method is certainly elegant and innovative, it once again introduces elements that we would prefer to avoid in a protocol designed for resource-limited settings, as it introduces additional expenses. Not only is the UNG enzyme itself another perishable reagent that would require cold storage, ideally at -20°C, but the 37°C temperature necessary for its function introduces the need for thermocycling, which is one of the fundamentals of PCR diagnostics that we seek to avoid in a more cost-effective LAMP alternative.
For this reason, we seek to cut the problem off at the source, and prevent aerosolized contaminant DNA in the first place. We thus designed our low-cost device such that LAMP tubes would never need to be opened after incubation in order to find out the results. While we recognize that the academic scientific community is very attached to its agarose gel images, which do a great job of showcasing DNA in discreet fragments whose sizes can be easily estimated with appropriate molecular rulers, we cannot in good conscience recommend this procedure for any LAMP experiments, simply because it

necessitates opening an amplified reaction tube. In any case, the characteristic ladder-like bands of LAMP reactions run on an agarose gel do not offer any additional information other than the actual occurrence of the reaction – unlike PCR, where one discreet band of a single size can be correlated to the anticipated fragment size in order to determine if the *correct* sequence was amplified. LAMP reactions unfortunately do not carry this inherent specificity test, and confirmation can only be done by sequencing of bands purified from the gel.

Aerosolized contamination by template DNA can also be a potential issue in LAMP. Just like in the case of opening amplified reaction tubes, template DNA can become airborne from concentrated samples of template DNA. Moreover, this type of contamination would not be remedied by the dUTP-UNG protocol, as it would contain no Uracil. It was for this reason that we decided to move away from molecular cloning and plasmid purification by miniprep as a source of template DNA and work solely with the lower copy numbers from PCR.

It is important once again to note, however, the LMIC applications for which LAMP is intended. Because of its ability to reliably detect low DNA concentrations on the order of 10^3, our recommendation would be to use LAMP as an early diagnostic tool in patients who may be at risk for an infection, well before symptoms arise. This is where LAMP can offer some of its most robust advantages over current diagnostic methods, which may come “too little, too late”. In such applications, the amount of template DNA would likely be very low, at several thousands of copy numbers of viral or parasitic DNA, and

this risk would be minimal. Thus, for practical LAMP-based diagnostics, we hypothesize that template concentrations high enough to pose significant airborne contamination threats would be excluded from the protocol naturally, and that laboratory-based LAMP experiments may be the few settings in which this is a real issue. In addition, for field applications of LAMP diagnostics in outdoor settings (which would likely be the primary sites for such diagnostics in LMICs), the large open area with extensive air circulation could itself provide a very effective means of dissipating template contamination.

All in all, we set out to validate the LAMP assay as a diagnostic tool in "ideal" laboratory conditions, and have concluded that, in fact, a laboratory setting may be one of the least ideal places in which to produce repeatable and clinically-relevant LAMP assays.

5.b LAMP Device: Detection and Output Platforms

Fortunately for LAMP, the magnesium pyrophosphate byproduct it produces is an excellent alternative for detection that does not require any additional reagents, and most importantly, can be done without opening amplified reaction tubes. By using optically transparent PCR tubes for LAMP reactions, visualization of results can be done through horizontal transillumination and measurement of light attenuation by the precipitate, without ever having to open the amplified mixtures post-reaction.

The principle can be accomplished using low-cost LEDs with very long lifespans, and relatively inexpensive CMOS image sensors which also have quite extensive lifespans,

and the costs of which are falling daily. This detection platform is extremely versatile, and can be customized based on the available resources in specific regions, as these image sensors are the most commonly used photodetectors in modern digital cameras and camera-phones. Instead of discarding old imaging electronics, users now have the option of salvaging the CMOS image sensors from their old cameras or camera-phones, and using their already integrated instrumentation and output platforms in order to obtain diagnostic results of LAMP-based assays. Our prototype uses a mini-USB/USB cable to interface with a laptop, and an open-source image processing software that is free to download anywhere in the world. Future users may wish to use different hardware connectors and different image-processing software platforms. This is not a problem to our design, and, indeed, is an added convenience, as a user seeking to recycle a CMOS image sensor from an old image-capturing device is likely to have the interface and processing platforms for the device already on-hand, and the transition can be a relatively seamless one. Even minimally-functioning image sensors can be used, so long as they can distinguish different levels of ~400nm light, and the sensors can be incorporated to the device through simple 3D-printing, or even just through the proper use of adhesives. Depending on their chosen user-interface platforms, health-care practitioners can then obtain rapid LAMP-based diagnostic results on their desktop computers, laptops, tablets, or smart-phones to share with other specialists in whatever system is most convenient for them.

It is important to keep in mind the unpredictable nature of light when designing a detection system for LAMP. As evident in our prototype, many variables may need to be adjusted before an appreciable difference in signal can be obtained for a successful

LAMP experiment versus a failed one. Variables such as incident light intensity, light scattering, infiltration of ambient light, absorption by the plastic of the reaction tubes, and even internal processing by the chosen software can all have substantial effects, and must be manipulated in concert for an ideal clinical tool, as will be further discussed in Section 6.

5.c LAMP Device: Power and Thermal Incubation

Recent work has succeeded in designing LAMP platforms that are entirely independent of electricity, which is a very exciting leap forward in terms of bringing diagnostics to LMICs. LaBarre, et al. have recently reported a device housed within a disassembled Thermos™ for heat insulation(94). Heat is generated chemically, via an exothermic reaction of calcium oxide (CaO) and water, much like what is found in many commercially available instant hand or foot warmers. The balanced chemical reaction equation is shown below.

$CaO_{(s)} + H_2O_{(l)} \rightarrow Ca(OH)_{2(aq)} + heat$

This heat is controlled and kept at a constant 65°C through an elegant exploitation of phase-changes. The group reports the synthesis of an “Engineered Phase Change Material” - a rationally designed oil-like molecule with a melting temperature of 65°C. The device is lined extensively with this synthetic oil, and it uses the heat generated by the calcium oxide reaction to transition from solid to liquid. Because heat energy during

phase changes is dedicated entirely to the shift in intermolecular distances and interactions of the substance, no temperature increase can occur during a phase change until the change is complete. By having the synthetic oil lining the device in great excess so that one calcium oxide reaction can never fully melt it all, it can be insured that the device's temperature will never climb beyond the 65°C needed for LAMP(94).

Though we found this approach innovative and very exciting, in the end we found three major flaws with the method that dissuaded us from attempting further electricity-free LAMP research. Firstly, the proprietary nature of the Engineered Phase Change Material goes against some of our aims for this application. Though the group reports that one “pack” can last for a minimum of 10 LAMP reactions, we question the economic merit of replacing this material after that point, as the molecule has been designed by a small group of North American scientists(94). Thus, it is not readily available in the regions that need it most, and very likely carries a significant cost to synthesize in a laboratory setting, by highly trained personnel. In addition, this not only means a potential for long delays in shipping before diagnoses can be made, which can often spell out a death sentence for patients in dire need of medical attention, but also fosters additional dependencies on developed nations by LMICs. It is our firmly held belief that economic circumstances in LMICs will never improve while they are still dependent on imported goods from the developed world, and wish to help change this as much as possible in the scope of our device. Secondly, this device has room for three LAMP reactions at a time: a positive control, a negative control, and one patient sample. It is a well-known fact to anyone familiar with laboratory work in molecular biology that molecular assays are not

100% reliable, and have a tendency to produce erratic results on occasion, for example, when DNA fragments have degraded in solution over time and their binding specificities have thus been reduced. For this reason, many laboratory experiments in molecular are carried out with redundancies – often in triplicate, so that researchers can be more certain of their findings when three separate assays all confirm one result. This is also the reason for rigorous implementation of both positive and negative controls in research. In addition to the decrease in credibility of only one test per patient, having room for only one patient sample at a time means that the Engineered Phase Change Material will have to be replaced more often, incurring more cost to the whole process. Finally, the fact that this device requires such elaborately engineered insulation as that found in a Thermos leads us to question its versatility. We wonder how much effect the outside ambient temperature will have on the temperature of the device, and, as we would ideally like to design a device that could be deployed at both 40°C and -40°C, we chose in the end to pursue an electrical device with minimal power requirements.

Perhaps the most economical triumph in this project was the build of a working system for incubation of LAMP reactions at an extremely low cost, by the recycling of disposed-of equipment. By using parts from a discarded computer, components of a broken PCR machine, some cardboard, and a length of wire, a device was constructed that could achieve a stable 63°C temperature in a time-frame that would allow it to be powered by a portable and rechargeable battery, as well as maintain that temperature stably for the duration of a LAMP experiment. The low power requirements of the device that allow it to be powered by a compact, lightweight, and readily-available rechargeable battery open

up various possibilities for powering the device in field applications where an electrical grid may not be available, as will be further discussed in Section 6. The computer power supply used in this prototype is already versatile in that, like most similar power supplies, it can be switched to operate from 120V or 240V AC power, which allows it to exploit power grids anywhere in the world. It is important to note that many PCR machines use power supplies similar to those of many computers (though discarded computers are certainly more abundant than discarded PCR machines), and thus the limiting regent in the construction of a low-cost LAMP device would essentially be the procurement of a PCR machine. Thermocyclers also offer the additional advantage of the aluminum sample-block cut specifically for the insertion of 0.2mL reaction tubes suitable for LAMP reactions as well as PCR. Though aluminum is a cheap metal, and this cutting is relatively simple and inexpensive to do in a factory setting, this once again introduces costs and resources into the project that may not be desirable to LMIC applications. All in all, our recommendation is for the PCR machine to become a primary focus for LAMP-based diagnostic devices, rather than being discarded. This offers an exciting new paradigm for PCR Machine recycling, as even the devices that are recycled rather than simply discarded, are currently recycled similarly to other microprocessor devices such as computers, and thus do not achieve their full reincarnate potential.

However, Peltier pads are also used in some other thermal applications, notably in small low-power coolers, such as for individual cups or portable coolers for camping. Because these pads would likely be of various dimensions, and possibly even different compositions, to the ones used in PCR machines, there would need to be some additional troubleshooting research done; however this could open many new possibilities to

recyclers, and the device could be made “from scratch”, still at no additional cost other than the wire needed for resistance and the cost of cutting an aluminum block to fit 0.2mL PCR tubes.

Overall, this project has demonstrated the conceptual feasibility of constructing a portable, rapid, and low-cost device for performing and analyzing LAMP reactions for diagnostic purposes in even the most resource-limited settings, where few health-care initiatives have succeeded so-far in bringing effective means of early diagnosis to patients suffering from, or at risk of, deadly MIDs.

6. FUTURE DIRECTIONS

The nature of this project was a proof-of-concept exploration of LAMP's feasibility as a tool to bring low-cost, point-of-care diagnostics to LMIC settings. Though we have seen some promising preliminary results that suggest the idea could very well materialize into a clinical tool in the near future, there is still much work to be done before this method can truly benefit those who need it the most. We have seen that the LAMP reaction relies on many biological and biochemical reagents. Many of these reagents are highly perishable, and are stored at temperatures of -20°C to minimize their degradation. A main future focus of this area of research should undoubtedly address the issues of these reagents' costs, both to obtain and to store.

Bst polymerase is perhaps one of the most expensive reagents required in the LAMP reaction. It is available from New England Biolabs, for example, at a cost of $365.00CAD for 1mL (8000 enzymatic units) of either the natural form or the company's proprietary “Bst2.0” engineered version, and at $404.00CAD for 1mL/8000U of a “WarmStart” version of Bst2.0 with a reversibly bound aptamer to inhibit polymerization below 45°C(75,95). These polymerases are kept in a buffered 50% glycerol, and the reagent tube is recommended for storage at -20°C. Clearly, it would be beneficial for LMIC applications to find a cheaper Bst source.

Our group has previously succeeded in cloning the Bst polymerase gene into the “pET-303” vector from Invitrogen, Inc.. This plasmid has its cloning site immediately upstream of a polyhistidine sequence, forming a chimeric protein with a His-tag at the C-terminus.

Through review of previous work, it was chosen to add the histidine tag at the C-terminus, as this would likely have a very minimal effect on the enzyme's function. The pET-303 vector is a bacterial expression plasmid suitable for transformation into *E. coli*, which can be conveniently cultured in a laboratory setting. Because pET-303 also contains a *Lac* promoter for protein expression, induction can be done relatively simply, using Isopropyl β-D-1-thiogalactopyranoside (IPTG). After confirmation of protein expression by Sodium Dodecyl Sulfate-Polyacrylamide Gel Electrophoresis (SDS-PAGE), induced bacterial cultures could then be lysed using a milder detergent designed to preserve protein structure, such as 3-((3-chloramidopropyl) dimethylammonio)-1-propanesulfonate (CHAPS), and Nickel-Nitrilotriacetic Acid (Ni-NTA) affinity chromatography with imidazole elution could be used to purify the enzyme. This cloning method would also yield a Bst polymerase in aqueous solution, rather than in 50% glycerol, which could be extremely beneficial for storing the enzyme in a more cost-effective way.

LAMP oligonucleotide primers are also stored at -20°C, albeit typically in simple aqueous solutions. This adds significant costs for anyone wishing to transport LAMP reagents, in what is termed a “cold-chain” that must be maintained throughout the transportation, in order to preserve the reagents.

However, this need not be the case. PCR reactions, for example have long been engineered to break free of the cold-chain through lyophilization. By addition of the trehalose disaccharide to the aqueous PCR mixture, at concentrations of ~5%, the mixture can be lyophilized, or freeze-dried, in such a way that functionality is maintained upon

rehydration, after up to 1 year storage at room temperature(96). The lyophilization process rapidly manipulated both temperature and pressure to take liquid mixtures around the triple-point of phase transitions, into a dried solid form. Initially, water is cooled so rapidly it vitrifies into an amorphous solid form of ice without crystal formation. This is crucial, as ice crystal formation can heavily disrupt protein structure; indeed, this is the main reason why commercial enzymes are sold in 50% glycerol solutions, so that they can be stored below 0°C without losing function. Next, the pressure in the lyophilizer is lowered such that the vitrified ice can sublimate into gaseous water vapor directly, and escape without having to transition back into its liquid form. Because of the rapid and atypical phase changes, relative positions of reagents in the aqueous mixture are preserved in ways that would not be possible if there were either a liquid->solid or a liquid->vapor transition. The addition of trehalose allows for a matrix to form that further helps to preserve this amorphous distribution of reagents even as the mixture is reduced to the volume of a tiny solid bead, particularly with respect to the structural integrities of both the Bst polymerase and the oligonucleotide primers. Of course, this process is greatly complicated if there is any glycerol component to the mixture, as glycerol has drastically different phase-change properties compared to water. Thus, the “home-grown” cloning of Bst polymerase would be doubly beneficial to reducing LAMP costs. After transportation at room temperature, a lyophilized LAMP mixture would simply have to be rehydrated, mixed thoroughly, and impregnated with a template (i.e. a patient sample), for a diagnostic test to be performed anywhere in the world.

We are aware of lyophilized LAMP diagnostic tests available from Eiken Chemical Co., the developers of LAMP technique, so it is certain that a LAMP mixture lacking only in

template can be engineered to be transportable without a cold-chain. Of course, the exact methods used by Eiken for their freeze-dried LAMP mixtures is proprietary; however, there exists a myriad of published research on various lyophilization protocols for similar PCR reactions, with which an optimal process for LAMP lyophilization could certainly be elucidated.

Finally, it would be beneficial to any low-cost LAMP application if patient samples could be utilized directly. In our idealized LAMP validations, we initially used purified genomic DNA in aqueous solutions. From there, we moved to purified plasmid DNA from liquid *E. coli* cultures in water, as well as in "Elution Buffer" mixtures from purification kits, which typically also contain Tris-HCl detergent, sodium chloride (NaCl), and isopropanol. Finally, we performed most of our reactions using template DNA directly from PCR mixtures, which contain many other components (see Section 3), all with success – often more than was convenient. This suggests that Bst is significantly more robust than Taq polymerase, and can generally tolerate more biochemical "contaminants" in its reaction mixtures. Indeed, this forgiving side of Bst has been reported in several previous works, where its increased tolerance over Taq to various buffer additives has been thoroughly described(76). However, these results are certainly mixed, with the improvement being only marginal in the cases of blood-derived contaminants such as serum and plasma(76). Some groups have reported improved success with heat-treated blood samples, ultimately suggesting that the inhibitors may be proteins that have a greatly reduced inhibitory effect once denatured(68). These results suggest the possibility of diluted and heat-treated blood samples being usable for

diagnostic LAMP tests, particularly as genetic-engineering efforts by commercial Bst distributors, such as New England Biolabs' “Bst2.0”, yield recombinant enzymes with even greater tolerances to contaminants. It remains to be seen how far the envelope will be pushed, and whether an engineered enzyme will emerge that can use blood-based templates at high enough concentrations to detect low levels of MID pathogens such as HIV, *Plasmodium*, or *Leishmania* earlier than current diagnostic alternatives. Interestingly enough, some groups have reported LAMP success for *Leishmania* detection using minimally-processed samples from sandflies, which suggests that the technique could easily be adopted to control the disease at the arthropod vector level, by mass screening of sandflies in areas known to be at risk for Leishmaniasis(97).

Aside from these key cost-reducing work-arounds for LAMP's costly reagents and need for purified template, future directions in LAMP-based diagnostics for resource-limited settings should focus on hardware optimization, while promoting accessibility. While our first prototype certainly has significant limitations to be addressed, particularly in its optics, further developments in the near future should certainly focus on exploiting the rechargeable battery-powered embodiment. The particular Nickel-Metal-Hydride battery pack selected for our device was chosen for its versatility with regard to recharging. This could include everything from more costly solar-powered recharging to a simple manually-power dynamo crank. However, the moderate power requirements of the heat-generating components of the device may prove difficult for such setups in the long-term, and more robust energy-generating methods, such as the burning of fossil-fuels, may prove to be better suited to this application. Setting up the hardware platform for

recharging the battery using power from a 12V car battery (rechargeable, of course, using the kinetic energy of the vehicle's internal combustion engine) should become an immediate priority, as this would allow the device to be taken almost anywhere that a full tank of gas will allow, even though it is an electrical device. We have seen how efforts to bring this exciting new diagnostic test to remote rural areas have produced intriguing and highly innovative electricity-free apparatuses, but also how these devices require highly specialized proprietary components, and have low throughputs. We hope with this project to begin to steer future directions in LAMP research toward simple devices that can be assembled from recycled parts that would have been otherwise discarded, at a very minimal costs, and with maximal versatility for data processing. In this way, we can not only help to bring these diagnostic methods to LMICs, but can lay a groundwork for local LAMP research and optimization in the regions themselves that would most benefit from it.

7. TEXT REFERENCES

(1) Berg RD. The indigenous gastrointestinal microflora. Trends Microbiol 1996 Nov;4(11):430-435.

(2) Nelson PN, Hooley P, Roden D, Davari Ejtehadi H, Rylance P, Warren P, et al. Human endogenous retroviruses: transposable elements with potential? Clin Exp Immunol 2004 Oct;138(1):1-9.

(3) Roth RR, James WD. Microbial ecology of the skin. Annu Rev Microbiol 1988;42:441-464.

(4) Walker LC, Jucker M. Neurodegenerative Diseases: Expanding the Prion Concept. Annu Rev Neurosci 2015 Mar 30.

(5) Weissmann C. The state of the prion. Nat Rev Microbiol 2004 Nov;2(11):861-871.

(6) Malaga-Trillo E, Solis GP, Schrock Y, Geiss C, Luncz L, Thomanetz V, et al. Regulation of embryonic cell adhesion by the prion protein. PLoS Biol 2009 Mar 10;7(3):e55.

(7) Pan KM, Baldwin M, Nguyen J, Gasset M, Serban A, Groth D, et al. Conversion of alpha-helices into beta-sheets features in the formation of the scrapie prion proteins. Proc Natl Acad Sci U S A 1993 Dec 1;90(23):10962-10966.

(8) Ridley RM, Baker HF. The nature of transmission in prion diseases. Neuropathol Appl Neurobiol 1997 Aug;23(4):273-280.

(9) Murayama Y, Yoshioka M, Okada H, Takata M, Yokoyama T, Mohri S. Urinary excretion and blood level of prions in scrapie-infected hamsters. J Gen Virol 2007 Oct;88(Pt 10):2890-2898.

(10) Auwaerter PG, Aucott J, Dumler JS. Lyme borreliosis (Lyme disease): molecular and cellular pathobiology and prospects for prevention, diagnosis and treatment. Expert Rev Mol Med 2004 Jan 19;6(2):1-22.

(11) Miller RG, Mitchell JD, Moore DH. Riluzole for amyotrophic lateral sclerosis (ALS)/motor neuron disease (MND). Cochrane Database Syst Rev 2012 Mar 14;3:CD001447.

(12) Caraballo H, King K. Emergency department management of mosquito-borne illness: malaria, dengue, and West Nile virus. Emerg Med Pract 2014 May;16(5):1-23; quiz 23-4.

(13) Barrett MP, Croft SL. Management of trypanosomiasis and leishmaniasis. Br Med Bull 2012;104:175-196.

(14) Lloyd-Smith JO, Poss M, Grenfell BT. HIV-1/parasite co-infection and the emergence of new parasite strains. Parasitology 2008 Jun;135(7):795-806.

(15) Joint United Nations Programme on HIV/AIDS (UNAIDS). Fact Sheet 2014. 2014;5.

(16) Tjotta E, Hungnes O, Grinde B. Survival of HIV-1 activity after disinfection, temperature and pH changes, or drying. J Med Virol 1991 Dec;35(4):223-227.

(17) Kripke C. Antiretroviral prophylaxis for occupational exposure to HIV. Am Fam Physician 2007 Aug 1;76(3):375-376.

(18) Sharp PM, Hahn BH. Origins of HIV and the AIDS pandemic. Cold Spring Harb Perspect Med 2011 Sep;1(1):a006841.

(19) Koop CE. Health and health care for the 21st century: for all the people. Am J Public Health 2006 Dec;96(12):2090-2092.

(20) Alimonti JB, Ball TB, Fowke KR. Mechanisms of CD4+ T lymphocyte cell death in human immunodeficiency virus infection and AIDS. J Gen Virol 2003 Jul;84(Pt 7):1649-1661.

(21) Voisset C, Weiss RA, Griffiths DJ. Human RNA "rumor" viruses: the search for novel human retroviruses in chronic disease. Microbiol Mol Biol Rev 2008 Mar;72(1):157-96, table of contents.

(22) Craigie R, Bushman FD. HIV DNA integration. Cold Spring Harb Perspect Med 2012 Jul;2(7):a006890.

(23) Dimmock NJ, Easton AJ, Leppard K. Introduction to modern virology. 6th ed. Malden, MA: Blackwell Pub.; 2007.

(24) Chan DC, Kim PS. HIV entry and its inhibition. Cell 1998 May 29;93(5):681-684.

(25) Moss JA. HIV/AIDS Review. Radiol Technol 2013 Jan-Feb;84(3):247-67; quiz p.268-70.

(26) Mehandru S, Poles MA, Tenner-Racz K, Horowitz A, Hurley A, Hogan C, et al. Primary HIV-1 infection is associated with preferential depletion of CD4+ T lymphocytes from effector sites in the gastrointestinal tract. J Exp Med 2004 Sep 20;200(6):761-770.

(27) Das K, Arnold E. HIV-1 reverse transcriptase and antiviral drug resistance. Part 1. Curr Opin Virol 2013 Apr;3(2):111-118.

(28) Doitsh G, Cavrois M, Lassen KG, Zepeda O, Yang Z, Santiago ML, et al. Abortive HIV infection mediates CD4 T cell depletion and inflammation in human lymphoid tissue. Cell 2010 Nov 24;143(5):789-801.

(29) Garg H, Mohl J, Joshi A. HIV-1 induced bystander apoptosis. Viruses 2012 Nov 9;4(11):3020-3043.

(30) Doitsh G, Galloway NL, Geng X, Yang Z, Monroe KM, Zepeda O, et al. Cell death by pyroptosis drives CD4 T-cell depletion in HIV-1 infection. Nature 2014 Jan 23;505(7484):509-514.

(31) Monroe KM, Yang Z, Johnson JR, Geng X, Doitsh G, Krogan NJ, et al. IFI16 DNA sensor is required for death of lymphoid CD4 T cells abortively infected with HIV. Science 2014 Jan 24;343(6169):428-432.

(32) Cowman AF, Berry D, Baum J. The cellular and molecular basis for malaria parasite invasion of the human red blood cell. J Cell Biol 2012 Sep 17;198(6):961-971.

(33) Giribaldi G, Ulliers D, Schwarzer E, Roberts I, Piacibello W, Arese P. Hemozoin- and 4-hydroxynonenal-mediated inhibition of erythropoiesis. Possible role in malarial dyserythropoiesis and anemia. Haematologica 2004 Apr;89(4):492-493.

(34) Fitch CD, Chevli R, Kanjananggulpan P, Dutta P, Chevli K, Chou AC. Intracellular ferriprotoporphyrin IX is a lytic agent. Blood 1983 Dec;62(6):1165-1168.

(35) Sullivan DJ,Jr, Gluzman IY, Russell DG, Goldberg DE. On the molecular mechanism of chloroquine's antimalarial action. Proc Natl Acad Sci U S A 1996 Oct 15;93(21):11865-11870.

(36) Greenwood B, Mutabingwa T. Malaria in 2002. Nature 2002 Feb 7;415(6872):670-672.

(37) Nadjm B, Behrens RH. Malaria: an update for physicians. Infect Dis Clin North Am 2012 Jun;26(2):243-259.

(38) McMahon-Pratt D, Alexander J. Does the Leishmania major paradigm of pathogenesis and protection hold for New World cutaneous leishmaniases or the visceral disease? Immunol Rev 2004 Oct;201:206-224.

(39) Rougeron V, De Meeus T, Kako Ouraga S, Hide M, Banuls AL. "Everything you always wanted to know about sex (but were afraid to ask)" in Leishmania after two decades of laboratory and field analyses. PLoS Pathog 2010 Aug 19;6(8):e1001004.

(40) Sundar S, Chakravarty J. Leishmaniasis: an update of current pharmacotherapy. Expert Opin Pharmacother 2013 Jan;14(1):53-63.

(41) Lozano R, Naghavi M, Foreman K, Lim S, Shibuya K, Aboyans V, et al. Global and regional mortality from 235 causes of death for 20 age groups in 1990 and 2010: a systematic analysis for the Global Burden of Disease Study 2010. Lancet 2012 Dec 15;380(9859):2095-2128.

(42) Krafts KP, Hempelmann E, Oleksyn BJ. The color purple: from royalty to laboratory, with apologies to Malachowski. Biotech Histochem 2011 Feb;86(1):7-35.

(43) Srivastava P, Dayama A, Mehrotra S, Sundar S. Diagnosis of visceral leishmaniasis. Trans R Soc Trop Med Hyg 2011 Jan;105(1):1-6.

(44) Lewis SM, Bain BJ, Bates I, Dacie JV, Dacie JV. Dacie and Lewis practical haematology. 10th ed. Philadelphia: Churchill Livingstone/Elsevier; 2006.

(45) Nikon Inc. "E200-LED Educational Microscope". Available at: http://www.nikon-instruments.com/layout/set/print/Store/E200. Accessed 05/02, 2015.

(46) Ridzon R, Gallagher K, Ciesielski C, Ginsberg MB, Robertson BJ, Luo CC, et al. Simultaneous transmission of human immunodeficiency virus and hepatitis C virus from a needle-stick injury. N Engl J Med 1997 Mar 27;336(13):919-922.

(47) Chronister CL. Serologic confirmation of HIV infection. Optom Vis Sci 1995 May;72(5):299-301.

(48) Chou R, Huffman LH, Fu R, Smits AK, Korthuis PT, US Preventive Services Task Force. Screening for HIV: a review of the evidence for the U.S. Preventive Services Task Force. Ann Intern Med 2005 Jul 5;143(1):55-73.

(49) Ling IT, Cooksley S, Bates PA, Hempelmann E, Wilson RJ. Antibodies to the glutamate dehydrogenase of Plasmodium falciparum. Parasitology 1986 Apr;92 (Pt 2)(Pt 2):313-324.

(50) Lee JH, Jang JW, Cho CH, Kim JY, Han ET, Yun SG, et al. False-positive results for rapid diagnostic tests for malaria in patients with rheumatoid factor. J Clin Microbiol 2014 Oct;52(10):3784-3787.

(51) Humar A, Ohrt C, Harrington MA, Pillai D, Kain KC. Parasight F test compared with the polymerase chain reaction and microscopy for the diagnosis of Plasmodium falciparum malaria in travelers. Am J Trop Med Hyg 1997 Jan;56(1):44-48.

(52) Murray CK, Gasser RA,Jr, Magill AJ, Miller RS. Update on rapid diagnostic testing for malaria. Clin Microbiol Rev 2008 Jan;21(1):97-110.

(53) Chen IT, Aung T, Thant HN, Sudhinaraset M, Kahn JG. Cost-effectiveness analysis of malaria rapid diagnostic test incentive schemes for informal private healthcare providers in Myanmar. Malar J 2015 Feb 5;14(1):55-015-0569-7.

(54) Boelaert M, Verdonck K, Menten J, Sunyoto T, van Griensven J, Chappuis F, et al. Rapid tests for the diagnosis of visceral leishmaniasis in patients with suspected disease. Cochrane Database Syst Rev 2014 Jun 20;6:CD009135.

(55) Strick LB, Wald A. Diagnostics for herpes simplex virus: is PCR the new gold standard? Mol Diagn Ther 2006;10(1):17-28.

(56) Iroegbu J, Birk M, Lazdina U, Sonnerborg A, Sallberg M. Variability and immunogenicity of human immunodeficiency virus type 1 p24 gene quasispecies. Clin Diagn Lab Immunol 2000 May;7(3):377-383.

(57) Li P, Ruel T, Fujimoto K, Hatano H, Yukl S, Eller LA, et al. Novel application of Locked Nucleic Acid chemistry for a Taqman assay for measuring diverse human immunodeficiency virus type 1 subtypes. J Virol Methods 2010 Dec;170(1-2):115-120.

(58) Tolle MA, Schwarzwald HL. Postexposure prophylaxis against human immunodeficiency virus. Am Fam Physician 2010 Jul 15;82(2):161-166.

(59) Beaucage SL. Oligodeoxyribonucleotides synthesis. Phosphoramidite approach. Methods Mol Biol 1993;20:33-61.

(60) Bartlett JM, Stirling D. A short history of the polymerase chain reaction. Methods Mol Biol 2003;226:3-6.

(61) Rittie L, Perbal B. Enzymes used in molecular biology: a useful guide. J Cell Commun Signal 2008 Jun;2(1-2):25-45.

(62) Voet D, Voet JG. Biochemistry. 4th ed. Hoboken, NJ: John Wiley & Sons; 2011.

(63) Saiki RK, Gelfand DH, Stoffel S, Scharf SJ, Higuchi R, Horn GT, et al. Primer-directed enzymatic amplification of DNA with a thermostable DNA polymerase. Science 1988 Jan 29;239(4839):487-491.

(64) Rowe DM. CRC handbook of thermoelectrics. Boca Raton, FL: CRC Press; 1995.

(65) Incropera FP, Incropera FP. Fundamentals of heat and mass transfer. 6th ed. Hoboken, NJ: John Wiley; 2007.

(66) Fisher Scientific I. **Thermo Scientific™ Arktik™ Thermal Cycler**. Available at: http://www.fishersci.com/ecomm/servlet/fsproductdetail_10652_13106393__-1_0. Accessed 05/02, 2015.

(67) LabX Classifieds. **For Sale: ABI Viia7 Real Time PCR System w/384 & 96 Blocks**. Available at: http://www.labx.com/item/abi-viia7-real-time-pcr-system-w-384-96-blocks/595349. Accessed 05/02, 2015.

(68) Poon LL, Wong BW, Ma EH, Chan KH, Chow LM, Abeyewickreme W, et al. Sensitive and inexpensive molecular test for falciparum malaria: detecting Plasmodium falciparum DNA directly from heat-treated blood by loop-mediated isothermal amplification. Clin Chem 2006 Feb;52(2):303-306.

(69) Donk PJ. A Highly Resistant Thermophilic Organism. J Bacteriol 1920 Jul;5(4):373-374.

(70) Bergey DH, Buchanan RE, Gibbons NE, American Society for Microbiology. Bergey's manual of determinative bacteriology. 8th ed. Baltimore: Williams & Wilkins Co; 1974.

(71) Watanabe T, Furukawa S, Hirata J, Koyama T, Ogihara H, Yamasaki M. Inactivation of Geobacillus stearothermophilus spores by high-pressure carbon dioxide treatment. Appl Environ Microbiol 2003 Dec;69(12):7124-7129.

(72) Duguid JP, Marmion BP, Swain RHA, Mackie TJ, Mackie TJ. Mackie & McCartney medical microbiology: a guide to the laboratory diagnosis and control of infection. 13th ed. Edinburgh ; New York: Churchill Livingstone; 1978.

(73) Kiefer JR, Mao C, Hansen CJ, Basehore SL, Hogrefe HH, Braman JC, et al. Crystal structure of a thermostable Bacillus DNA polymerase I large fragment at 2.1 A resolution. Structure 1997 Jan 15;5(1):95-108.

(74) Notomi T, Okayama H, Masubuchi H, Yonekawa T, Watanabe K, Amino N, et al. Loop-mediated isothermal amplification of DNA. Nucleic Acids Res 2000 Jun 15;28(12):E63.

(75) New England Biolabs I. ***Bst* 2.0 DNA Polymerase**. Available at: https://www.neb.com/products/m0537-bst-20-dna-polymerase. Accessed 05/02, 2015.

(76) Kaneko H, Kawana T, Fukushima E, Suzutani T. Tolerance of loop-mediated isothermal amplification to a culture medium and biological substances. J Biochem Biophys Methods 2007 Apr 10;70(3):499-501.

(77) Nagamine K, Hase T, Notomi T. Accelerated reaction by loop-mediated isothermal amplification using loop primers. Mol Cell Probes 2002 Jun;16(3):223-229.

(78) Mori Y, Nagamine K, Tomita N, Notomi T. Detection of loop-mediated isothermal amplification reaction by turbidity derived from magnesium pyrophosphate formation. Biochem Biophys Res Commun 2001 Nov 23;289(1):150-154.

(79) Nzelu CO, Gomez EA, Caceres AG, Sakurai T, Martini-Robles L, Uezato H, et al. Development of a loop-mediated isothermal amplification method for rapid mass-screening of sand flies for Leishmania infection. Acta Trop 2014 Apr;132:1-6.

(80) Han ET. Loop-mediated isothermal amplification test for the molecular diagnosis of malaria. Expert Rev Mol Diagn 2013 Mar;13(2):205-218.

(81) Geojith G, Dhanasekaran S, Chandran SP, Kenneth J. Efficacy of loop mediated isothermal amplification (LAMP) assay for the laboratory identification of Mycobacterium tuberculosis isolates in a resource limited setting. J Microbiol Methods 2011 Jan;84(1):71-73.

(82) Jiang T, Liu J, Deng YQ, Su JL, Xu LJ, Liu ZH, et al. Development of RT-LAMP and real-time RT-PCR assays for the rapid detection of the new duck Tembusu-like BYD virus. Arch Virol 2012 Dec;157(12):2273-2280.

(83) Curtis KA, Rudolph DL, Owen SM. Rapid detection of HIV-1 by reverse-transcription, loop-mediated isothermal amplification (RT-LAMP). J Virol Methods 2008 Aug;151(2):264-270.

(84) Zhao X, Chen X, Zhang Y, He X, Li W, Shi L, et al. Development and evaluation of reverse-transcription loop-mediated isothermal amplification for rapid detection of human immunodeficiency virus type 1. Indian J Med Microbiol 2012 Oct-Dec;30(4):391-396.

(85) Takagi H, Itoh M, Islam MZ, Razzaque A, Ekram AR, Hashighuchi Y, et al. Sensitive, specific, and rapid detection of Leishmania donovani DNA by loop-mediated isothermal amplification. Am J Trop Med Hyg 2009 Oct;81(4):578-582.

(86) Gray PR. Analysis and design of analog integrated circuits. 5th ed. New York: Wiley; 2009.

(87) Saetiew C, Limpaiboon T, Jearanaikoon P, Daduang S, Pientong C, Kerdsin A, et al. Rapid detection of the most common high-risk human papillomaviruses by loop-mediated isothermal amplification. J Virol Methods 2011 Dec;178(1-2):22-30.

(88) Tomita N, Mori Y, Kanda H, Notomi T. Loop-mediated isothermal amplification (LAMP) of gene sequences and simple visual detection of products. Nat Protoc 2008;3(5):877-882.

(89) Newark I. **NTE ELECTRONICS WH22-00-100 HOOK UP WIRE, 100FT, 22AWG COPPER, BLACK**. Available at: http://canada.newark.com/nte-electronics/wh22-00-100/hook-up-wire-100ft-22awg-copper/dp/33C7334. Accessed 05/02, 2015.

(90) Tie Z, Chunguang W, Xiaoyuan W, Xinghua Z, Xiuhui Z. Loop-mediated isothermal amplification for detection of Staphylococcus aureus in dairy cow suffering from mastitis. J Biomed Biotechnol 2012;2012:435982.

(91) Life Technologies I. **Oligo Purity Selection Guide**. Available at: https://www.lifetechnologies.com/ca/en/home/products-and-services/product-types/primers-oligos-nucleotides/invitrogen-custom-dna-oligos/oligo-ordering-details/oligo-purity-selection-guide.html. Accessed 05/02, 2015.

(92) Nimesh M, Joon D, Varma-Basil M, Saluja D. Development and clinical evaluation of sdaA loop-mediated isothermal amplification assay for detection of Mycobacterium tuberculosis with an approach to prevent carryover contamination. J Clin Microbiol 2014 Jul;52(7):2662-2664.

(93) He L, Xu HS, Wang MZ, Rong HN. Development of rapid detection of infectious hypodermal and hematopoietic necrosis virus by loop-mediated isothermal amplification. Bing Du Xue Bao 2010 Nov;26(6):490-495.

(94) LaBarre P, Hawkins KR, Gerlach J, Wilmoth J, Beddoe A, Singleton J, et al. A simple, inexpensive device for nucleic acid amplification without electricity-toward instrument-free molecular diagnostics in low-resource settings. PLoS One 2011 May 9;6(5):e19738.

(95) New England Biolabs I. ***Bst* 2.0 WarmStart® DNA Polymerase**. Available at: https://www.neb.ca/detail.php?id=M0538. Accessed 05/02, 2015.

(96) Mair G, Vilei EM, Wade A, Frey J, Unger H. Isothermal loop-mediated amplification (LAMP) for diagnosis of contagious bovine pleuro-pneumonia. BMC Vet Res 2013 May 27;9:108-6148-9-108.

(97) Nzelu CO, Gomez EA, Caceres AG, Sakurai T, Martini-Robles L, Uezato H, et al. Development of a loop-mediated isothermal amplification method for rapid mass-screening of sand flies for Leishmania infection. Acta Trop 2014 Apr;132:1-6.

8. FIGURE REFERENCES

[1] “Figure 1: World wealth levels in year 2000.”: Davies JB, Sandström S, Shorrocks A, Wolff EN. The world distribution of household wealth. WIDER Discussion Paper. UNU-WIDER. 2008 Feb;2008/03 [Online] Available from: http://www.wider.unu.edu/publications/working-papers/discussion-papers/2008/en_GB/dp2008-03/
Accessed 05/02, 2015.

[2] “World: Adult HIV prevalence (15-49 years), 2013 – By WHO Region”: World Health Organization (WHO). [Online] Available from: http://gamapserver.who.int/mapLibrary/app/searchResults.aspx
Accessed 06/23, 2015.

[3] “Figure 1: Schematic overview of the HIV-1 replication cycle.”: Engelman A, Cherepanov P. The structural biology of HIV-1: mechanistic and therapeutic insights. Nat Rev Microbiol 2012 Mar;10(4):279-290.
Reprinted with permission: see Appendix III (License ID [3]).

[4] “Countries with ongoing transmission of malaria, 2013”: World Health Organization (WHO). [Online] Available from: http://www.who.int/gho/malaria/malaria_003.jpg?ua=1
Accessed 06/23, 2015.

[5] “Status of endemicity of leishmaniasis, worldwide, 2013”: World Health Organization (WHO). [Online] Available from: http://gamaps-erver.who.int/mapLibrary/Files/Maps/Leishmaniasis_2013_VL.png
Accessed 06/23, 2015.

[6] “Figure1. Schematic diagram of the mechanism of LAMP.”: Notomi T, Okayama H, Masubuchi H, Yonekawa T, Watanabe K, Amino N, et al. Loop-mediated isothermal amplification of DNA. Nucleic Acids Res 2000 Jun 15;28(12):E63.
Reprinted with permission: see Appendix III (License ID [6])

[7] “Fig. 3. B”: Nagamine K, Hase T, Notomi T. Accelerated reaction by loop-mediated isothermal amplification using loop primers. Mol Cell Probes 2002 Jun;16(3):223-229.
Reprinted with permission: see Appendix III (License ID [7])

APPENDIX I: Prototype Component Data-Sheets

1. HR-DF3 battery pack:

FDK TWICELL

Cell Type HR-D

Specifications

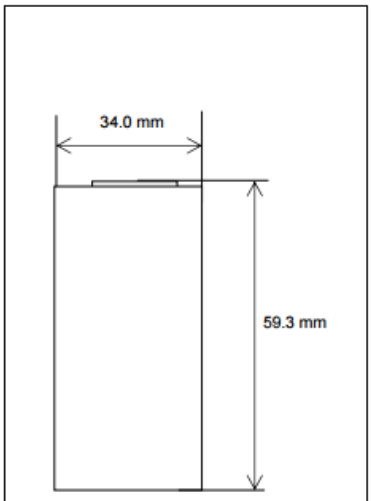

Dimensions (with tube)	D	34.0 mm
	H	59.3 mm

Type : Nickel-Metal Hydride Battery			Size : D
Capacity 1)	Typical		7300mAh
	Minimum		6500mAh
Nominal Voltage			1.2V
Charging Current x Time		Fast Charge 2)	5000 mA x about 1.7h
Ambient Temp.	Charge Condition	Fast Charge 2)	0℃ - 40℃
	Discharge Condition		0℃ - 50℃
	Storage Condition	Less than 30days	-20℃ - 50℃
		Less than 90days	-20℃ - 40℃
		Less than 1year	-20℃ - 30℃
Internal Impedance 3) (after discharge to E.V.=1.0V)			Approx. 5mΩ(at 1000Hz)
Weight 4)			Approx. 175 g
Size 4) :(Diameter) x (Height)			34.0(D) x 59.3(H) mm

1)Single cell capacity under the following condition.
Charge : 730mA×16h, Discharge : 1460mA(E.V.=1.0V) at 20℃
2)Use recommended charging system.
3)After a few charge and discharge cycles under the above 1) condition.
4)With tube.

Typical Characteristics

Charge

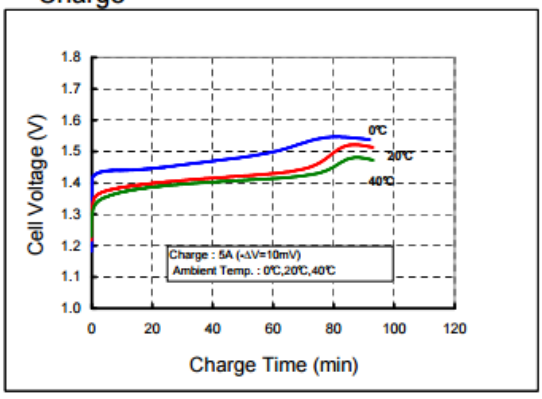

Discharge

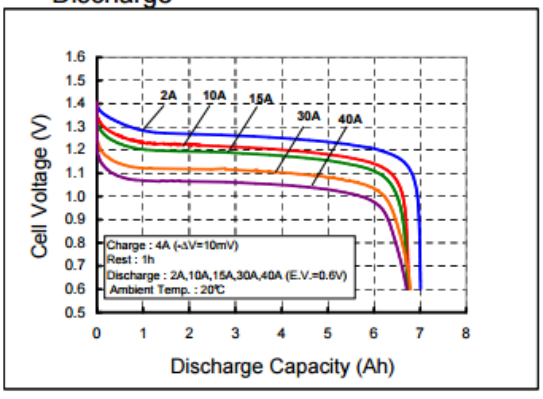

2010/03

2. 405nm LED:

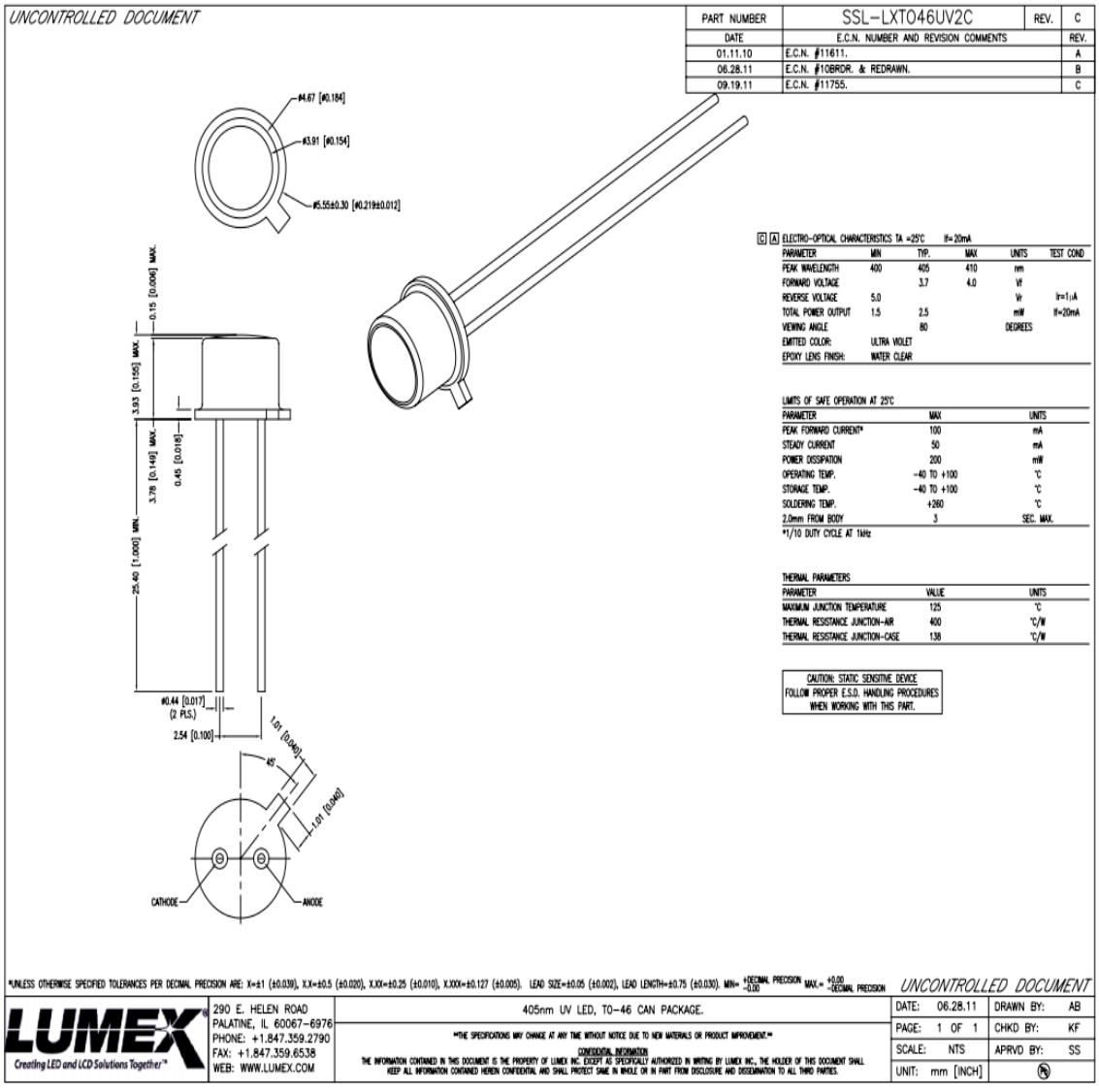
UNCONTROLLED DOCUMENT
PART NUMBER
SSL-LXT046UV2C
REV.
C
DATE
E.C.N. NUMBER AND REVISION COMMENTS
REV.
01.11.10
E.C.N. #11611.
A
06.28.11
E.C.N. #10BROR. & REDRAWN.
B
09.19.11
E.C.N. #11755.
C
ELECTRO-OPTICAL CHARACTERISTICS TA =25°C If=20mA
PARAMETER
MIN
TYP.
MAX
UNITS
TEST COND
PEAK WAVELENGTH
400
405
410
nm
FORWARD VOLTAGE
3.7
4.0
Vf
REVERSE VOLTAGE
5.0
Vr
Ir=1μA
TOTAL POWER OUTPUT
1.5
2.5
mW
If=20mA
VIEWING ANGLE
80
DEGREES
EMITTED COLOR:
ULTRA VIOLET
EPOXY LENS FINISH:
WATER CLEAR
LIMITS OF SAFE OPERATION AT 25°C
PARAMETER
MAX
UNITS
PEAK FORWARD CURRENT*
100
mA
STEADY CURRENT
50
mA
POWER DISSIPATION
200
mW
OPERATING TEMP.
-40 TO +100
°C
STORAGE TEMP.
-40 TO +100
°C
SOLDERING TEMP.
+260
°C
2.0mm FROM BODY
3
SEC. MAX.
*1/10 DUTY CYCLE AT 1kHz
THERMAL PARAMETERS
PARAMETER
VALUE
UNITS
MAXIMUM JUNCTION TEMPERATURE
125
°C
THERMAL RESISTANCE JUNCTION-AIR
400
°C/W
THERMAL RESISTANCE JUNCTION-CASE
138
°C/W
CAUTION: STATIC SENSITIVE DEVICE
FOLLOW PROPER E.S.D. HANDLING PROCEDURES
WHEN WORKING WITH THIS PART.
ø4.67 [ø0.184]
ø3.91 [ø0.154]
ø5.55±0.30 [ø0.219±0.012]
0.15 [0.006] MAX.
3.93 [0.155] MAX.
3.78 [0.149] MAX.
0.45 [0.018]
25.40 [1.000] MIN.
ø0.44 [0.017]
(2 PLS.)
2.54 [0.100]
1.01 [0.040]
45°
1.01 [0.040]
CATHODE
ANODE
*UNLESS OTHERWISE SPECIFIED TOLERANCES PER DECIMAL PRECISION ARE: X=±1 (±0.039), X.X=±0.5 (±0.020), X.XX=±0.25 (±0.010), X.XXX=±0.127 (±0.005). LEAD SIZE=±0.05 (±0.002), LEAD LENGTH=±0.75 (±0.030). MIN= +DECIMAL PRECISION -0.00 MAX.= +0.00 -DECIMAL PRECISION
UNCONTROLLED DOCUMENT
LUMEX
Creating LED and LCD Solutions Together™
290 E. HELEN ROAD
PALATINE, IL 60067-6976
PHONE: +1.847.359.2790
FAX: +1.847.359.6538
WEB: WWW.LUMEX.COM
405nm UV LED, TO-46 CAN PACKAGE.
THE SPECIFICATIONS MAY CHANGE AT ANY TIME WITHOUT NOTICE DUE TO NEW MATERIALS OR PRODUCT IMPROVEMENT.
CONFIDENTIAL INFORMATION
THE INFORMATION CONTAINED IN THIS DOCUMENT IS THE PROPERTY OF LUMEX INC. EXCEPT AS SPECIFICALLY AUTHORIZED IN WRITING BY LUMEX INC., THE HOLDER OF THIS DOCUMENT SHALL KEEP ALL INFORMATION CONTAINED HEREIN CONFIDENTIAL AND SHALL PROTECT SAME IN WHOLE OR IN PART FROM DISCLOSURE AND DISSEMINATION TO ALL THIRD PARTIES.
DATE: 06.28.11
DRAWN BY: AB
PAGE: 1 OF 1
CHKD BY: KF
SCALE: NTS
APRVD BY: SS
UNIT: mm [INCH]

3. UI-1222LE-M-GL camera:

All uEye®LE Features at a Glance

CS-Mount Housing Model	UI-1225LE-C/M	UI-1545LE-M	UI-1645LE-C	UI-1555LE-C	UI-1465LE-C	UI-1485LE-C/M
S-Mount, M12 Model	UI-1226LE-C/M	UI-1546LE-M	UI-1646LE-C	UI-1556LE-C	UI-1466LE-C	UI-1486LE-C/M
S-Mount, M14 Model	-	UI-1547LE-M	-	-	UI-1467LE-C	UI-1487LE-C/M
Boardlevel Model	UI-1228LE-C/M	UI-1548LE-M	UI-1648LE-C	UI-1558LE-C	UI-1468LE-C	UI-1488LE-C/M
CMOS Sensor	Monochrome/RGB Color	Monochrome	RGB Color	RGB Color	RGB Color	Monochrome/RGB Color
Resolution	752 x 480	1280 x 1024	1280 x 1024	1600 x 1200	2048 x 1536	2560 x 1920
Resolution Category / Pixel Class	WVGA	SXGA/1.3 MP	SXGA/1.3 MP	UXGA/2 MP	SUXGA/3,3 MP	QSXGA/5 MP
Sensor Class	1/3"	1/2"	1/3"	1/3"	1/2"	1/2"
Shutter	Global	Rolling	Rolling	Rolling	Rolling	Rolling/Global Start
max. fps in Freerun Mode at full resolution	87 fps	25 fps	25 fps	18 fps	11 fps	6 fps
Exposure Time in Freerun Mode	80 µs - 5,5 s	35 µs - 980 ms	37 µs - 10 s	39 µs - 13,4 s	57 µs - 1,75 s	71 µs- 2,74 s
AOI Modes	$H^2 + V^2$	$H^2 + V^2$	$H^2 + V^2$	$H^2 + V^2$	$H^2 + V^2$	$H^2 + V^2$
AOI with 320 x 240 Pixels (CIF)	215 fps	232 fps	270 fps	240 fps	220 fps	126 fps
Subsampling Modes	-	$H^2 + V^2$ (pairing)	$H^2 + V^2$	$H^2 + V^2$	$H^2 + V^2$	$H^2 + V^2$
Subsampling Factores	-	x2, x4	x2, x4	x2, x4	x2, x4	x2, x4
Resolution, fps	-	640 x 512, 79 fps	640 x 512, 83 fps	800 x 600, 59 fps	1024 x 768, 37 fps	1280 x 960, 19 fps
	-	320 x 256, 219 fps	320 x 256, 248 fps	400 x 300, 172 fps	512 x 384, 113 fps	640 x 480, 53 fps
Binning Modes	$H + V^2$ (Mono)	-	-	$H^2 + V^2$	$H^2 + V^2$	$H^2 + V^2$
Binning Method	H + V: Average	-	-	H + V: Average	H: Sum V: Average	H: Sum V: Average
Binning Factors	x2, x4	-	-	x2	x2, x4	x2, Color: x4
Resolution, fps	368 x 240, 162 fps	-	-	800 x 600, 52 fps	1024 x 768, 30 fps	1280 x 960, 15 fps
	176 x 120, 286 fps				512 x 384, 52 fps	640 x 480, 23 fps
I/Os	LE models xxx6, xxx7, xxx8: trigger in, flash out, 2 digital outs (TTL compatible)					
Sensor Model	MT9V032	MT9M001	MT9M131	MT9D131	MT9T001	MT9P031
Pixel Clock	5 - 40 MHz	5 - 43 MHz	5 - 40 MHz	5 - 40 MHz	5 - 43 MHz	5 - 43 MHz
Pixelpitch in µm	6,0	5,2	3,6	2,8	3,2	2,2
Optical Size	4,51 x 2,88 mm	6,66 x 5,32 mm	4,61 x 3,69 mm	4,48 x 3,36 mm	6,55 x 4,92 mm	5,63 x 4,22 mm
Aspect Ratio	14:9	5:4	5:4	4:3	4:3	4:3
Exact Real Diagonal	5,4 mm	8,5 mm	5,9 mm	5,6 mm	8,2 mm	7,0 mm
Exact Real Diagonal	1/3,0"	1/1,9"	1/2,7"	1/2,9"	1/2,0"	1/2,3"
Regulations	CE class A, CE class B, FCC (depending on model)					

[2] Function increases frame rate
Performance data is based on driver 3.22

APPENDIX II: Table of Wire Resistance per 1000ft and per Kilometer by awg for Copper Wires

AWG gauge	Conductor Diameter Inches	Conductor Diameter mm	Ohms per 1000 ft.	Ohms per km
OOOO	0.46	11.684	0.049	0.16072
OOO	0.4096	10.40384	0.0618	0.202704
OO	0.3648	9.26592	0.0779	0.255512
0	0.3249	8.25246	0.0983	0.322424
1	0.2893	7.34822	0.1239	0.406392
2	0.2576	6.54304	0.1563	0.512664
3	0.2294	5.82676	0.197	0.64616
4	0.2043	5.18922	0.2485	0.81508
5	0.1819	4.62026	0.3133	1.027624
6	0.162	4.1148	0.3951	1.295928
7	0.1443	3.66522	0.4982	1.634096
8	0.1285	3.2639	0.6282	2.060496
9	0.1144	2.90576	0.7921	2.598088
10	0.1019	2.58826	0.9989	3.276392
11	0.0907	2.30378	1.26	4.1328
12	0.0808	2.05232	1.588	5.20864
13	0.072	1.8288	2.003	6.56984
14	0.0641	1.62814	2.525	8.282
15	0.0571	1.45034	3.184	10.44352
16	0.0508	1.29032	4.016	13.17248
17	0.0453	1.15062	5.064	16.60992
18	0.0403	1.02362	6.385	20.9428
19	0.0359	0.91186	8.051	26.40728
20	0.032	0.8128	10.15	33.292
21	0.0285	0.7239	12.8	41.984
22	0.0254	0.64516	16.14	52.9392
23	0.0226	0.57404	20.36	66.7808
24	0.0201	0.51054	25.67	84.1976
25	0.0179	0.45466	32.37	106.1736
26	0.0159	0.40386	40.81	133.8568
27	0.0142	0.36068	51.47	168.8216
28	0.0126	0.32004	64.9	212.872

29	0.0113	0.28702	81.83	268.4024
30	0.01	0.254	103.2	338.496
31	0.0089	0.22606	130.1	426.728
32	0.008	0.2032	164.1	538.248
Metric 2.0	0.00787	0.2	169.39	555.61
33	0.0071	0.18034	206.9	678.632
Metric 1.8	0.00709	0.18	207.5	680.55
34	0.0063	0.16002	260.9	855.752
Metric 1.6	0.0063	0.16002	260.9	855.752
35	0.0056	0.14224	329	1079.12
Metric 1.4	0.00551	0.14	339	1114
36	0.005	0.127	414.8	1360
Metric 1.25	0.00492	0.125	428.2	1404
37	0.0045	0.1143	523.1	1715
Metric 1.12	0.00441	0.112	533.8	1750
38	0.004	0.1016	659.6	2163
Metric 1	0.00394	0.1	670.2	2198
39	0.0035	0.0889	831.8	2728
40	0.0031	0.07874	1049	3440

Source: Mark Lund, PowerStream, Inc. “American Wire Gauge Table and AWG Electrical Current Load Limits. [Online] Available from: http://www.powerstream.com/Wire_Size.htm

Accessed 05/02, 2015.

APPENDIX III: Licenses for Reprinting of Copyrighted Figures

[3]

NATURE PUBLISHING GROUP LICENSE TERMS AND CONDITIONS

Apr 30, 2015

This is a License Agreement between Paul M Mintchev ("You") and Nature Publishing Group ("Nature Publishing Group") provided by Copyright Clearance Center ("CCC"). The license consists of your order details, the terms and conditions provided by Nature Publishing Group, and the payment terms and conditions.

All payments must be made in full to CCC. For payment instructions, please see information listed at the bottom of this form.

License Number

3618980600086

License date

Apr 30, 2015

Licensed content publisher

Nature Publishing Group

Licensed content publication

Nature Reviews Microbiology

Licensed content title

The structural biology of HIV-1: mechanistic and therapeutic insights

Licensed content author

Alan Engelman and Peter Cherepanov

Licensed content date

Apr 1, 2012

Volume number

10

Issue number

4

Type of Use

reuse in a dissertation / thesis

Requestor type

academic/educational

Format

print and electronic

Portion

figures/tables/illustrations

Number of figures/tables/illustrations

1

High-res required

no

Figures

FIGURE 3: Schematic representation of the HIV cycle of infection/replication, with some common drug therapies listed at the steps they inhibit.

Author of this NPG article

no

Your reference number

None

Title of your thesis / dissertation

Loop-Mediated Isothermal Amplification for Diagnosis of Major Infectious Diseases in Resource-Limited Seetings

Expected completion date

Jun 2015

Estimated size (number of pages)

110

Total

0.00 CAD

Terms and Conditions

Terms and Conditions for Permissions

Nature Publishing Group hereby grants you a non-exclusive license to reproduce this material for this purpose, and for no other use,subject to the conditions below:

1. NPG warrants that it has, to the best of its knowledge, the rights to license reuse of this material. However, you should ensure that the material you are requesting is original to Nature Publishing Group and does not carry the copyright of another entity (as credited in the published version). If the credit line on any part of the material you have requested indicates that it was reprinted or adapted by NPG with permission from another source, then you should also seek permission from that source to reuse the material.

2. Permission granted free of charge for material in print is also usually granted for any electronic version of that work, provided that the material is incidental to the work as a whole and that the electronic version is essentially equivalent to, or substitutes for, the print version.Where print permission has been granted for a fee, separate permission must be obtained for any additional, electronic re-use (unless, as in the case of a full paper, this has already been accounted for during your initial request in the calculation of a print run).NB: In all cases, web-based use of full-text articles must be authorized separately through the 'Use on a Web Site' option when requesting permission.

3. Permission granted for a first edition does not apply to second and subsequent editions and for editions in other languages (except for signatories to the STM Permissions Guidelines, or where the first edition permission was granted for free).

4. Nature Publishing Group's permission must be acknowledged next to the figure, table or abstract in print. In electronic form, this acknowledgement must be visible at the same time as the figure/table/abstract, and must be hyperlinked to the journal's homepage.

5. The credit line should read:
   Reprinted by permission from Macmillan Publishers Ltd: [JOURNAL NAME] (reference citation), copyright (year of publication)
   For AOP papers, the credit line should read:
   Reprinted by permission from Macmillan Publishers Ltd: [JOURNAL NAME], advance online publication, day month year (doi: 10.1038/sj.[JOURNAL ACRONYM].XXXXX)

Note: For republication from the *British Journal of Cancer*, the following credit lines apply.
Reprinted by permission from Macmillan Publishers Ltd on behalf of Cancer Research UK: [JOURNAL NAME] (reference citation), copyright (year of publication)For AOP papers, the credit line should read:
Reprinted by permission from Macmillan Publishers Ltd on behalf of Cancer Research UK: [JOURNAL NAME], advance online publication, day month year (doi: 10.1038/sj.[JOURNAL ACRONYM].XXXXX)

6. Adaptations of single figures do not require NPG approval. However, the adaptation should be credited as follows:

   Adapted by permission from Macmillan Publishers Ltd: [JOURNAL NAME] (reference citation), copyright (year of publication)

   Note: For adaptation from the *British Journal of Cancer*, the following credit line applies.
   Adapted by permission from Macmillan Publishers Ltd on behalf of Cancer Research UK: [JOURNAL NAME] (reference citation), copyright (year of publication)

7. Translations of 401 words up to a whole article require NPG approval. Please visithttp://www.macmillanmedicalcommunications.com for more information.Translations of up to a 400 words do not require NPG approval. The translation should be credited as follows:

   Translated by permission from Macmillan Publishers Ltd: [JOURNAL NAME] (reference citation), copyright (year of publication).

   Note: For translation from the *British Journal of Cancer*, the following credit line applies.
   Translated by permission from Macmillan Publishers Ltd on behalf of Cancer Research UK: [JOURNAL NAME] (reference citation), copyright (year of publication)

We are certain that all parties will benefit from this agreement and wish you the best in the use of this material. Thank you.

Special Terms:

v1.1

Questions? customercare@copyright.com or +1-855-239-3415 (toll free in the US) or +1-978-646-2777.

Gratis licenses (referencing $0 in the Total field) are free. Please retain this printable license for your reference. No payment is required.

[6]

OXFORD UNIVERSITY PRESS LICENSE

TERMS AND CONDITIONS

May 03, 2015

This is a License Agreement between Paul M Mintchev ("You") and Oxford University Press ("Oxford University Press") provided by Copyright Clearance Center ("CCC"). The license consists of your order details, the terms and conditions provided by Oxford University Press, and the payment terms and conditions.

All payments must be made in full to CCC. For payment instructions, please see information listed at the bottom of this form.

License Number	3621581094039
License date	May 03, 2015
Licensed content publisher	Oxford University Press
Licensed content publication	Nucleic Acids Research
Licensed content title	Loop-mediated isothermal amplification of DNA:
Licensed content author	Tsugunori Notomi, Hiroto Okayama, Harumi Masubuchi, Toshihiro Yonekawa, Keiko Watanabe, Nobuyuki Amino, Tetsu Hase
Licensed content date	06/15/2000
Type of Use	Thesis/Dissertation
Institution name	None

Title of your work	Loop-Mediated Isothermal Amplification for Diagnosis of Major Infectious Diseases in Resource-Limited Seetings
Publisher of your work	n/a
Expected publication date	Jun 2015
Permissions cost	0.00 USD
Value added tax	0.00 USD
Total	0.00 USD
Total	0.00 USD

Terms and Conditions

STANDARD TERMS AND CONDITIONS FOR REPRODUCTION OF MATERIAL FROM AN OXFORD UNIVERSITY PRESS JOURNAL

1. Use of the material is restricted to the type of use specified in your order details.

2. This permission covers the use of the material in the English language in the following territory: world. If you have requested additional permission to translate this material, the terms and conditions of this reuse will be set out in clause 12.

3. This permission is limited to the particular use authorized in (1) above and does not allow you to sanction its use elsewhere in any other format other than specified above, nor does it apply to quotations, images, artistic works etc that have been reproduced from other sources which may be part of the material to be used.

4. No alteration, omission or addition is made to the material without our written consent. Permission must be re-cleared with Oxford University Press if/when you decide to reprint.

5. The following credit line appears wherever the material is used: author, title, journal, year, volume, issue number, pagination, by permission of Oxford University Press or the sponsoring society if the journal is a society journal. Where a journal is being published on behalf of a learned society, the details of that society must be included in the credit line.

6. For the reproduction of a full article from an Oxford University Press journal for whatever purpose, the corresponding author of the material concerned should be informed of the proposed use. Contact details for the corresponding authors of all Oxford University Press journal contact can be found alongside either the abstract or full text of the article concerned, accessible from www.oxfordjournals.org Should there be a problem clearing these rights, please contact journals.permissions@oup.com

7. If the credit line or acknowledgement in our publication indicates that any of the figures, images or photos was reproduced, drawn or modified from an earlier source it will be necessary for you to clear this permission with the original publisher as well. If this permission has not been obtained, please note that this material cannot be included in your publication/photocopies.

8. While you may exercise the rights licensed immediately upon issuance of the license at the end of the licensing process for the transaction, provided that you have disclosed complete and accurate details of your proposed use, no license is finally effective unless and until full payment is received from you (either by Oxford University Press or by Copyright Clearance Center (CCC)) as provided in CCC's Billing and Payment terms and conditions. If full payment is not received on a timely basis, then any license preliminarily granted shall be deemed automatically revoked and shall be void as if never granted. Further, in the event that you breach any of these terms and conditions or any of CCC's Billing and Payment terms and conditions, the license is automatically revoked and shall be void as if never granted. Use of materials as described in a revoked license, as well as any use of the materials beyond the scope of an unrevoked license, may constitute copyright infringement and Oxford University Press reserves the right to take any and all action to protect its copyright in the materials.

9. This license is personal to you and may not be sublicensed, assigned or transferred by you to any other person without Oxford University Press's written permission.

10. Oxford University Press reserves all rights not specifically granted in the combination of (i) the license details provided by you and accepted in the course of this licensing transaction, (ii) these terms and conditions and (iii) CCC's Billing and Payment terms and conditions.

11. You hereby indemnify and agree to hold harmless Oxford University Press and CCC, and their respective officers, directors, employs and agents, from and against any and all claims arising out of your use of the licensed material other than as specifically authorized pursuant to this license.

12. Other Terms and Conditions:

v1.4

Questions? customercare@copyright.com or +1-855-239-3415 (toll free in the US) or+1-978-646-2777.

Gratis licenses (referencing $0 in the Total field) are free. Please retain this printable license for your reference. No payment is required.

[7]

ELSEVIER LICENSE

TERMS AND CONDITIONS

May 03, 2015

This is a License Agreement between Paul M Mintchev ("You") and Elsevier ("Elsevier") provided by Copyright Clearance Center ("CCC"). The license consists of your order details, the terms and conditions provided by Elsevier, and the payment terms and conditions.

All payments must be made in full to CCC. For payment instructions, please see information listed at the bottom of this form.

Supplier	Elsevier Limited The Boulevard,Langford Lane Kidlington,Oxford,OX5 1GB,UK
Registered Company Number	1982084
Customer name	Paul M Mintchev
Customer address	3280 Hospital Drive NW Calgary, AB T2N 4N1
License number	3621601203014
License date	May 03, 2015
Licensed content publisher	Elsevier
Licensed content publication	Molecular and Cellular Probes

Licensed content title	Accelerated reaction by loop-mediated isothermal amplification using loop primers
Licensed content author	K. Nagamine,T. Hase,T. Notomi
Licensed content date	June 2002
Licensed content volume number	16
Licensed content issue number	3
Number of pages	7
Start Page	223
End Page	229
Type of Use	reuse in a thesis/dissertation
Intended publisher of new work	other
Portion	figures/tables/illustrations
Number of figures/tables/illustrations	1
Format	both print and electronic
Are you the author of this Elsevier article?	No
Will you be translating?	No
Original figure numbers	Figure 3B

Title of your thesis/dissertation	Loop-Mediated Isothermal Amplification for Diagnosis of Major Infectious Diseases in Resource-Limited Seetings
Expected completion date	Jun 2015
Estimated size (number of pages)	110
Elsevier VAT number	GB 494 6272 12
Permissions price	0.00 CAD
VAT/Local Sales Tax	0.00 CAD / 0.00 GBP
Total	0.00 CAD

Terms and Conditions

INTRODUCTION

1. The publisher for this copyrighted material is Elsevier. By clicking "accept" in connection with completing this licensing transaction, you agree that the following terms and conditions apply to this transaction (along with the Billing and Payment terms and conditions established by Copyright Clearance Center, Inc. ("CCC"), at the time that you opened your Rightslink account and that are available at any time at http://myaccount.copyright.com).

GENERAL TERMS

2. Elsevier hereby grants you permission to reproduce the aforementioned material subject to the terms and conditions indicated.

3. Acknowledgement: If any part of the material to be used (for example, figures) has appeared in our publication with credit or acknowledgement to another source, permission must also be sought from

that source. If such permission is not obtained then that material may not be included in your publication/copies. Suitable acknowledgement to the source must be made, either as a footnote or in a reference list at the end of your publication, as follows:

"Reprinted from Publication title, Vol /edition number, Author(s), Title of article / title of chapter, Pages No., Copyright (Year), with permission from Elsevier [OR APPLICABLE SOCIETY COPYRIGHT OWNER]." Also Lancet special credit - "Reprinted from The Lancet, Vol. number, Author(s), Title of article, Pages No., Copyright (Year), with permission from Elsevier."

4. Reproduction of this material is confined to the purpose and/or media for which permission is hereby given.

5. Altering/Modifying Material: Not Permitted. However figures and illustrations may be altered/adapted minimally to serve your work. Any other abbreviations, additions, deletions and/or any other alterations shall be made only with prior written authorization of Elsevier Ltd. (Please contact Elsevier atpermissions@elsevier.com)

6. If the permission fee for the requested use of our material is waived in this instance, please be advised that your future requests for Elsevier materials may attract a fee.

7. Reservation of Rights: Publisher reserves all rights not specifically granted in the combination of (i) the license details provided by you and accepted in the course of this licensing transaction, (ii) these terms and conditions and (iii) CCC's Billing and Payment terms and conditions.

8. License Contingent Upon Payment: While you may exercise the rights licensed immediately upon issuance of the license at the end of the licensing process for the transaction, provided that you have disclosed complete and accurate details of your proposed use, no license is finally effective unless and until full payment is received from you (either by publisher or by CCC) as provided in CCC's Billing and Payment terms and conditions. If full payment is not received on a timely basis, then any license pre-

liminarily granted shall be deemed automatically revoked and shall be void as if never granted. Further, in the event that you breach any of these terms and conditions or any of CCC's Billing and Payment terms and conditions, the license is automatically revoked and shall be void as if never granted. Use of materials as described in a revoked license, as well as any use of the materials beyond the scope of an unrevoked license, may constitute copyright infringement and publisher reserves the right to take any and all action to protect its copyright in the materials.

9. Warranties: Publisher makes no representations or warranties with respect to the licensed material.

10. Indemnity: You hereby indemnify and agree to hold harmless publisher and CCC, and their respective officers, directors, employees and agents, from and against any and all claims arising out of your use of the licensed material other than as specifically authorized pursuant to this license.

11. No Transfer of License: This license is personal to you and may not be sublicensed, assigned, or transferred by you to any other person without publisher's written permission.

12. No Amendment Except in Writing: This license may not be amended except in a writing signed by both parties (or, in the case of publisher, by CCC on publisher's behalf).

13. Objection to Contrary Terms: Publisher hereby objects to any terms contained in any purchase order, acknowledgment, check endorsement or other writing prepared by you, which terms are inconsistent with these terms and conditions or CCC's Billing and Payment terms and conditions. These terms and conditions, together with CCC's Billing and Payment terms and conditions (which are incorporated herein), comprise the entire agreement between you and publisher (and CCC) concerning this licensing transaction. In the event of any conflict between your obligations established by these terms and conditions and those established by CCC's Billing and Payment terms and conditions, these terms and conditions shall control.

14. Revocation: Elsevier or Copyright Clearance Center may deny the permissions described in this License at their sole discretion, for any reason or no reason, with a full refund payable to you. Notice

of such denial will be made using the contact information provided by you. Failure to receive such notice will not alter or invalidate the denial. In no event will Elsevier or Copyright Clearance Center be responsible or liable for any costs, expenses or damage incurred by you as a result of a denial of your permission request, other than a refund of the amount(s) paid by you to Elsevier and/or Copyright Clearance Center for denied permissions.

LIMITED LICENSE

The following terms and conditions apply only to specific license types:

15. **Translation**: This permission is granted for non-exclusive world **English** rights only unless your license was granted for translation rights. If you licensed translation rights you may only translate this content into the languages you requested. A professional translator must perform all translations and reproduce the content word for word preserving the integrity of the article. If this license is to re-use 1 or 2 figures then permission is granted for non-exclusive world rights in all languages.

16. **Posting licensed content on any Website**: The following terms and conditions apply as follows: Licensing material from an Elsevier journal: All content posted to the web site must maintain the copyright information line on the bottom of each image; A hyper-text must be included to the Homepage of the journal from which you are licensing at http://www.sciencedirect.com/science/journal/xxxxx or the Elsevier homepage for books at http://www.elsevier.com; Central Storage: This license does not include permission for a scanned version of the material to be stored in a central repository such as that provided by Heron/XanEdu.

Licensing material from an Elsevier book: A hyper-text link must be included to the Elsevier homepage at http://www.elsevier.com . All content posted to the web site must maintain the copyright information line on the bottom of each image.

Posting licensed content on Electronic reserve: In addition to the above the following clauses are

applicable: The web site must be password-protected and made available only to bona fide students registered on a relevant course. This permission is granted for 1 year only. You may obtain a new license for future website posting.

17. **For journal authors:** the following clauses are applicable in addition to the above:

Preprints:

A preprint is an author's own write-up of research results and analysis, it has not been peer-reviewed, nor has it had any other value added to it by a publisher (such as formatting, copyright, technical enhancement etc.).

Authors can share their preprints anywhere at any time. Preprints should not be added to or enhanced in any way in order to appear more like, or to substitute for, the final versions of articles however authors can update their preprints on arXiv or RePEc with their Accepted Author Manuscript (see below).

If accepted for publication, we encourage authors to link from the preprint to their formal publication via its DOI. Millions of researchers have access to the formal publications on ScienceDirect, and so links will help users to find, access, cite and use the best available version. Please note that Cell Press, The Lancet and some society-owned have different preprint policies. Information on these policies is available on the journal homepage.

Accepted Author Manuscripts: An accepted author manuscript is the manuscript of an article that has been accepted for publication and which typically includes author-incorporated changes suggested during submission, peer review and editor-author communications.

Authors can share their accepted author manuscript:

- – immediately
    - o via their non-commercial person homepage or blog
    - o by updating a preprint in arXiv or RePEc with the accepted manuscript
    - o via their research institute or institutional repository for internal institutional uses or as part of an invitation-only research collaboration workgroup

    - directly by providing copies to their students or to research collaborators for their personal use
    - for private scholarly sharing as part of an invitation-only work group on commercial sites with which Elsevier has an agreement
- – after the embargo period
    - via non-commercial hosting platforms such as their institutional repository
    - via commercial sites with which Elsevier has an agreement

In all cases accepted manuscripts should:

- – link to the formal publication via its DOI
- – bear a CC-BY-NC-ND license - this is easy to do
- – if aggregated with other manuscripts, for example in a repository or other site, be shared in alignment with our hosting policy not be added to or enhanced in any way to appear more like, or to substitute for, the published journal article.

Published journal article (JPA): A published journal article (PJA) is the definitive final record of published research that appears or will appear in the journal and embodies all value-adding publishing activities including peer review co-ordination, copy-editing, formatting, (if relevant) pagination and online enrichment.

Policies for sharing publishing journal articles differ for subscription and gold open access articles:

Subscription Articles: If you are an author, please share a link to your article rather than the full-text. Millions of researchers have access to the formal publications on ScienceDirect, and so links will help your users to find, access, cite, and use the best available version.

Theses and dissertations which contain embedded PJAs as part of the formal submission can be posted publicly by the awarding institution with DOI links back to the formal publications on ScienceDirect.

If you are affiliated with a library that subscribes to ScienceDirect you have additional private sharing rights for others' research accessed under that agreement. This includes use for classroom teaching and internal training at the institution (including use in course packs and courseware programs), and inclusion of the article for grant funding purposes.

Gold Open Access Articles: May be shared according to the author-selected end-user license and should contain a CrossMark logo, the end user license, and a DOI link to the formal publication on ScienceDirect.

Please refer to Elsevier's posting policy for further information.

18. **For book authors** the following clauses are applicable in addition to the above: Authors are permitted to place a brief summary of their work online only. You are not allowed to download and post the published electronic version of your chapter, nor may you scan the printed edition to create an electronic version. **Posting to a repository:** Authors are permitted to post a summary of their chapter only in their institution's repository.

19. **Thesis/Dissertation**: If your license is for use in a thesis/dissertation your thesis may be submitted to your institution in either print or electronic form. Should your thesis be published commercially, please reapply for permission. These requirements include permission for the Library and Archives of Canada to supply single copies, on demand, of the complete thesis and include permission for Proquest/UMI to supply single copies, on demand, of the complete thesis. Should your thesis be published commercially, please reapply for permission. Theses and dissertations which contain embedded PJAs as part of the formal submission can be posted publicly by the awarding institution with DOI links back to the formal publications on ScienceDirect.

Elsevier Open Access Terms and Conditions

You can publish open access with Elsevier in hundreds of open access journals or in nearly 2000 established subscription journals that support open access publishing. Permitted third party re-use of these open access articles is defined by the author's choice of Creative Commons user license. See our open access license policy for more information.

CC BY NC ND: The CC BY-NC-ND license allows users to copy and distribute the Article, provided this is not done for commercial purposes and further does not permit distribution of the Article if it is changed or edited in any way, and provided the user gives appropriate credit (with a link to the formal publication through the relevant DOI), provides a link to the license, and that the licensor is not represented as endorsing the use made of the work. The full details of the license are available at http://creativecommons.org/licenses/by-nc-nd/4.0. Any commercial reuse of Open Access articles published with a CC BY NC SA or CC BY NC ND license requires permission from Elsevier and will be subject to a fee.

Commercial reuse includes:

- – Associating advertising with the full text of the Article
- – Charging fees for document delivery or access
- – Article aggregation
- – Systematic distribution via e-mail lists or share buttons

Posting or linking by commercial companies for use by customers of those companies.

20. **Other Conditions**:

v1.7

Questions? customercare@copyright.com or +1-855-239-3415 (toll free in the US) or+1-978-646-2777.

Gratis licenses (referencing $0 in the Total field) are free. Please retain this printable license for your reference. No payment is required.